

ABSTRACT

Title of Document: USE OF 2-DEOXYFLAVIN
MONONUCLEOTIDE TO PROBE
SUBSTRATE-FLAVIN INTERACTIONS
WITHIN IODOTYROSINE DEIODINASE.

Petrina Abiola Boucher,
Doctor of Philosophy, 2015

Directed By: Professor Steven E. Rokita, Department of
Chemistry and Biochemistry

The catalytic versatility of flavins encompasses the ability to catalyze one and two electron redox processes as well as dioxygen activation. In flavoenzymes, protein-cofactor interactions modulate flavin chemistry enabling these enzymes to perform a diverse set of biological roles. Flavin analogs, such as deoxyflavins, provide a convenient method for identifying which polar contacts to FMN are necessary for enzymatic activity.

Iodotyrosine deiodinase (IYD) is responsible for the deiodination of byproducts from thyroxine biosynthesis (mono- and diiodotyrosine (MIT and DIT)) in the thyroid. A unique flavoenzyme, IYD, is one of few known aerobic enzymes able to catalysis reductive dehalogenation. Literature precedence for the deiodination mechanism of IYD has not been found. Detection of the flavin semiquinone (Fl_{sq}) intermediate during anaerobic reduction of IYD in the presence of substrate suggests deiodination occurs via two single electron transfer processes. Proposed one electron

mechanisms for IYD involving formation of a substrate keto-tautomer are supported by the enzyme's preference for the phenolate form of substrate during binding. Previous analysis of a co-crystal of IYD and MIT showed the involvement of substrate in extensive interactions with the FMN cofactor, including a hydrogen bond between the FMN ribityl 2'-OH and the phenolic OH of MIT. This hydrogen bond has been hypothesized to activate substrate for deiodination.

To probe the significance of the polar interaction between the ribityl 2'-OH and the phenolic OH of MIT in IYD, 2-deoxyriboflavin was synthesized and enzymatically phosphorylated using riboflavin kinase. Reconstitution of human IYD (hIYD) with 2-deoxyFMN produced an enzyme with a significantly decreased affinity for MIT. Deiodinase activity was retained in 2-deoxyhIYD with a 10-fold decrease in catalytic efficiency. Detection of the Fl_{sq} was not observed during anaerobic reduction of 2-deoxyhIYD in the presence of mono-fluorotyrosine (MFT). The enzyme's preference for the phenol versus phenolate form of substrate could not be determined due to the low solubility of DIT at concentrations necessary for pH dependent binding analysis. Removal of the ribityl 2'-OH did not support turnover of O-methyl MIT, a substrate analog incapable of undergoing tautomerization.

USE OF 2-DEOXYFLAVIN MONONUCLEOTIDE TO PROBE SUBSTRATE-
FLAVIN INTERACTIONS WITHIN IODOTYROSINE DEIODINASE.

By

Petrina Abiola Boucher

Dissertation submitted to the Faculty of the Graduate School of the
University of Maryland, College Park, in partial fulfillment
of the requirements for the degree of
Doctor of Philosophy
2015

Advisory Committee:
Professor Steven E. Rokita, Chair
Professor Jeffery Davis
Professor Daniel Falvey
Professor Lai-Xi Wang
Professor Jonathan Dinman

© Copyright by
Petrina Abiola Boucher
2015

Dedication

To my family, for your love, support and encouragement.

Acknowledgements

All praise and thanks are due to the Most High for getting me through this process, allowing me to see the light at the end of the tunnel and bringing so many amazing people into my life along the way.

Dr. Rokita, thank you for taking me into your lab, bringing me to Hopkins and supporting me throughout the ups and downs of science. You have helped me to become a more critical thinker, a better writer and a more thoughtful scientist. Thank you for teaching me to anticipate both positive and negative results, to always fill the white space and check sig figs.

Thank you to my committee Professors Davis, Falvey, DeShong, Wang and Dinman for taking the time to be there. To Professors Davis, Falvey and DeShong thank you for helping to mold my scientific mind in the first years of graduate school and taking the time to be there whenever I needed to discuss science. Professor Wang, many thanks to you for stepping in last minute and allowing the show to go on. To Professors Eichorn, Issacs, Sintim, Dixon and the other faculty members that I have encountered during my time at College Park thank you for helping grow as a scientist.

Thank you to all the departmental staff for managing the paperwork and being my translator with the rest of the University. Thanks to Tia, Elizabeth and Diane at UMD as well as Jean, Joe and Boris at JHU for making things happen. To Drs. Yui-Fai Lam, Yue Li, Phil Mortimer and Joel Tang, thank you for all your assistance with instrumentation.

To the Rokita lab members past and present thank you. Every one of you has helped to make me a better scientist, person and friend. Patrick McTamney, thank you showing me what a dedicated scientist looks like. Jim Watson, though we never overlapped in lab, I'm glad to have met you. Your advice, kind words and humor made all the difference. Jen Buss words do no justice to your influence on me as a scientist and person. Jimin Hu thanks for your help with the biochemistry side of things. To Mike McCrane and Shalini Saha thank you both for being there to talk through science and life. Mark, Blessing, Abhishek and Patt thanks for making the transition to Hopkins and Baltimore a smooth one. I wish you guys all the best in finishing up. See you all on the other side soon! Chris and Zuodong thanks for your help, best of luck.

Many thanks to my extended NOBCChE family for keeping me sane through this process called graduate school. Drs. Jackie Smith, Kathy Goodson and many more thank you being my science big sisters, offering both professional and personal advice. To the Hopkins Chapter, I wish you all the best. Thanks to the Hopkins MSA and Grad-MSA for keeping me grounded and connected to my Lord through your friendship and kindness. I am forever grateful to know you all.

Last but definitely not least, a huge thank you to my entire family. Mommy and Anisha, you two have been my rocks through this entire journey. Thanks for believing in me and encouraging me when I needed it the most. Mom, I pray I can repay you for all the sacrifices. To Poppy, Bonnie, Aminah and Eian thank you for being there when I truly needed you and everything else you do to keep me sane. RIP Grandmother, Uncle Kenrick and Royston.

Table of Contents

Dedication.....	ii
Acknowledgements.....	iii
Table of Contents.....	v
List of Tables.....	vii
List of Figures.....	viii
Chapter 1: Introduction.....	1
<u>1.1</u> The Chemistry of Flavoenzyme.....	1
1.1.1 Cofactor with Diverse Activity.....	1
1.1.2 Unusual Role of Flavoenzymes in Reductive Dehalogenation.....	7
1.2 IYD is a Flavoenzyme that Catalyzes Reductive Dehalogenation.....	9
1.2.1 Iodide Salvage.....	9
1.2.2 Characterization of IYD as a nitro-FMN reductase.....	12
1.2.3 Comparison of IYD within nitro-FMN reductase Superfamily.....	12
1.3 Proposed Mechanism for IYD.....	15
1.4 Specific Aims.....	18
Chapter 2: Preparation of a 2-DeoxyFMN Analog.....	19
2.1 Introduction.....	19
2.2 Results and Discussion.....	22
2.2.1 Synthesis of 2-Deoxyriboflavin.....	22
2.2.2 Enzymatic Phosphorylation of 2-Deoxyriboflavin using Riboflavin Kinase 29.....	
2.3 Summary.....	32
2.4 Experimental Procedures.....	33
Chapter 3: Preparation and Reconstitution of IYD.....	39
3.1 Introduction.....	39
3.2 Results and Discussion.....	40
3.2.1 Reconstitution of hIYD with FMN and 2-DeoxyFMN.....	40
3.2.2 Deiodinase Activity of FMN and 2-DeoxyFMN Reconstituted hIYD... ..	49
3.3 Summary.....	52
3.4 Experiments.....	52
3.4.1 Protein Expression and Purification of hIYD.....	53
3.4.2 Generation of apo-hIYD.....	54
3.4.3 Reconstitution of apo-hIYD.....	55
3.4.4 Fluorescence Binding.....	55
3.4.5 Deiodinase Activity.....	56
Chapter 4: 2-DeoxyhIYD Activity with Substrate Analogs.....	59
4.1 Introduction.....	59
4.2 Results and Discussion.....	62
4.2.1 The Effects of 2'OH on Flavin Reduction.....	62
4.2.2 Importance of 2'OH for Substrate Binding.....	65

4.2.3	2-DeoxyhIYD does not Support Turnover of OMeMIT.....	68
4.3	Summary	70
4.4	Experimental	70
4.4.1	Anaerobic Redox Titration	70
4.4.2	Fluorescence Binding.....	71
4.4.3	HPLC Deiodinase Activity Assay of OMeMIT.....	71
Chapter 5:	Conclusions.....	72
Appendices.....		75
Appendix A.	Supporting Information for Chapter 2.....	75
Appendix B.	Supporting Information for Chapter 3.....	80
Appendix C.	Supporting Information for Chapter 4.....	83
Reference		85

List of Tables

Chapter 1

No tables.

Chapter 2

No tables.

Chapter 3

Table 3.1 Kinetic parameters of hIYD.....	43
Table 3.2 Equilibrium binding constants of native, FMN reconstituted and 2-deoxyhIYD.....	48
Table 3.3 Kinetic parameters of native, FMN reconstituted and 2-deoxyhIYD with DIT.....	50

Chapter 4

No tables.

Chapter 5

No tables.

List of Figures

Chapter 1

Figure 1.1 The chemical structure of flavin.....	2
Figure 1.2 Hydrogen bond of acyl-CoA with FAD ribityl 2'OH and Glu376 in medium chain acyl-CoA dehydrogenase (MCAD). PBD ID: 3MDE ²⁶	7
Figure 1.3 The biosynthesis of the thyroid hormones, T4 and T3, in the thyroid follicular cells. Figure modified from ⁴⁶	10
Figure 1.4 Crystal structure of hIYD (left) and its co-crystal with MIT.	13
Figure 1.5 Comparison of IYD to nitro-FMN reductase superfamily.	14
Figure 1.6 Crystal structure of the active site of hIYD, highlighting the interaction between MIT, the protein and FMN. PBD ID: 4TTC ⁶⁴	15

Chapter 2

Figure 2.1 Structure of 1-deaza and 5-deazariboflavin.....	20
Figure 2.2 Structure of 2-deoxyriboflavin.	21
Figure 2.3 HPLC chromatographs of the 2-deoxyriboflavin purification	27
Figure 2.4 HPLC chromatograph of 2-Deoxyriboflavin purification using riboflavin as a standard. Product purification was monitored at 450 nm using a 30 min linear gradient from 100% 0.1% trifluoroacetic acid in water to 50% acetonitrile.	28
Figure 2.5 Comparison of 2-deoxyriboflavin final purification using HPLC and Waters Sep-Pak®. Product purification was monitored at 450 nm using a 30 min linear gradient from 100% 0.1% trifluoroacetic acid in water to 50% acetonitrile. ...	28
Figure 2.6 Denaturing SDS-page gel of hsRFK Ni ²⁺ affinity purification.	30
Figure 2.7 HPLC chromatograph of riboflavin kinase (RFK) phosphorylation of riboflavin to FMN. Product formation was monitored at 450 nm using a 25 min linear gradient from 0% to 55% acetonitrile with 100 mM ammonium formate (pH 3.7) as the aqueous buffer.....	31
Figure 2.8 HPLC chromatograph of RFK catalyzed phosphorylation of 2-deoxyriboflavin to 2-deoxyFMN. Product formation was monitored at 450 nm using a 30 min linear gradient from 0% to 50% acetonitrile.....	32

Chapter 3

Figure 3.1 DIT deiodinase activity of native, apo and FMN reconstituted hIYD under 500 mM NaCl conditions. The activity of hIYD (0.08 μM) with DIT was determined using the standard discontinuous D ¹²⁵ IT iodide release assay.....	41
Figure 3.2 DIT deiodinase activity of native, apo and holo-hIYD reconstituted with 5 eq of FMN. The activity of hIYD (0.08 μM) was determined using the standard D ¹²⁵ IT iodide release assay. Assays were performed in triplicate and the average data sets were fit to Michaelis-Menten kinetics using Origin 7.0. Error bars represent standard deviation at each concentration.	43

Figure 3.3 D ¹²⁵ IT deiodinase activity of native, apo and holo-hIYD reconstituted with 5 and 10 equivalents of FMN. Activity was determined using the standard D ¹²⁵ IT iodide release assay.....	44
Figure 3.4 D ¹²⁵ IT deiodinase activity of native, apo and holo-hIYD reconstituted on Ni ²⁺ affinity column using 100 μM FMN. Activity of hIYD (0.08 μM) was determined using the standard D ¹²⁵ IT iodide release assay. Assays were performed at least twice. Error bars represent standard deviation at each concentration.	46
Figure 3.5 DIT deiodinase activity of native, apo and holo-hIYD reconstituted on Ni ²⁺ affinity column using 100 μM FMN. The activity of hIYD (0.08 μM) was determined using the standard D ¹²⁵ IT iodide release assay. Assays were performed in triplicate. The averaged data was fit to Michaelis-Menten kinetics using Origin 7.0. Error bars represent standard deviation at each concentration.	47
Figure 3.6 Equilibrium binding of MIT to FMN reconstituted hIYD and 2-deoxyhIYD. Binding was monitored by the change in fluorescence of flavin bound to enzyme (4.5 μM) in solution of 100 mM potassium phosphate and 200 mM potassium chloride (pH 7.4) at 25°C using λ _{ex} of 450 nm and λ _{em} of 527 nm. The average of three independent measurements were normalized and plotted against MIT concentrations. Error bars represents the standard deviation of three measurements.	49
Figure 3.7 MIT deiodinase activity of 2-deoxyhIYD.	51

Chapter 4

Figure 4.1 Selected spectra from the redox titration of 15 μM FMN reconstituted hIYD by xanthine/xanthine oxidase.....	63
Figure 4.2 Selected spectra from the redox titration of 15 μM 2-deoxyhIYD in the presence of 5 mM MFT by xanthine/xanthine oxidase. The data was recorded every 2 mins for over 120 mins.	65
Figure 4.3 Polar contacts between the ribityl chain 2'-OH and N1 of FMN in IYD. .	65
Figure 4.4 Equilibrium binding of OMeMIT to A) native hIYD and B) 2-deoxyhIYD. Binding was monitored by the change in fluorescence of flavin bound to enzyme (4.5 μM) in solution of 100 mM potassium phosphate and 200 mM potassium chloride (pH 7.4) at 25°C using λ _{ex} of 450 nm and λ _{em} of 527 nm.....	68
Figure 4.5 HPLC chromatograph of the deiodination of OMeMIT by A) 4.5 μM hIYD and B) 4.5 μM 2-deoxyhIYD using a 45 min linear gradient from 100% TEAA pH 5.5 to 45% acetonitrile. Production formation was monitored at 274 nm. Reaction were conducted for 4 hr and spiked with 10 μM OMeTyr to confirm no turnover had occurred.....	69

Chapter 5

No figures.

List of Schemes

Chapter 1

Scheme 1.1 Physiologically relevant redox and protonation states of riboflavin.....	3
Scheme 1.2 Proposed mechanism for the reductive dehalogenation of pentachlorophenol catalyzed by tetrachlorohydroquinone dehalogenase (TD).....	8
Scheme 1.3 Proposed mechanism for the reductive dehalogenation of thyroxine catalyzed by iodothyronine deiodinase (ID).....	9
Scheme 1.4 Dehalogenation of mono- and diiodotyrosine catalyzed by IYD.....	11
Scheme 1.5 Proposed one electron transfer mechanisms for the reductive dehalogenation catalyzed by IYD.....	17

Chapter 2

Scheme 2.1 Proposed 1e- mechanism for the reductive dehalogenation of MIT by IYD.	21
Scheme 2.2 Initial A) and modified B) synthetic schemes for the formation of 2-deoxyribityl- 3,4- dimethylaniline (2.2).....	23
Scheme 2.3 Diazotization of 2-deoxyribitylated-3,4-dimethylaniline (2.2).....	24
Scheme 2.4 Formation of 2-Deoxyriboflavin.	26

Chapter 4

Scheme 4.1 Proposed 1 e- mechanism for the reductive dehalogenation catalyzed by IYD.	60
--	----

Chapter 5

No schemes.

List of Abbreviations

ATP	Adenosine Triphosphate
DIT	3,5,-Diiodo-L-tyrosine
EC	Enzyme Commission
ESI-MS	Electrospray Ionization Mass Spectrometry
ETF	Electron Transfer Flavoprotein
FAD	Flavin Adenine Dinucleotide
FMN	Flavin Mononucleotide
Fl _{ox}	Flavoquinone
Fl _{red}	Flavohydroquinone
Fl _{sq}	Flavosemiquinone
FPLC	Fast Protein Liquid Chromatography
GdnHCl	Guanidine hydrochloride
hIYD	Human Iodotyrosine Deiodinase
HPLC	High Performance Liquid Chromatography
ID	Iodothyronine Deiodinase
ITPG	Isopropyl β -D-1-thiogalactopyranoside
IYD	Iodotyrosine Deiodinase
IYD(Δ tm)	Truncated Iodotyrosine Deiodinase
k _{cat}	Catalytic rate
K _D	Dissociation constant
K _M	Michaelis-Menten constant
MCAD	Medium chain Acyl-CoA Dehydrogenase

MIT	3-Iodo-L-tyrosine
mIYD	Mouse Iodotyrosine Deiodinase
NADPH	Nicotinamide Adenine Dinucleotide Phosphate
NADH	Nicotinamide Adenine Dinucleotide
NMR	Nuclear Magnetic Resonance
OMeMIT	O-Methyl-3-iodo-L-tyrosine
OMeTyr	O-Methyl-tyrosine
PBD	Protein Data Bank
PCP	pentrachlorophenol
RFK	Riboflavin Kinase
T ₄	Thyroxine
T ₃	3,3',5 – Triiodothyronine
TD	Tetrachlorohydroquinone Deiodinase
TCHQ	Tetrachlorohydroquinone
TriCHQ	Trichlorohydroquinone
TLC	Thin Layer Chromatography
TFA	Trifluoroacetic acid
TEAA	Triethylammonium acetate
t _r	Retention time
UPLC-MS	Ultra High Performance Liquid Chromatography Mass Spectrometry
UV-Vis	Ultraviolet-Visible Spectroscopy

Chapter 1: Introduction

1.1 The Chemistry of Flavoenzyme

1.1.1 Cofactor with Diverse Activity

The biological importance of flavin has been under investigation since its recognition as a component of the vitamin B complex¹. Initially isolated from cow's milk in 1879 by the English chemist A. Wynter Blyth as a bright yellow pigment, it was not until the mid-1930s that a chemical structure was determined in parallel by Richard Kuhn and Paul Karrer¹. It was from that chemical structure (**Figure 1.1**) that the name riboflavin was derived, on the basis of its N10 ribityl side chain, yellow colored conjugated ring system and the compound's classification as a vitamin.

The biological active forms of riboflavin, flavin mononucleotide (FMN) and flavin adenine dinucleotide (FAD) were discovered to be necessary for enzymatic catalysis through the removal of the native cofactor and reconstitution with riboflavin in old yellow enzyme and D-amino acid oxidase¹. These cofactors differ from riboflavin in their modification at the N10 ribityl chain (**Figure 1.1**) where phosphorylation of the terminal 5'-OH produces FMN. Further adenylation of FMN with AMP results in the formation of FAD.

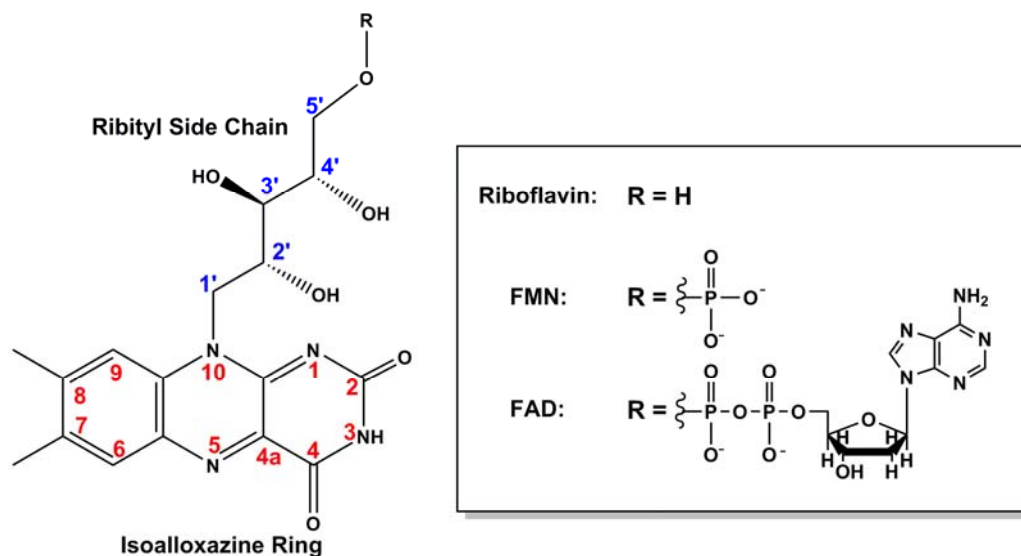
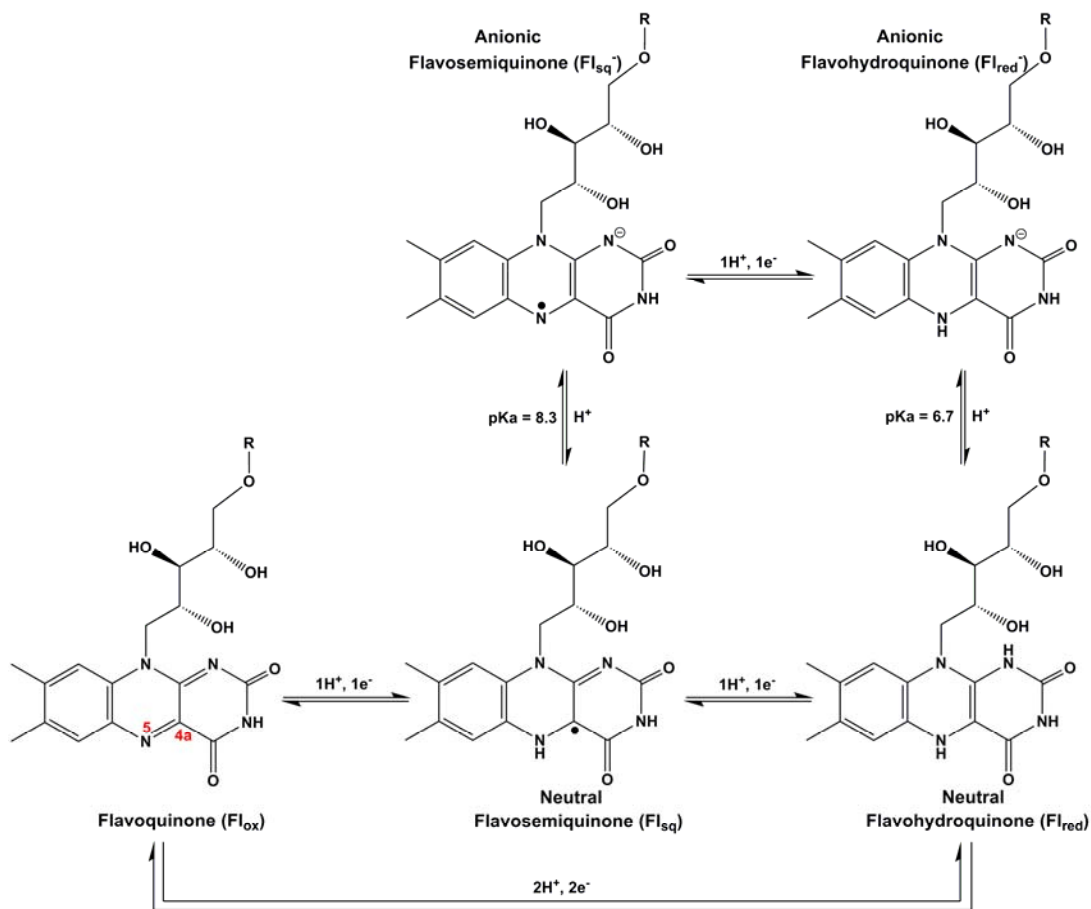


Figure 1.1 The chemical structure of flavin.

In general, flavins are defined by their tricyclic isoalloxazine ring system, comprised of a hydrophobic dimethylbenzene, a hydrophilic uracil ring and a central pyrazine ring (**Figure 1.1**). The isoalloxazine ring is the center of reactivity and responsible for the catalytic versatility of the cofactor that encompasses the ability to catalyze 1 and 2 electron redox processes as well as dioxygen activation^{2,3}. Flavins can exist in major redox states with each state occurring as a neutral, anionic and cationic species⁴. Of these nine variants, only five are physiologically relevant: the neutral flavoquinone (Fl_{ox}), the neutral and anionic flavohydroquinone (Fl_{red} , Fl_{red}^-), and the neutral and anionic flavosemiquinone (Fl_{sq} , Fl_{sq}^-) (**Scheme 1.1**)^{4,5}. Reduction of the fully oxidized Fl_{ox} can occur via one of two pathways: 1) a single two electron transfer or 2) two sequential one electron transfers, forming a stable radical intermediate at the either the N5 or C4a position of the isoalloxazine ring (**Figure 1.1**)⁶. Each state can be differentiated by way its characteristic optical spectrum. The Fl_{ox} is yellow with absorbance maximum at 445 nm. The neutral Fl_{sq} is blue with an

absorbance maximum around 500-600 nm and the anionic Fl_{sq}^- is red with an absorbance maximum around 370-400 nm. The Fl_{red} is colorless.



Scheme 1.1 Physiologically relevant redox and protonation states of riboflavin.

The Chemical Environment of Flavin Controls Redox Chemistry

Studies on both free and protein bound flavin have shown that its redox properties can be fine-tuned by its surrounding chemical environment⁶⁻¹¹. For flavoenzymes, the presence of non-covalent interactions plays a substantial role in the modulation of cofactor chemistry, and therefore enzymatic catalysis. Interactions such as hydrogen bonding, aromatic stacking and flavin conformation are known to

control the site of hydrogen transfer, the modes of electron transfer pathways and the modes of O₂ reductive activation^{3,12}. Site directed mutagenesis and/or enzymatic reconstitution with chemical modification of flavin have helped to decipher which of the non-covalent interactions between the cofactor and apoprotein are critical for activity^{1,3,12}. The process of enzymatic reconstitution involves removal of the enzyme's native cofactor and reinsertion of a flavin derivative, producing enzymes with different catalytic properties. The protein environment surrounding the pyrimidine ring is particularly important in control of the flavin redox potential^{7,8}. The N1 and N5 atoms at either end of the ethylenediamine linkage of the isoalloxazine nucleus, as well as their neighboring carbonyl groups (O2 and O4), are crucial for stabilization of the anionic and neutral forms of the semiquinone and hydroquinone states. For example, positively charged amino acid side chains near N1 and O2 increase the redox potential of flavin as well as stabilize the anionic form of the reduced flavin, whereas negatively charged amino acid side chains have the opposite effect and decrease the redox potential^{8,11}. This trend is seen in a number of flavoenzymes where the N1 position is in close proximity to protein residues such as a lysine or arginine¹¹ or even the flavin ribityl side chain. Additionally, intraflavin hydrogen bonding between the 4'OH and N1 in human and bacterial electron transfer flavoproteins (ETFs) has been implicated in the stabilization of the Fl_{sq}⁻ and Fl_{red}⁻ redox states of FAD¹³. The N5 position of the isoalloxazine ring is also important for stabilization of the neutral Fl_{sq} and dioxygen activation^{14,15,3}. Hydrogen bonding at this position by donors such as lysine or threonine has been shown to activate the relative reactivity of the C4a position towards molecular oxygen^{3,16}.

Numerous reconstitution studies have confirmed the significance of N1 and N5 by utilizing 1-deaza and/or 5-deazaflavins analogs as mechanistic probes^{2, 8, 17}. Substitution of the N1 with carbon decreases the redox potential of this analog from -208 mV to -280 mV, making it harder to reduce than the native flavin¹⁸. However, this substitution does not eliminate the ability of 1-deaza analog to support both 1 and 2 electron transfers¹⁸. In contrast, carbon substitution of the N5 converts the central pyrazine ring into a pyridine ring. This modification not only decreases the redox potential from -208 mV to -311 mV but also suppresses single electron transfer and converts this analog into a nicotinamide equivalent¹⁸.

The Ribose Chain of Flavin Affects Substrate Recognition and Activation

Crystal structures of several flavoenzymes including old yellow enzyme¹⁹, glutathione reductase²⁰, lipoamide dehydrogenase²¹ and human monoamine oxidase B²² have shown networks of hydrogen bonding to the N10 ribityl chain hydroxyls, implying the significance of these groups for anchoring the cofactor and modulating catalytic activity. The 4'-OH has been observed by x-ray crystallography to form an intraflavin hydrogen bond with N1 of FAD in human and bacterial ETFs¹³. Elimination of the 4'-OH-N1 hydrogen bond by reconstitution of the human ETF with 4-deoxyFAD resulted in a 0.116 V decreased redox potential of the Fl_{ox}/Fl_{sq} half reaction, making it difficult to reduce the cofactor in the presence of either xanthine/xanthine oxidase or sodium dithionite¹³. These observations strongly suggest that the 4'-OH is necessary for stabilization of the Fl_{sq}⁻.

Removal of the ribityl chain 2'-OH can also have significant effects on enzyme activity^{23, 24 25}. The best characterized example involves acyl-CoA

dehydrogenase that promotes dehydrogenation of acyl CoAs from either β -oxidation cycle or amino acid metabolism^{26,27}. Crystal structures of the medium chain acyl-CoA dehydrogenase (MCAD) show the presence of two hydrogen bonds to the thioester carbonyl oxygen of acyl-CoA, one from the NH of Glu376 and the other from the 2'-OH of FAD (**Figure 1.2**)²⁶. These interactions were hypothesized to lower the pK_a of the acyl-CoA α proton as well as align acyl-CoA, FAD, and Glu376 for dehydrogenation. Reconstitution studies utilizing 2-deoxyFAD to eliminate the polar contact between 2'-OH and the thioester carbonyl resulted in a 1.5×10^7 fold decrease in substrate dehydrogenation²⁸. Additionally, studies with wild type MCAD and an acyl-CoA substrate analog also measured the effects of hydrogen bonding on substrate pK_a and showed a 6 unit increase in pK_a for the substrate when bound to native MCAD versus 2-deoxyFAD-MCAD ($pK_a \sim 5$ for wild type MCAD; $pK_a \sim 11$ for 2-deoxyFAD-MCAD)²⁸. This difference was attributed solely to the loss of substrate hydrogen bonding with the 2'-OH, confirming the necessity of this hydrogen bond for of acyl-CoA activation.

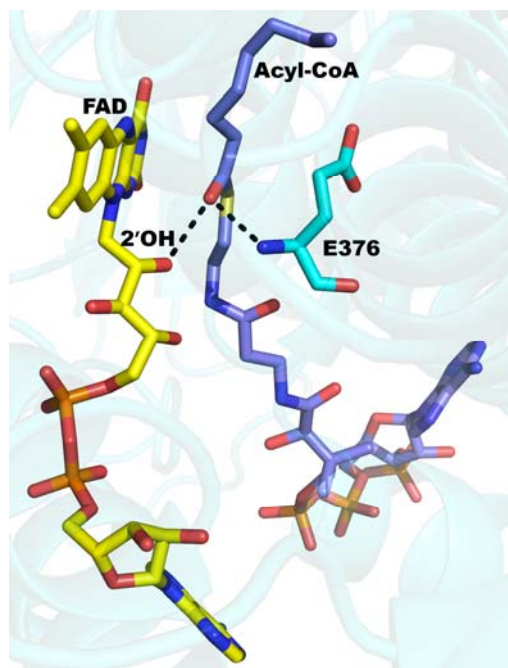
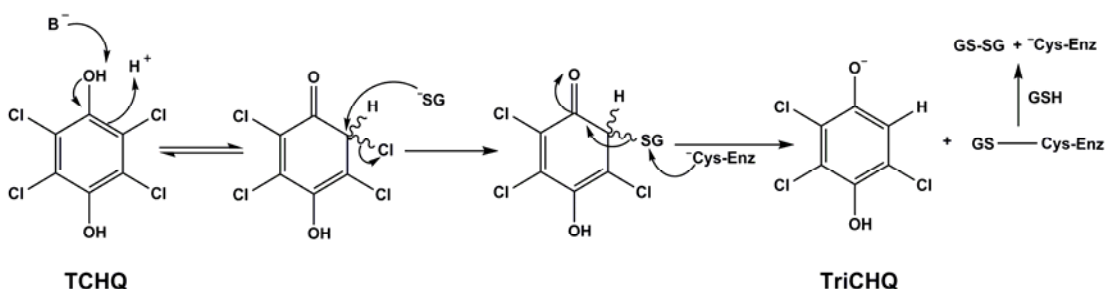


Figure 1.2 Hydrogen bond of acyl-CoA with FAD ribityl 2'OH and Glu376 in medium chain acyl-CoA dehydrogenase (MCAD). PDB ID: 3MDE ²⁶.

1.1.2 Unusual Role of Flavoenzymes in Reductive Dehalogenation

Efforts to correlate cofactor chemistry with mechanism of action led to a classification of flavin-dependent enzymes on the basis of their catalytic activity, with more than 90% of flavoenzymes classified as oxidoreductases ²⁹. The chemical versatility of flavins support a range of biological processes including bioluminescence ³⁰, photosynthesis ³¹, dehalogenation ^{32,33}, and halogenation ^{34,35}. Of the more than 300 known flavoenzymes, few are associated with reductive dehalogenation ³⁶. As a result, mechanisms for reductive dehalogenation are often expanded to include aerobic systems, with tetrachlorohydroquinone dehalogenase and iodothyronine deiodinase being the best studied examples.

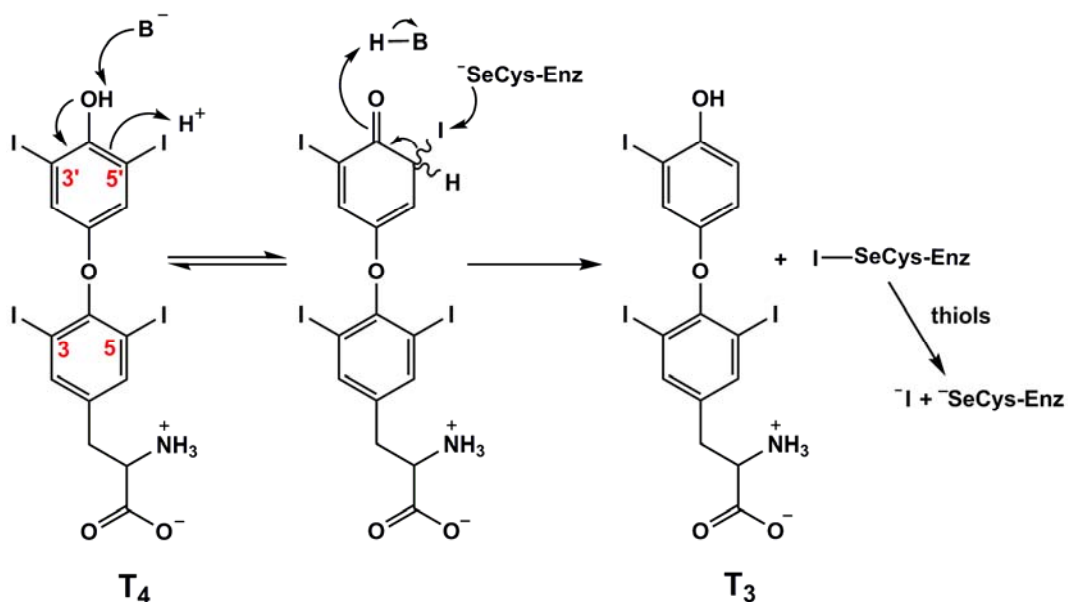
Tetrachlorohydroquinone dehalogenase (TD) from the soil bacterium *Sphingobium chlorophenicum*, catalyzes the reductive dechlorination of tetrachlorohydroquinone (TCHQ) and trichlorohydroquinone (TriCHQ) in the biodegradation of the pentachlorophenol³⁷. The mechanism of this dechlorination has been proposed to start with the tautomerization of TCHQ to an electrophilic enone (**Scheme 1.2**). Nucleophilic attack of the enone by glutathione, results in the elimination of a chloride ion. The sulfur atom of the glutathionyl intermediate is then attacked by a neighboring cysteine residue, releasing TriCHQ. A second glutathione is then hypothesized to regenerate the active site cysteine residue, completing the catalytic cycle (**Scheme 1.2**)^{38, 39}.



Scheme 1.2 Proposed mechanism for the reductive dehalogenation of pentachlorophenol catalyzed by tetrachlorohydroquinone dehalogenase (TD).

The second example, iodothyronine deiodinase (ID), is responsible for the reductive deiodination of the prohormone thyroxine (T_4), converting it to the thyroid hormone, 3,3',5' - triiodothyronine (T_3)⁴⁰. Similarly to TD, the propose mechanism of deiodination for ID, begins with tautomerization of T_4 to a non-aromatic intermediate (**Scheme 1.3**)⁴⁰. Nucleophilic attack of the C5' iodide of T_4 by an active site selenocysteine residue forms T_3 and a selenoleyl iodide intermediate. The catalytic

cycle is completed upon reduction of the selenoleyl iodide by substrate thiols, regenerating the active site selenocysteine and releasing iodide ^{40, 41}.



Scheme 1.3 Proposed mechanism for the reductive dehalogenation of thyroxine catalyzed by iodothyronine deiodinase (ID).

As an important constituent of T₃ and T₄, iodide is indispensable to regulation of metabolism and energy balance, growth and development, and development of the nervous system ⁴². Therefore, access to this micronutrient is critical for mammalian health. However, iodide is scarce in the environment and the majority of earth's supply is found in the ocean ⁴³. Nature has found a way to maintain iodide in the body through the action of another reductive dehalogenase, iodothyrosine deiodinase (IYD).

1.2 IYD is a Flavoenzyme that Catalyzes Reductive Dehalogenation

1.2.1 Iodide Salvage

IYD is a mammalian flavoenzyme that catalyzes the reductive deiodination of iodothyrosine, the byproduct of thyroid hormone synthesis. In the body, iodide is

transported by the Na/I symporter to the follicular cells of the thyroid where it is concentrated up to 40-fold over the levels found in the plasma (**Figure 1.3**)⁴⁴. This iodide is then transported across the apical membrane into the colloid where it is oxidatively coupled to tyrosine residues of thyroglobulin by thyroid peroxidase in the presence of H₂O₂ to form mono- and diiodotyrosines (MIT and DIT, respectively). A second oxidative coupling, also catalyzed by thyroid peroxidase, then couples adjacent iodotyrosines to produce thyroglobulin bound iodothyronines, T₃ and T₄. Secretion of the thyroid stimulating hormone is required for endocytosis of the iodinated thyroglobulin into the follicular cell where it is hydrolyzed to release T₄/T₃ into the bloodstream and residual iodotyrosines back into the cell for reutilization⁴⁵.

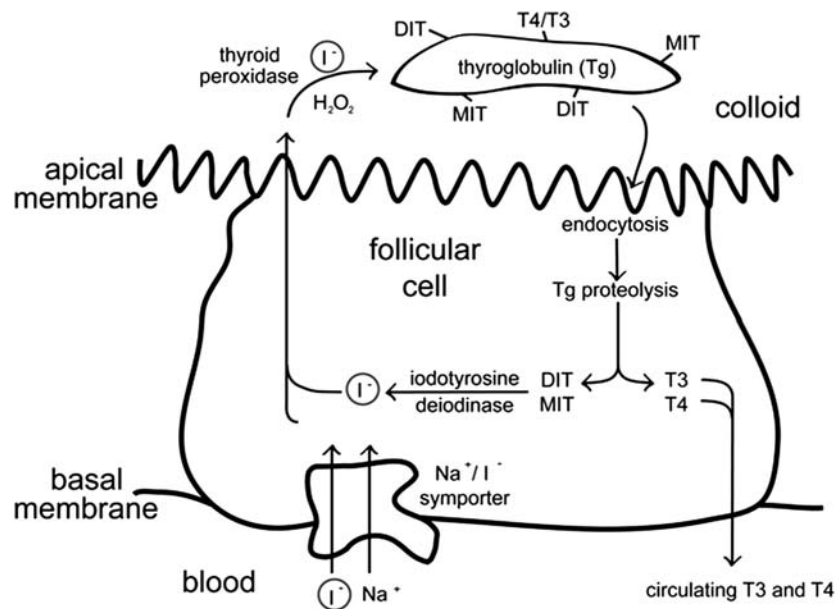
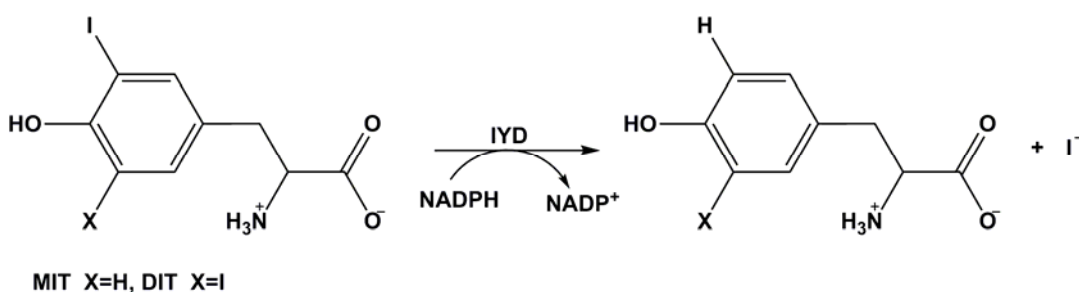


Figure 1.3 The biosynthesis of the thyroid hormones, T₄ and T₃, in the thyroid follicular cells. Figure modified from⁴⁶.

Iodination of thyroglobulin typically produces approximately 7 MIT and 6 DIT per molecule of T_4/T_3 ⁴⁷. Excretion of these byproducts as waste from the body would increase the physiological demand for iodide. While MIT and DIT are direct precursors to the thyroid hormones, these compounds cannot be directly reused for biosynthesis of T_4 and T_3 , as thyroglobulin requires free iodide. Instead these byproducts must be metabolized by IYD to release free iodide that can then be recycled for production of more T_4 and T_3 (**Scheme 1.4**).



Scheme 1.4 Dehalogenation of mono- and diiodotyrosine catalyzed by IYD.

Salvage of iodide by IYD is crucial for proper thyroid function as deficiencies in iodide homeostasis result in a number of health disorders, including hypothyroidism and goiter as the classic examples. The most detrimental of these consequences occur during fetal and adolescent brain development⁴⁸. The IQ of children with iodide deficiency is on average 15 points lower than those with adequate iodide nutrition⁴⁸. The World Health Organization has listed iodine deficiency as the most preventable cause of mental impairment worldwide⁴⁹. Although the introduction of iodide via iodized salt has significantly helped to decrease iodide deficiency, it remains a global problem. Insufficient dietary iodine is estimated to affect approximately 2 billion people worldwide⁴⁸.

1.2.2 Characterization of IYD as a nitro-FMN reductase

The first reports of a thyroidal deiodinase specific for MIT and DIT were made by Roche et al in the early 1950s^{50,51}. Reports of similar deiodinase activity in various tissue homogenate samples including those from thyroid, liver and kidney soon followed⁵². Once Rosenberg was able to partially purify the IYD from bovine thyroid, it was found to be a FMN dependent enzyme^{53,54}. The gene encoding for IYD, DEHAL1, was identified a few decades later⁵⁵⁻⁵⁷. Discovery of DEHAL1 confirmed clinical hypotheses from the 1950s that mutations of IYD were responsible for certain forms of congenital hypothyroidism and goiter⁵⁸⁻⁶⁰. Shortly thereafter, IYD was assigned as a member of the nitro-FMN reductase structural superfamily on the basis of peptide sequence homology⁶¹. This assignment made IYD the first mammalian member of this superfamily that had previously been identified only in bacteria.

1.2.3 Comparison of IYD within nitro-FMN reductase Superfamily

Structural Comparison

Classification of IYD as a nitro-FMN reductase generated interest in the enzyme's molecular structure in order to understand the mechanism of its reductive dehalogenation. Advances in protein expression and purification have led to the large scale production of IYD in Sf9 insect cells and *E. coli*⁶². As a direct result, crystal structures for both the mouse and human IYD (mIYD and hIYD, respectively) have been solved^{63,64} revealing important structural details about the relationship between protein, cofactor and substrate that have been helpful in directing mechanistic studies. Structural, IYD is homodimer comprised of an α - β fold pattern with the enzyme

active site sitting at the dimer interface⁶³. The active site is comprised of residues from both subunits and forms a lid upon substrate binding (**Figure 1.4**)⁶³. These features are shared by all members of the nitro-FMN reductase superfamily.

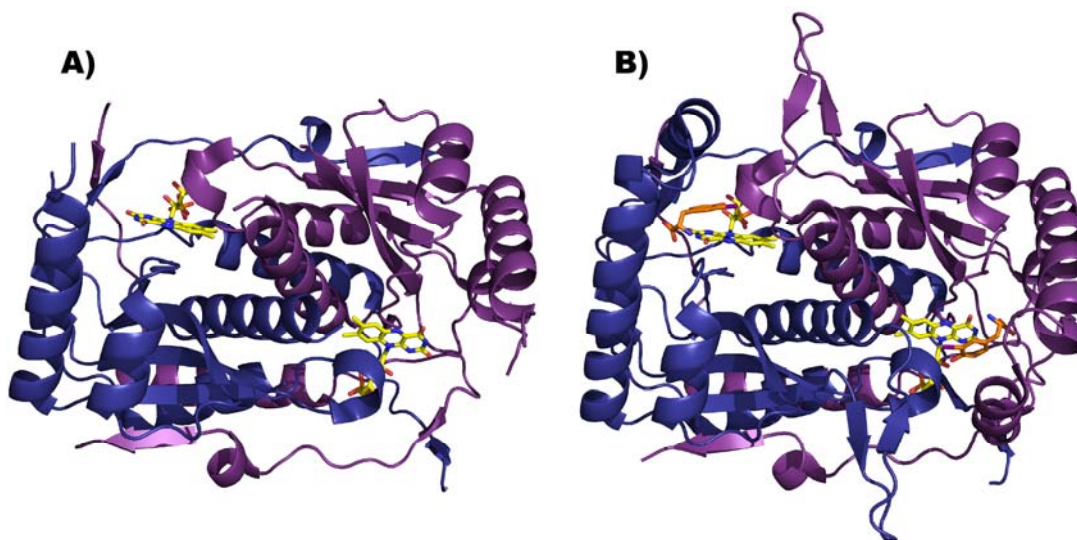


Figure 1.4 Crystal structure of hIYD (left) and its co-crystal with MIT. hIYD is shown in dark blue and purple. PDB ID: 4TTB, 4TTC⁶⁴.

IYD and BluB form a Distinct Subgroup

Several factors differentiate IYD and one other member, BluB, from the majority of the nitro-FMN reductase enzymes including active site lid formation and FMN protein interaction⁶³. Nitro-FMN reductase enzymes are divided into two subgroups based on the protein region used to form the active site lid. These two groups are represented by NADH oxidase (*Thermus thermophilus*), which forms its lid using a central α -helix region, and flavin reductase P (*Vibrio harveyi*), which uses a C-terminal extension (**Figure 1.5A**). Both IYD and BluB, however, utilize the same distinct α -helix region near the N-terminal to form their active site lid (**Figure 1.5A**), differentiating these enzymes from the two previously mentioned groups and creating a new subgroup within the superfamily. In addition, active site cofactor-protein

interactions for IYD and BluB, especially around the FMN pyrimidine ring, are minimal compared to the rest of the superfamily (**Figure 1.4B**). BluB cannibalizes its FMN cofactor for the biosynthesis of the lower ligand of vitamin B₁₂⁶⁵. Although the mechanism of this transformation is still unknown, the lack of flavin-protein interactions may aid in the degradation of the cofactor.

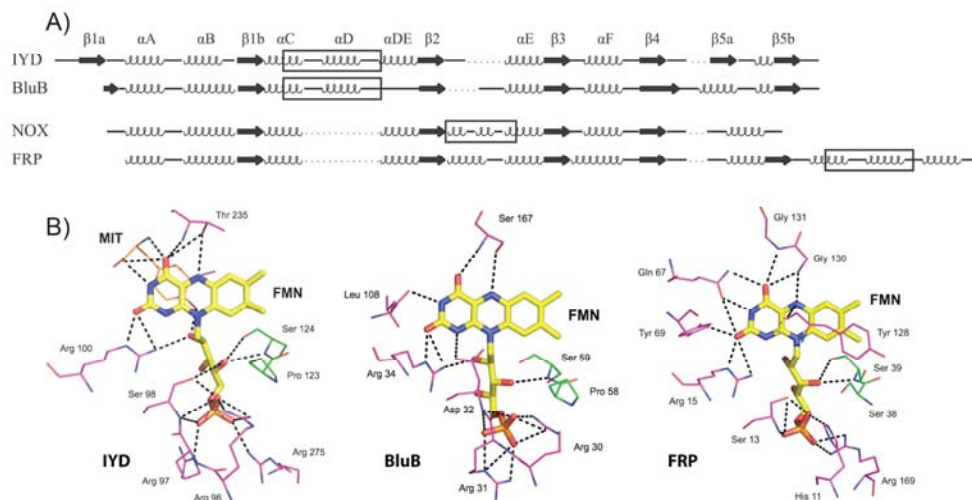


Figure 1.5 Comparison of IYD to nitro-FMN reductase superfamily.

A) Alignment of the secondary structure for representative members of the nitro-FMN reductase superfamily, highlighted in the box is the region used to form the active site lid. B) Comparison of the active site interaction of IYD, BluB, and FRP. Figure modified from⁶³.

For IYD, active site interactions for flavin and protein are largely dependent on the presence of substrate. Upon substrate binding, hydrogen bonding between the zwitterionic amino acid MIT and three active site residues (Glu157, Tyr161, and Lys182 in mIYD) as well as the C3 carbonyl and N3 of the isoalloxazine ring (**Figure 1.6**) form a bridge between FMN and the active site lid. The phenolic ring of MIT is observed to π – stack over the isoalloxazine ring of FMN. Another hydrogen bond is formed between phenolic hydroxyl group of MIT and the 2'-OH of the FMN ribityl chain. These interactions may guide substrate recognition, as well as orient the phenol

ring of MIT over FMN for proper stacking and positioning of the C-I bond of MIT over the C4a position of FMN. Equivalent to the need for the FAD 2'-OH of acyl CoA dehydrogenase to promote catalysis, the FMN 2'-OH of IYD may also be necessary for its catalysis as well. Additionally, hydrogen bond donors Arg104 and Thr239 in hIYD positioned near the N1 and N5 of FMN were also observed. Hydrogen bonding to these positions has been known to play a role in stabilization of the Fl_{sq} ⁸. These interactions between protein, substrate and FMN have proven to be very helpful in directing mechanistic studies of IYD.

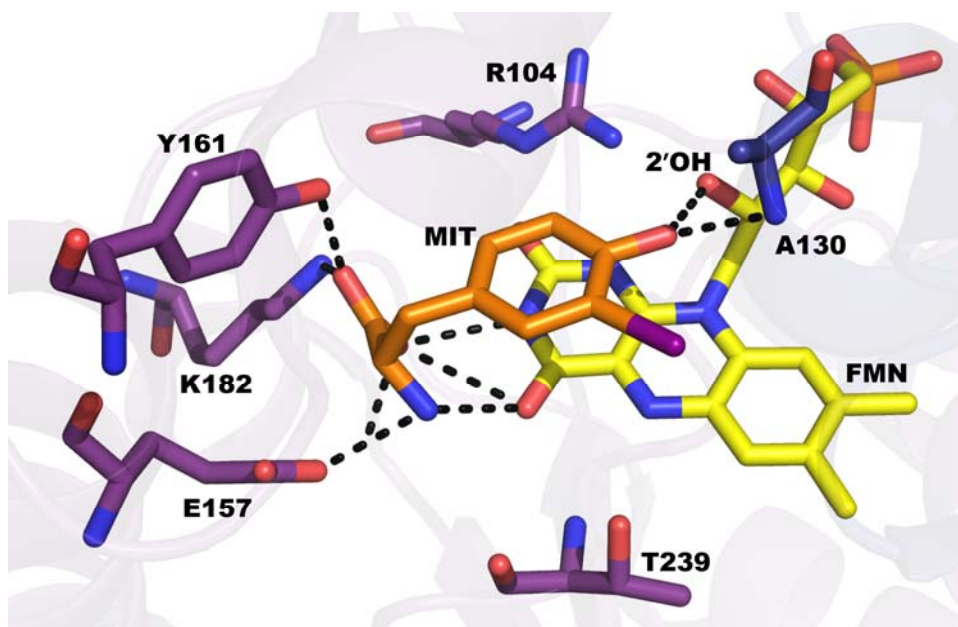


Figure 1.6 Crystal structure of the active site of hIYD, highlighting the interaction between MIT, the protein and FMN. PDB ID: 4TTC⁶⁴.

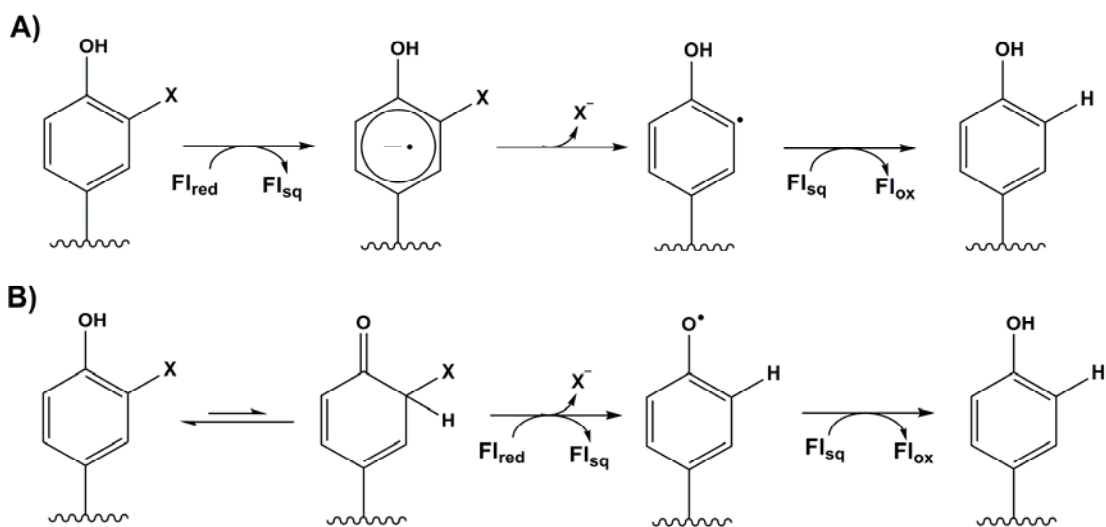
1.3 Proposed Mechanism for IYD

While it is widely accepted that IYD deiodinates MIT and DIT via a reductive process⁶⁶, the mechanism of this deiodination is still not well understood. *In vivo* NADPH acts as the physiological reductant for IYD. However *in vitro* this activity is

lost and dithionite is required for enzymatic reduction^{53, 54}. Precedence for aerobic reductive dehalogenation is limited to TD and ID. The mechanism for these, both depend on the use of an active site residue (cysteine or selenocysteine) during dehalogenation^{39, 40}. A mechanism was initially hypothesized for IYD but quickly abandoned after site directed mutagenesis of C217A and C293A in mIYD proved that cysteine was not required for deiodination activity⁶⁷. This observation was later supported by the crystal structures of IYD that show the cysteine residues reside in regions away from the active site⁶³. The crystal structures of IYD also show no other nucleophilic amino acid residues within the active site^{63, 64}.

As a flavoprotein, IYD is capable of reducing iodotyrosine via either a one or two electron transfer process. Within the active site, π – stacking of iodotyrosine over the N10 axis of FMN, aligns the C-I bond 3.65Å above the C4a-N5 position of the isoalloxazine ring, a sufficient distance for direct electron transfer from FMN to substrate⁶³. The C4a-N5 region of flavin is a key site radical formation as well as the site dioxygen activation in other flavoenzymes^{2, 3}. EPR and UV-Vis measurements during the redox titration of IYD in the presence of substrate indicate formation of the neutral Fl_{sq} as monitored by an increasing absorbance at ~560 nm^{64, 68}. This data strongly suggest that IYD catalyzes reductive dehalogenation via a one electron transfer process. Two mechanisms have been proposed for this one electron reduction dehalogenation (**Scheme 1.5**)⁴⁶. The first mechanism proceeds via radical aromatic substitution ($S_{RN}1$) (**Scheme 1.5A**). Transfer of a single electron from Fl_{red} into the phenyl ring of MIT would generate an aromatic anion radical intermediate. Collapse of this intermediate would result in formation of aryl radical and a free

iodide. Transfer of a second electron from Fl_{sq} and a proton would then yield tyrosine and Fl_{ox} . The second proposed mechanism involves an initial tautomerization of substrate to a non-aromatic ketone (**Scheme 1.5B**). Transfer of a single electron from Fl_{red} would then result in release of iodide, forming a tyrosyl radical. Addition of a second electron followed by proton transfer would complete the catalytic cycle to give tyrosine and Fl_{ox} .



Scheme 1.5 Proposed one electron transfer mechanisms for the reductive dehalogenation catalyzed by IYD.

The role of the substrate protein hydrogen bonds have been explored using site directed mutagenesis studies with mIYD. Mutation of the amino acid residues that make polar contact to the zwitterion of MIT have resulted in either a decrease (Y157F) or total loss (E153Q) of enzymatic activity⁶². Removal of the lysine hydrogen bond appeared to destabilization of protein structure as expression of a K178Q mutant gave ⁶², highlighting the importance of these interactions. These results have led to questions about the significance of the substrate hydrogen bond to the FMN ribityl 2'-OH for enzymatic activity.

1.4 Specific Aims

This dissertation will address:

- 1) Modified flavin analogs are often used to explore the role of cofactor interactions for enzymatic catalysis. 2-deoxyFAD has been used as a mechanistic probe to identify the importance of hydrogen bonding to this position in flavoenzymes such as MCAD, where the ribityl 2'-OH has been shown to be necessary for substrate activation. The synthesis of 2-deoxyFMN was carried out to investigate the dependence of the 2'-OH for reductive deiodination of IYD.
- 2) Though most flavins are bound to the apoprotein through non-covalent interactions, the process necessary for cofactor removal can often be detrimental to the recovery of enzymatic activity. Characterization of hIYD reconstituted with both FMN and 2-deoxyFMN was performed to determine the effects of reconstitution on IYD activity. The FMN reconstitution was used as a positive control to verify whether changes in the enzymatic activity of IYD were due to the reinsertion of the cofactor or disruption of the FMN-substrate hydrogen bond.
- 3) The hydrogen bond between the FMN ribityl 2'-OH and phenolic OH of MIT has been hypothesized to facilitate the tautomerization of MIT for deiodination by IYD. Additionally, it is believed that this bond may be necessary for substrate recognition. The role of this interaction was examined using an O-methyl MIT analog, which is unable to tautomerize to the proposed substrate keto-intermediate.

Chapter 2: Preparation of a 2-DeoxyFMN Analog

2.1 Introduction

The extensive range of reactions catalyzed by flavoenzymes can be attributed to the chemical versatility of the flavin cofactor its capacity to catalyze both one and two electron transfer processes. The ability of specific flavoenzymes to promote these processes is controlled by the chemical environment surrounding the cofactor. To distinguish which feature controls enzymatic activity, the cofactor environment can be perturbed by either site directed mutagenesis of the protein or by chemical modification of either the substrate or cofactor.

An extensive collection of flavin analogues have been created via organic synthesis^{24, 69}. These analogs have long been used to probes of features of flavoenzymes catalysis such as active site polarity, reaction stereochemistry and flavin electron transfer processes^{7, 24 70}. Analogs such as the 1-deaza and 5-deazaflavins (**Figure 2.1**) have been used to differentiate between a 1 or 2 electron transfer process flavoenzymes such as isopentyl diphosphate isomerase^{17, 71}. 1-Deazariboflavin retains the ability to undergo both types of electron transfer processes, as the central pyrazine ring remains intact. However, replacement of the N1 with carbon of the isoalloxazine ring decreases the redox potential of this analog from -208 mV to -280 mV¹⁸. Substitution of the N5 with a carbon converts the central pyrazine ring into a pyridine ring, rendering this analog incapable of stabilizing radical formation at the C4a position, allowing only transfer of electron pairs¹⁸.

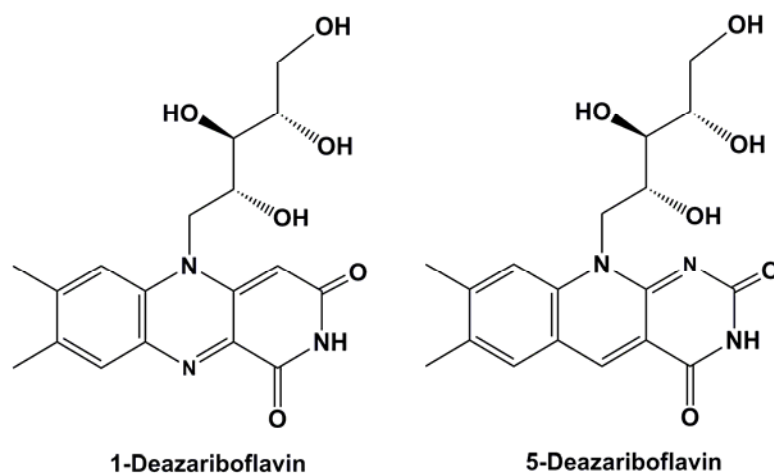
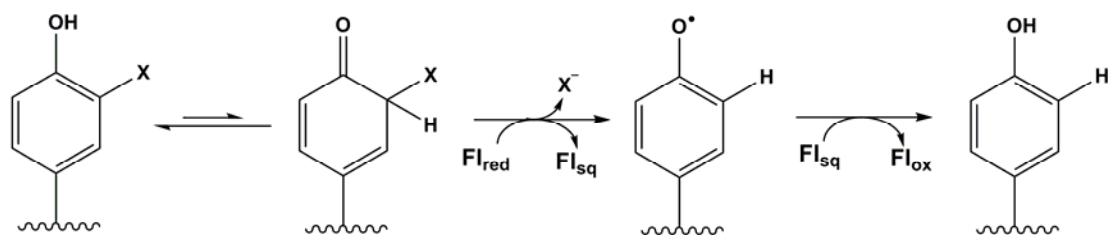


Figure 2.1 Structure of 1-deaza and 5-deazariboflavin.

The role of the flavin N10 ribityl side chain hydroxyls has been studied through the use of deoxyflavins, such as 2-deoxyflavin, in a number of flavoenzymes such as monoamine oxidases A and B ⁷², electron-transfer flavoprotein ¹³ and medium chain acyl-CoA dehydrogenase (MCAD) ²⁸. The deoxyflavins lack the ribityl OH group and provide a convenient method for identifying the significance of hydrogen bonds to this portion of flavin. In particular, mechanistic studies of MCAD with 2-deoxyFAD strongly suggest that an observed hydrogen bond between the 2'-OH of FAD to the thioester carbonyl of CoA is important for substrate orientation and activation during dehydrogenation ²⁸. An analogous role has been proposed for IYD. Co-crystal of mIYD and MIT show a hydrogen bond between the 2'-OH of the FMN ribityl chain and phenolic OH of iodotyrosine ⁶³. Active site interactions between FMN and the protein are minimal when compared to those between the cofactor and MIT. Therefore all cofactor-substrate interactions, including the hydrogen bond to the ribityl 2'-OH, are thought to be critical for enzymatic activity.



Scheme 2.1 Proposed 1e⁻ mechanism for the reductive dehalogenation of MIT by IYD.

The currently proposed mechanism for the reductive dehalogenation of MIT catalyzed by IYD, involves the formation and stabilization of a non-aromatic keto tautomer before direct electron transfer from FMN to the substrate and expulsion of iodide (**Scheme 2.1**)⁴⁶. The 2'-OH of the FMN has been suggested to act as a general acid/base, promoting tautomerization of MIT to an electron deficient species. To test this hypothesis, mechanistic studies of IYD reconstituted with 2-deoxyFMN were pursued. The goal of this chapter was to reproduce the chemical synthesis of 2-deoxyriboflavin as described by Massey²³ and enzymatically phosphorylate this analog (**Figure 2.2**) for use as mechanistic probe.

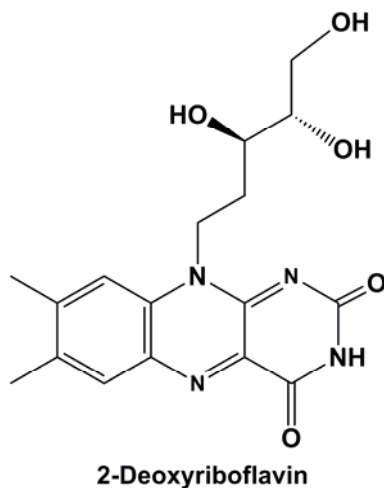


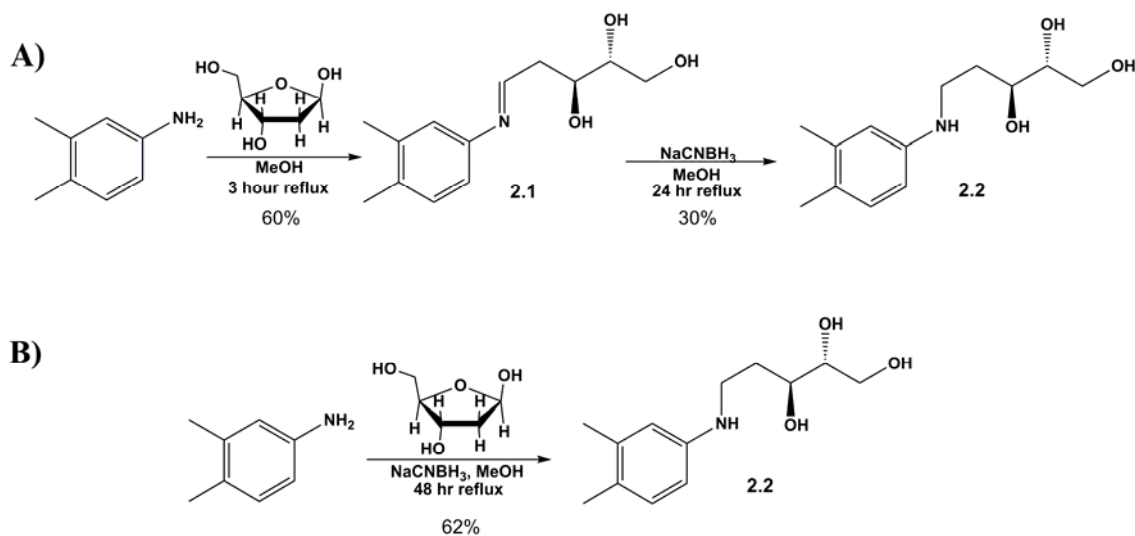
Figure 2.2 Structure of 2-deoxyriboflavin.

2.2 Results and Discussion

2.2.1 Synthesis of 2-Deoxyriboflavin

Ribitylation of 3,4-Dimethylaniline

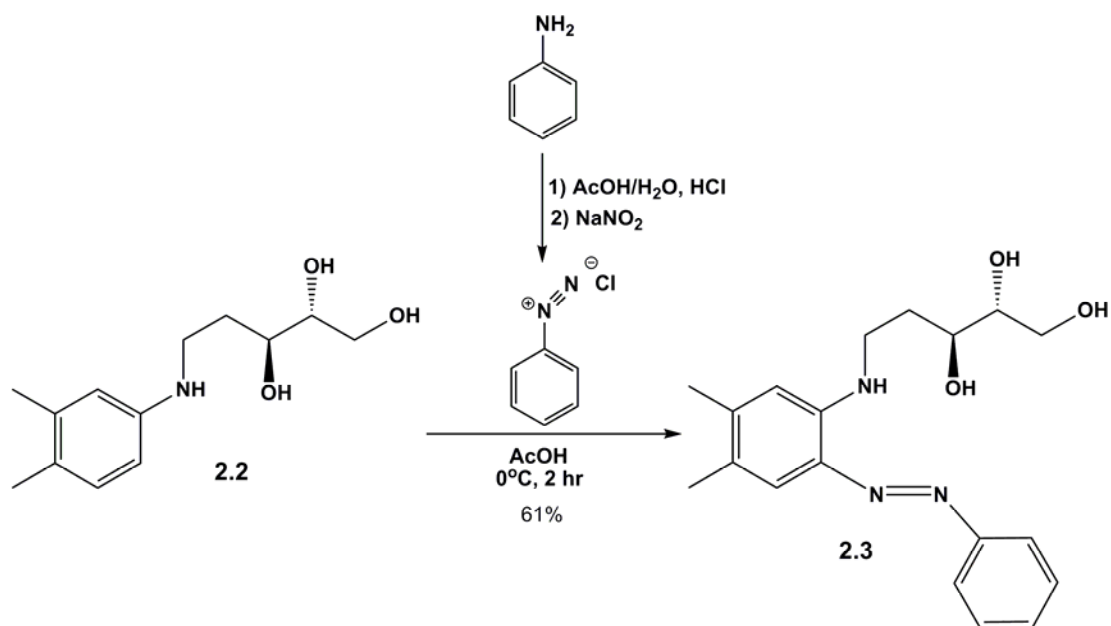
Preparation of 2-deoxyriboflavin started with ribitylation of the commercially available 3,4-dimethylaniline with 2-deoxyriboflavin (**Scheme 2.2**). The synthetic route described by Massey utilized the Tishler-condensation method for flavin synthesis⁷³. Isolation and crystallization of the Schiff base **2.1** formed from the condensation of 2-deoxyribose and the dimethylaniline produced the expected imine in 59% yield. However, subsequent reduction in the presence sodium borohydride gave only 30% of the desired ribitylated aniline **2.2**. The starting material could not be recovered. Another published method made use of a one pot reductive amination of the dimethylaniline and D-ribose in the presence of sodium cyanoborohydride to form a similar ribitylated aniline⁷⁴. Following this method the yield of **2.2** was approximately doubled to 62%. Increase in yields which resulted from changing procedures can be attributed to the milder reductant and the immediate reduction of the imine upon formation in the one-pot reaction, driving the reaction equilibrium to the right. ¹H NMR spectra showed chemical shifts corresponding to the aromatic ring (δ 6.86 (1H); 6.50 (1H); 6.43 (1H) ppm) and ribityl chain (δ 3.73 - 3.12 (6); 1.99 (1H) and 1.74 (1H) ppm) of the ribitylated product (**Appendix A.1**). ESI-MS confirmed formation of **2.2** showing a mass at 240.1 m/z (**Appendix A.2**). These data were in line with the computational estimates (ChemDraw Ultra 7.0) for **2.2**.



Scheme 2.2 Initial **A)** and modified **B)** synthetic schemes for the formation of 2-deoxyribityl- 3,4- dimethylaniline (**2.2**).

Diazotization of 2-Deoxyribitylated-3,4-Dimethylaniline

Diazotization of **2.2** with freshly prepared benzene diazonium chloride resulted in formation of a dark red oil (**Scheme 2.3**)²³. ¹H NMR analysis of this product showed a very complex aromatic region (**Appendix A.3**). Signals at δ 7.88 (d), 7.86 (d), 7.52 (t), 6.67 (d) ppm correspond to the expected signals of the diaza substituted aromatic ring of **2.3**. Some additional signals at δ 7.06 (t) and 6.55 (t) ppm may correspond to aniline, suggesting either a mixture of starting materials and product or decomposition. ESI –MS spectra showed the mass of the diazotization product **2.3** at 344.2645 m/z (theoretical m/z = 344.1929), and masses corresponding to aniline and its two derivatives used in the reaction (aniline at 94.0 m/z; 3,4-dimethylaniline at 122.1 m/z and 2-deoxyribitylated-3,4-dimethylaniline at 240.1 m/z). Carrying crude **2.3** onto the final condensation step without further purification gave no product. Therefore, a method of purification for **2.3** had to be devised.



Scheme 2.3 Diazotization of 2-deoxyribose-3,4-dimethylamine (**2.2**).

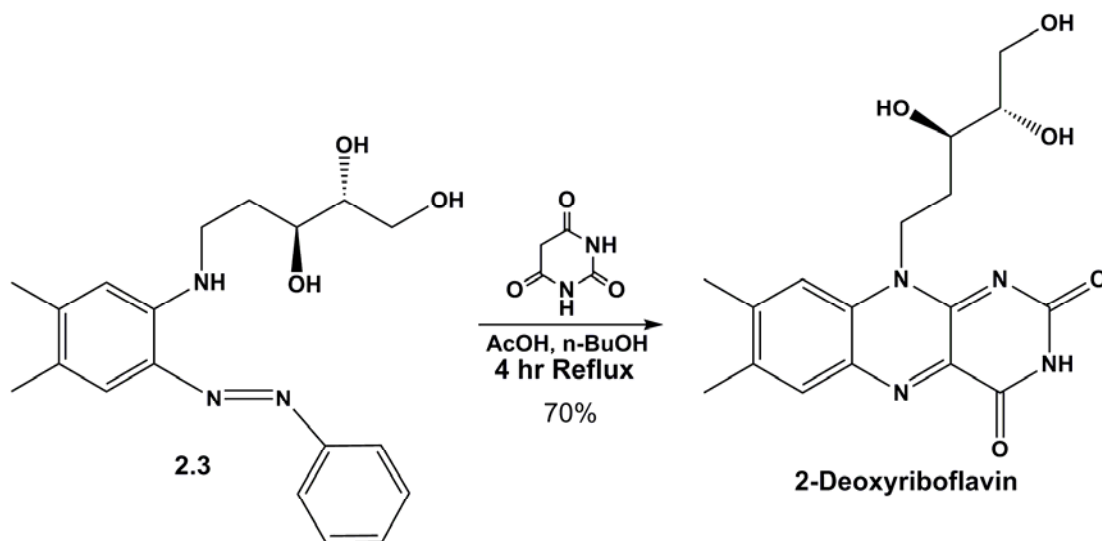
TLC monitoring of the diazotization reaction in ethyl acetate showed 4 spots with relatively good separation. The crude product was purified on silica using ethyl acetate, followed by elution with chloroform and methanol gave 7 fractions. ¹H NMR analysis of these fractions showed them to contain four different mixtures, confirming separation of the crude reaction mixture. The ¹H NMR spectrum of one fraction in particular (Fraction 4) showed signals corresponding to the aromatic ring (δ 7.88 - 6.77 ppm) and ribityl chain (δ 4.80 - 3.50 ppm) (**Appendix A.4**) of the expected diazotization product **2.3** as estimated by a ¹H NMR prediction (ChemDraw Ultra 7.0). MS-ESI of this fraction (**Appendix A.5**) was also comparable to computational estimates (ChemDraw Ultra 7.0) for **2.3**.

Formation of 2-Deoxyriboflavin

The final step towards the synthesis of 2-deoxyriboflavin (**Scheme 2.4**) was the acid-catalyzed condensation of barbituric acid to the diazo-aniline **2.3** to yield the target compound **2.4**. Once purified, **2.3** must be used within 24 hours to avoid

degradation back to starting materials (aniline and 2-deoxyribitylated-3,4-dimethylaniline). **2.3** and barbituric acid were suspended in *n*-butanol and heated to reflux in the presence of glacial acetic acid. This conversion was monitored using a dual TLC solvent system to enable observation of both starting material consumption and product formation. Since the diazo starting material **2.3** was soluble in ethyl acetate and the expected product, due to its higher polarity, was more soluble in a mixture of 30% methanol in chloroform, the reaction was monitored via TLC using either of these solvents as the eluent. In addition, the product displays a yellow fluorescence under UV light, whereas the starting material does not. After 4 hours, TLC of the reaction mixture using ethyl acetate as the eluent showed a decrease in starting material and a yellow fluorescent spot at the baseline. TLC using 30% methanol in chloroform as the eluent showed a yellow fluorescent spot mid-way up the plate, indicative of product formation according to the literature²³. The reaction was continued overnight to ensure full consumption of starting material. A TLC taken the next day showed no difference to that taken at 4 hours and it was assumed that the reaction had reach completion after 4 hours. The reaction was then stopped, cooled to room temperature and *n*-butanol was removed to give a reddish orange solid. The crude solid was purified on HPLC initially using an isocratic system of 85% 10 mM ammonium formate buffer and 15% methanol. Two peaks were observed with the expected UV signal around 445 nm and 370 nm for 2-deoxyriboflavin (t_r =16 and 19 minutes respectively). However due to the strong tailing observed (**Figure 2.3**), the method was optimizes for better separation to a linear gradient of 27% - 30% methanol over 45 minutes. While this condition resulted

in an improved separation of 2-deoxyriboflavin from the crude material (**Figure 2.3**), this procedure prove to be irreproducible as a buildup of air bubbles was created in the organic pumps from methanol overtime. To overcome this issue, the organic solvent was changed to acetonitrile and the HPLC method was again modified, this time to a linear gradient of 0.1% trifluoroacetic acid in water to 50% acetonitrile over 30 minutes described by Kiessling ⁷⁴. These conditions were reproducible and gave the best separation of the final product from the crude mixture (**Figure 2.4**). ¹H NMR analysis (**Appendix A.6**) of the material collected at 15 minutes showed chemical shifts for the aromatic ring (δ 7.98 and δ 7.90 ppm) and ribose chain (δ 3.76 - δ 3.47 ppm), consisted with the predicted spectrum(ChemDraw Ultra7.0) and were comparable to ¹H NMR of 2-deoxyriboflavin taken in DMSO ⁷⁵. ESI-MS observed $[M^+]$ for the synthesis 2-deoxyriboflavin (**Appendix A.7**) agreed with the literature value of 361.1 m/z ²³.



Scheme 2.4 Formation of 2-Deoxyriboflavin.

Efforts made to scale up the production of 2-deoxyriboflavin for phosphorylation, revealed the limitations of using preparative HPLC for purification. Low solubility of the crude product mixture in 0.1% TFA in water resulted in product loss during sample filtration as well as increased pressure during HPLC runs. These issues inspired the use of a Waters Sep-Pak® Plus C18 cartridge for large scale purification. The Sep-Pak proved to be a suitable alternative to preparative HPLC (**Figure 2.5**). Since the crude reaction mixture did not have to be filtered before purification, product that had previously been discarded due to low solubility in the aqueous buffer could now be purified as this material became more soluble when washed with increasing amounts of acetonitrile.

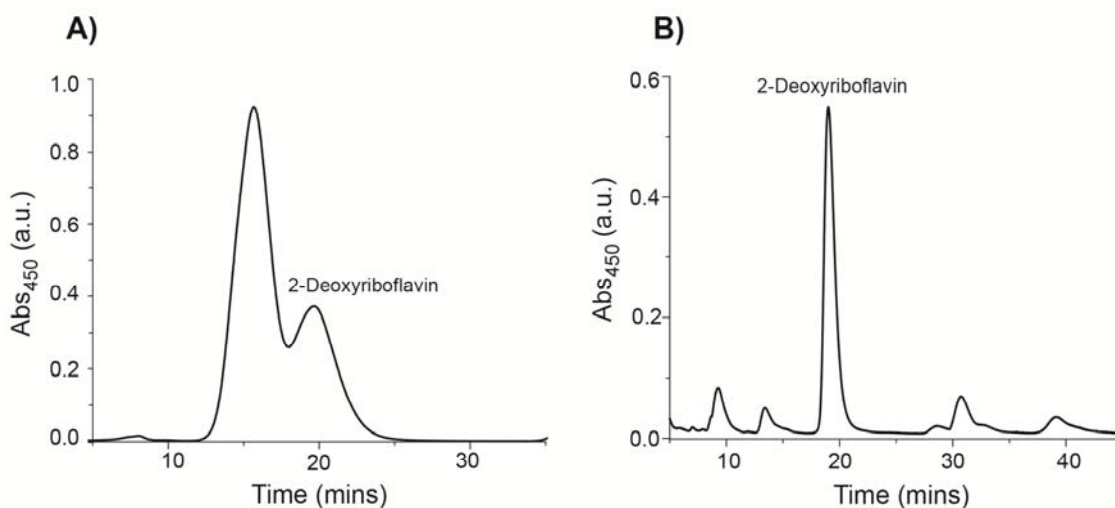


Figure 2.3 HPLC chromatographs of the 2-deoxyriboflavin purification using A) an isocratic system of 15% methanol in 10 mM ammonium formate pH 6.02 and B) a linear gradient system of 27% methanol in 10 mM ammonium formate pH 6.02 going to 30% methanol over 45 min. Retention time approximately 19 min.

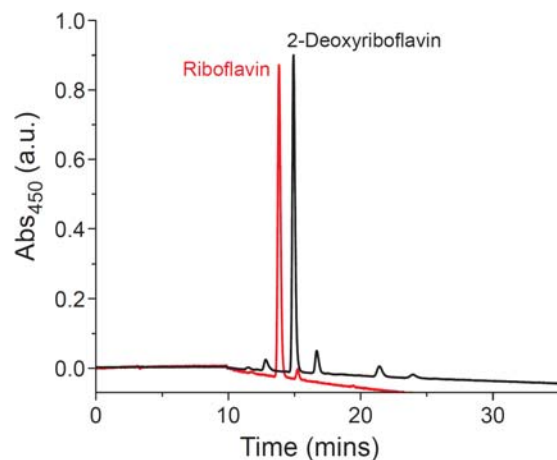


Figure 2.4 HPLC chromatogram of 2-Deoxyriboflavin purification using riboflavin as a standard. Product purification was monitored at 450 nm using a 30 min linear gradient from 100% 0.1% trifluoroacetic acid in water to 50% acetonitrile.

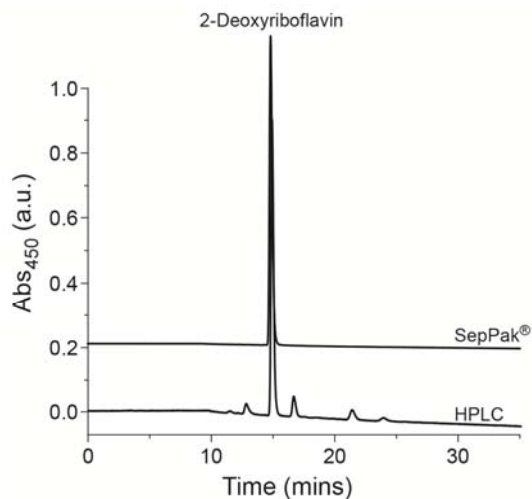


Figure 2.5 Comparison of 2-deoxyriboflavin final purification using HPLC and Waters Sep-Pak®. Product purification was monitored at 450 nm using a 30 min linear gradient from 100% 0.1% trifluoroacetic acid in water to 50% acetonitrile.

2.2.2 Enzymatic Phosphorylation of 2-Deoxyriboflavin using Riboflavin Kinase

Phosphorylation of riboflavin following both chemical and enzymatic methods has been described in the literature⁷⁰. There are two traditional methods for the enzymatic formation of FMN from riboflavin. The first utilizes flavokinase (ATP:riboflavin-5'-phosphotransferase, EC 2.7.1.26) to directly transfer a phosphoryl group from ATP to the 5' hydroxyl group of riboflavin. The second requires the phosphodiester cleavage of FAD formed from the flavokinase-FAD synthetase complex historically isolated from *Brevibacterium ammoniagenes*¹⁸. Conversion of FAD to FMN is then achieved by phosphodiester cleavage using Naja Naja snake venom¹⁸. The second method is most commonly used, due to the lower substrate fidelity of FAD synthetase from *B. ammoniagenes* compared to flavokinase¹⁸. Since the co-factor of IYD is FMN, with hopes of avoiding the additional cleavage step, we decided to follow the former method using flavokinase. The human riboflavin kinase (RFK) plasmid was provided by Dr. Zhang from UT-Southwestern, whose lab solved the crystal structure in 2003⁷⁶. RFK was expressed and purified as described via a Ni²⁺ affinity column⁷⁷. Protein purity was determined by SDS-Page (**Figure 2.6**)

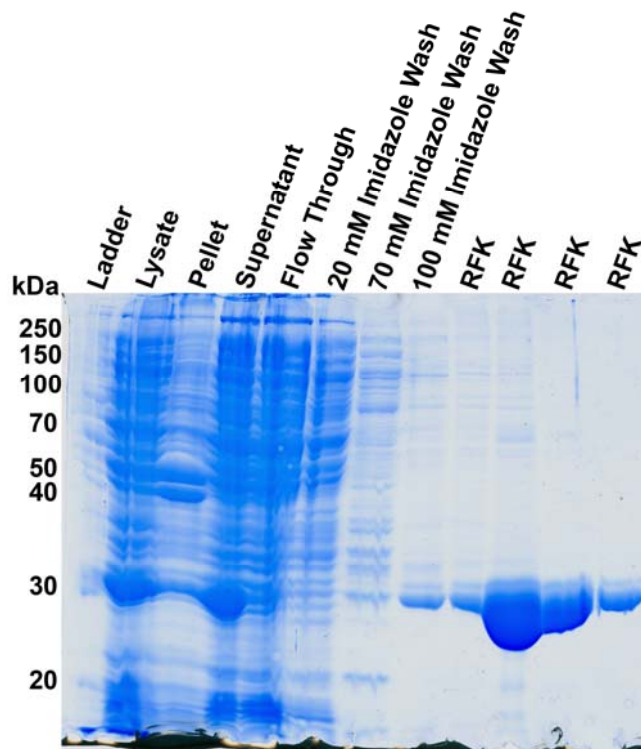


Figure 2.6 Denaturing SDS-page gel of hsRFK Ni²⁺ affinity purification.

Although the Zhang papers provided detailed protocols for the expression and purification of RFK^{76,77}, no procedures were listed for the conversion of riboflavin to FMN. Again many protocols for this phosphorylation reaction are present in the literature however, the method describe by Mack⁷⁸ was chosen due to its simplicity. The reported HPLC analysis conditions used 100 mM ammonium formate (pH 3.7) and methanol. However, due to the introduction of air bubbles into HPLC pump as discovered during the initial use of methanol for purification of 2-deoxyriboflavin, the organic solvent was changed to acetonitrile. Using the modified conditions of a 25 minute linear gradient from 0% to 55% acetonitrile over 25 with 100 mM ammonium formate (pH 3.7) as the aqueous buffer, HPLC chromatographs of the assay (**Figure 2.7**) showed that after 24 hours approximately 60% of the riboflavin ($t_r = 15$ min) was converted to FMN ($t_r = 10$ mins).

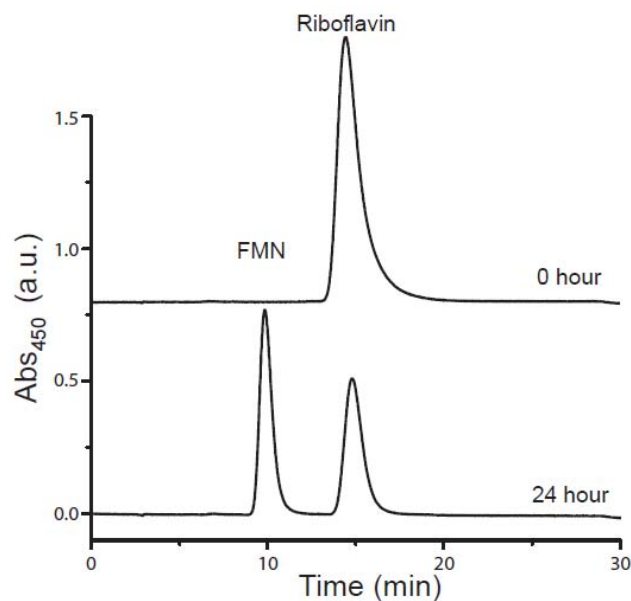


Figure 2.7 HPLC chromatograph of riboflavin kinase (RFK) phosphorylation of riboflavin to FMN. Product formation was monitored at 450 nm using a 25 min linear gradient from 0% to 55% acetonitrile with 100 mM ammonium formate (pH 3.7) as the aqueous buffer.

While these conditions worked well for the separation of riboflavin from FMN, the previously described HPLC protocol optimized for the purification of 2-deoxyriboflavin was ultimately used to monitor 2-deoxyFMN formation. Additionally, the final phosphorylation conditions were modified to remove the reported 10 mM sodium sulfite⁷⁸. During earlier attempts made to form the 1-deazaFMN analog with this protocol, the presence of sodium sulfite had been observed to prevent phosphorylation. Optimization of the reaction conditions ultimately showed sodium sulfite to be unnecessary for the conversion of riboflavin to FMN. Due to the comparable UV-Vis absorption of the 2-deoxy analog and riboflavin, the phosphorylation reaction was monitored at 450 nm. After a 24 hour incubation at 37°C, an approximate 10% conversion of 2-deoxyriboflavin to 2-deoxyFMN was observed (**Figure 2.8**). Allowing the reaction to go an additional 36

hours resulted in full conversion to the desired FMN derivative. Again, a Sep-Pak was used for final purification of 2-deoxyFMN during reaction scale up. ^1H NMR and UPLC-MS data collected for the final product confirmed its formation based on computation estimates (ChemDraw Ultra 7.0) for 2-deoxyFMN (**Appendix A.8** and **A.9**).

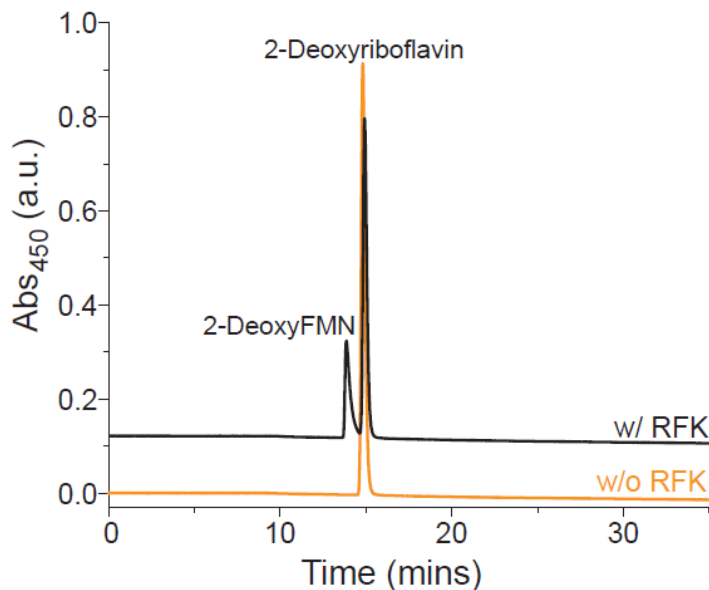


Figure 2.8 HPLC chromatograph of RFK catalyzed phosphorylation of 2-deoxyriboflavin to 2-deoxyFMN. Product formation was monitored at 450 nm using a 30 min linear gradient from 0% to 50% acetonitrile.

2.3 Summary

2-Deoxyriboflavin was synthesized following a modified protocol utilizing a one pot reductive amination to yield 2-deoxyribitylated dimethylaniline. Reaction of the deoxyribitylated aniline with benzene diazonium chloride afforded the 2-deoxyriboflavin precursor. Condensation of the diazo-aniline with barbituric acid in *n*-butanol, gave the final product in modest yield. Using RFK, 2-deoxyFMN was prepared directly from 2-deoxyriboflavin. This method proved to be a suitable

phosphorylation method and eliminated the need of phosphodiester cleavage as would be necessary with the more traditional enzymatic route of FAD synthetase.

2.4 Experimental Procedures

Materials and Methods

All moisture and oxygen sensitive reaction were carried out in flame dried glassware under nitrogen atmosphere. All other reagents were obtained at the highest grade available and used without further purification. Water was purified to a resistivity of 18.2 M Ω -cm. Plasmids containing pPROEX-Hta-RFK His₆ were provided by Dr. Hong Zhang (UT Southwestern) and transformed into *Escherichia coli* Top10 by Dr. Patrick McTamney. All protein purifications were carried out on an AKTA Prime FPLC (GE Healthcare Bio-sciences Corp.) unless otherwise stated. HisPurTM Ni-NTA resin and HisTrap HP column (1 mL) were purchased from ThermoScientific (Rockford, IL). Amicon Ultra-15 centrifugal filters were purchased from Millipore (Billerica, MA). UV-Vis measurements were made using a Hewlett-Packard 8453 spectrophotometer. ¹H NMR spectra were collected on a Bruker DRX-400 MHz spectrometer or Bruker AV-400 MHz spectrometer. Chemical shifts are reported as δ values relative to residual solvent as an internal standard in parts per million (¹H: CD₃COCD₃ δ 2.05 ppm; D₂O δ 4.81; MeOD δ 4.51 ppm). Coupling constants (*J*) are reported as Hertz (Hz). Column chromatography was performed on Sigma-Aldrich kieselgel 60 Å silica (2-25 μ M) with fluorescent indicator. High performance liquid chromatography (HPLC) was performed on an Econosphere C₁₈ reverse-phase semi-preparative column (250 mm x10.0 mm) using water (A) and

acetonitrile (B) buffered with 0.1% trifluoroacetic acid as the elution solvent.

Compound elution was detected by UV at 280, 360 nm, and 450nm. Mass spectrometry analysis at University of Maryland, College Park was performed on a JEOL AccuToF-CS ESI-MS in ESI⁺ ionization mode. Mass spectrometry analysis at The Johns Hopkins University was performed on either a Thermo Finnigan LCQ Deca ESI-MS in ESI⁺ ionization mode or on a Waters Acquity/Xevo G2 UPLC-MS/MS in ESI⁺ ionization mode.

2.1.1 Synthesis of 2-Deoxyriboflavin^{23, 74}

2-Deoxyribitylated-3,4-dimethylaniline (2.2)

3,4-Dimethylaniline (394 mg, 3.25 mmol), 2-deoxy-D-ribose (485 mg, 3.62 mmol) and sodium cyanoborohydride (385 mg, 6.13 mmol) were dissolved in methanol (50 mL) and heated to 65°C for 48 hours. Solvent was removed via rotary evaporation and the residue was stirred with 1 N HCl (35 mL) (to quench the excess sodium cyanoborohydride) until gas evolution ceased. The solution was then neutralized with a saturated sodium bicarbonate solution and extracted with ethyl acetate (2 x 50 mL). The combined organic layers were washed with brine, dried over anhydrous magnesium sulfate and filtered. The filtrate evaporated to yield the desired product as a light yellow/tan solid (558 mg, 71.7 % yield). ¹H NMR (400 MHz, d₄-MeOD) δ 6.90 (d, *J* = 8.15 Hz, 1H), 6.54 (s, 1H), 6.47 (dd, *J* = 2.45, 8.15 Hz, 1H), 3.70 (dd, *J* = 3.84, 11.4 Hz, 1H), 3.65 (m, 1H), 3.60 (dd, *J* = 6.51, 4.73 Hz, 1H), 3.49 (m, 2H), 3.20 (m, 2H), 2.16 (s, 3H), 2.11 (s, 3H), 1.98(m, 1H) 1.74 (m, 1H). ESI⁺ (m/z) [M+H] for C₁₃H₂₁NO₃ calculated: 240.1555, found: 240.1464. Values agree with computational estimates (ChemDraw Ultra 7.0).

Benzene Diazonium Chloride

Aniline (189 mg, 2.03 mmol) was dissolved in acetic acid (2 mL) and diluted with water (2 mL). This solution was cooled on ice and concentrated HCl (1 mL) was then added drop wise. Solid sodium nitrite (171 mg, 2.48 mmol) was then added to this solution slowly while maintaining a temperature below 5°C. This mixture was stirred at 0°C for 10 minutes for the completion its formation. The product was used without further purification.

Diazo-2-Deoxyribitylated-3,4-Dimethylaniline (2.3)

The ribitylated aniline **2.2** (538 mg, 2.25 mmol) obtained from the previous reaction (used without further purification) was suspended in a minimum amount of acetic acid (~2 mL), cooled on ice and stirred at 0°C for 10 minutes. The solution containing benzene diazonium chloride was then added drop wise to this mixture over ~5 minutes and stirred at 0°C for 10 min. A concentrated solution of sodium hydroxide (approx. 400 mg NaOH in 1 mL water) was added with care taken to maintain a pH below 4 (monitored by pH paper) and the mixture was stirred at 0°C for 2 hours. The reaction mixture was extracted with ether (100 mL), followed by two more extractions of the aqueous layer (50 mL of ether x 2). The organic layers were combined, neutralized with a saturated sodium bicarbonate solution, washed with water and dried over anhydrous magnesium sulfate. The solvent was then removed via rotary evaporation to yield the crude azo product as a red oil (468 mg, 60.6% yield). Chromatography purification on silica using ethyl acetate as the eluant resulted in the desired product as a red solid. ¹H NMR (400 MHz, d₆-Acetone) δ 7.87 (d, *J* = 8.19 Hz, 2H), 7.57 (s, 1H), 7.50 (t, *J* = 7.32, 5.2 Hz, 2H), 7.40

(d, $J = 6.75$ Hz, 1H) 6.77 (s, 1H), 4.06 (d, $J = 6.98$ Hz, 1H), 3.85 (m, 1H) 3.75 (m, 1H) 3.67 (m, 1H), 3.56 (m, 1H), 3.52 (m, 2H), 2.32 (s, 3H) 2.26 (s, 3H), 1.85 (m, 2H). ESI+ (m/z) [M+H] for C₁₉H₂₅N₃O₃ calculated: 344.1929, found: 344.2645. Values agree with computational estimates (ChemDraw Ultra 7.0).

2-Deoxyriboflavin

Purified diazotized material **2.3** (468 mg, 1.36 mmol) and barbituric acid (180 mg, 1.40 mmol) were suspended in *n*-butyl alcohol (10 mL). Acetic acid (2.5 mL) was then added and the mixture heated to reflux and allowed to stir overnight. TLC of the reaction mixture at this time using ethyl acetate as the elutant showed a yellow fluorescent spot at the base line. In comparison a TLC of the reaction mixture using 30% methanol in chloroform as the elutant showed the yellow fluorescent spot closer to solvent head. *n*-Butanol was then removed via rotary evaporation to give the crude material as a reddish orange solid (438 mg). This solid was purified by HPLC (100% → 50% A:B; 0.1% Trifluoroacetic acid in water: Acetonitrile, retention time approx. 15 min) to yield a yellow solid (34 mg, 70 % yield). ¹H NMR (400 MHz, d₄-MeOD): δ 7.98 (s, 1H), 7.90 (s, 1H), 3.62-3.55 (m, 6H), 2.60 (s, 3H), 2.48 (s, 3H), 2.28 (m, 1H), 1.98 (m, 1H). Values agree with computational estimates (ChemDraw Ultra 7.0) and were comparable to literature⁷⁵. ESI⁺ (m/z) [M+H] for C₁₇H₂₀N₄O₅ calculated: 361.1467, found: 361.1508. Value agreed with literature²³.

2-DeoxyFMN

200 μM 2-deoxyriboflavin, 10 mM MgCl₂, and 4mM ATP were combined in potassium phosphate buffer pH 7.4 (total reaction volume, 1mL) and pre-incubated at 37°C for 5 minutes before the addition of 4.42 nM RFK to initiation the reaction. The

reaction was incubated at 37°C for 24-48 hours to allow for full conversion of 2-deoxyriboflavin to 2-deoxyFMN before HPLC purification using the condition described above to yield a yellow solid. ¹H NMR (400 MHz, D₂O): δ 7.57 (s, 1H), 7.55 (s, 1H), 3.85 (m, 1H), 3.75 (m, 1H), 3.60 (m, 1H), 3.52 (m, 1H), 2.36 (s, 3H), 2.24 (s, 3H), 2.04 (m, 2H), 1.78 (m, 1H). ESI⁺ (m/z) [M+H] for C₁₇H₂₀N₄O₅ calculated: 441.1131, found: 441.1166.

Protein Expression and Purification of hsRFK

Clones containing pPROEX-Hta-RFK His₆ were grown in LB media contain ampicillin (100 µg/ml) at 37°C to an OD₆₀₀ between 0.6 and 0.8. The medium was then cooled to 18°C and cells were induced via incubation with 0.4 mM IPTG at 18°C with shaking for 4 hours. Cells were then harvested by centrifugation at 5,000 x g for 6 mins (4°C) and the cell pellet was resuspended for affinity purification (500 mM sodium chloride, 50 mM sodium phosphate pH 8).

Cells were lysed via 4 passages through a French press at approximately 10,000 psi. Lysates were centrifuged with 150 µM FMN at 40,000 x g for 1.5 hr (4°C) to remove cellular debris. Supernatant was filtered (0.22 µm PES) to remove any additional particulate matter before being loaded onto a HisTrap HP column (1 mL) chelated with Ni²⁺ using an AKTA Prime FPLC. Soluble lysates were applied to the affinity column, washed with 5 column volumes of wash buffer (500 mM sodium chloride, 50 mM sodium phosphate pH 8.0, 20 mM imidazole) and eluted using a linear gradient of 20-250 mM imidazole in the wash buffer (20 mL). Fractions containing RFK-His₆, as identified by SDS-PAGE, were pooled and dialyzed against 500 mM sodium chloride, 50 mM sodium phosphate pH 8.0 at 4°C. Concentrations of

the final purified hsRFK-His₆ were determined using an ϵ_{280} of $21,430^{-1} \text{ cm}^{-1}$. The concentration of bound FMN cofactor was determined using an ϵ_{450} $12,500 \text{ M}^{-1} \text{ cm}^{-1}$.

Chapter 3: Preparation and Reconstitution of IYD

3.1 Introduction

The association and dissociation of flavoproteins into apoprotein and the flavin cofactor is a well-accepted phenomenon⁷⁰. This reversible relationship has been manipulated for biochemical studies by replacement of the native cofactor with synthetic flavin analogs^{7,70}. In order to examine the nature of the flavin ribityl hydrogen bond to MIT in IYD, its FMN cofactor was removed, to generate apoenzyme that was then reconstituted with 2-deoxyFMN. Preliminary reconstitution studies were performed utilizing mIYD expressed isolated from Sf9 insect cells⁷⁹. Expression of IYD in this cell line while efficient was expensive and time consuming. Engineering of IYD fusion constructs using either thioredoxin or SUMO proteins has allowed for heterologous expression in *E. coli*⁶². This method has provided a cost and time efficient way to obtain large quantities of soluble IYD from several organisms, including human for mechanistic studies^{80 64}.

Mechanistic studies with 2-deoxyIYD are only possible if a method of reconstitution can be developed. As reconstitution requires unfolding of the native enzyme under harsh denaturing conditions, it is possible that the generated apoenzyme could be irreversible denatured, making it impossible to recovery enzymatic activity. Previous attempts at developing a reconstitution protocol for IYD were successful in generation of the apoenzyme using stepwise increases of guanidine hydrochloride to denature IYD^{54,79}. However, the reincorporation of FMN did not result in 100% active site occupancy⁷⁹. As a flavoenzyme, the flavin occupancy of

IYD is critical for an accurate measurement of its enzymatic activity. Therefore, optimizations of the IYD reconstitution protocol were made using the enzyme's native cofactor FMN. This served as a positive control and would be used to differentiate whether observed changes were due to formation of the apoenzyme and its reconstitution or cofactor modification. Discussed in this chapter is the development of an IYD reconstitution protocol and its use to generate both FMN and 2-DeoxyFMN reconstituted hIYD. Substrate dissociation constants (K_D) as well as Michaelis-Menten kinetic were determined for each reconstituted enzyme. These values were then compared to native hIYD to measure the effects of reconstitution on catalytic ability.

3.2 Results and Discussion

3.2.1 Reconstitution of hIYD with FMN and 2-DeoxyFMN

Apo-hIYD was initially generated as described in a modified protocol utilizing stepwise increases of guanidine hydrochloride to denature hIYD⁵⁴. This method resulted in the release the non-covalently bound FMN and loss of hIYD's characteristic yellow color. UV-Vis measurements taken of the freshly formed apoenzyme showed no absorbance at 450 nm. A discontinuous D¹²⁵IT activity assay⁸¹ of apo-hIYD showed the expected loss of deiodinase activity (**Figure 3.1**). Incubation of apo-hIYD with 2 equivalents of FMN follow by an overnight dialysis in the standard hIYD purification buffer containing 500 mM NaCl should have produced the reconstituted haloenzyme, marked by the return of deiodinase activity. Surprisingly, UV-Vis spectra showed little to no uptake of FMN and D¹²⁵IT

deiodinase activity assay of this prepared enzyme were comparable to that of apoenzyme (**Figure 3.1**).

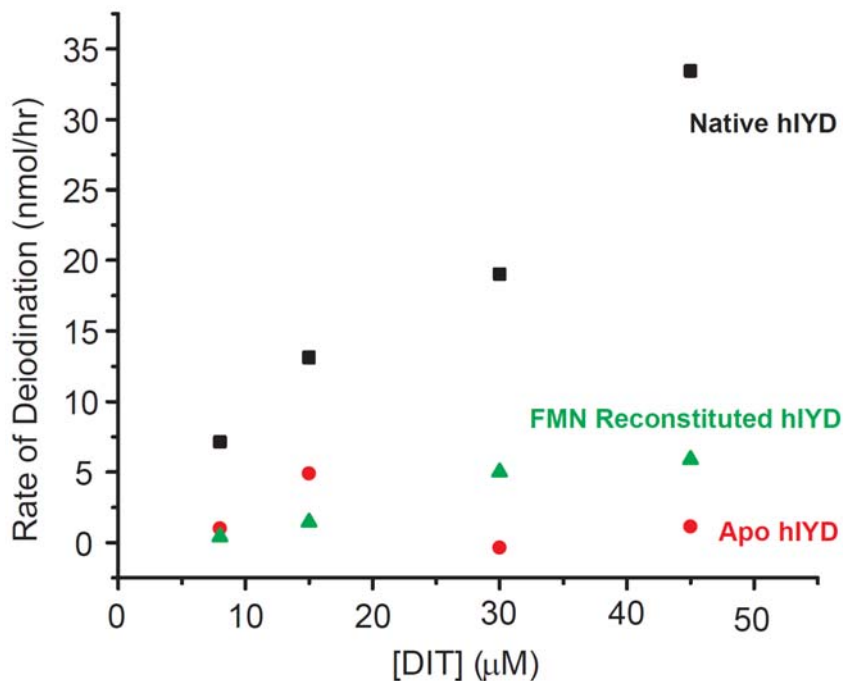


Figure 3.1 DIT deiodinase activity of native, apo and FMN reconstituted hIYD under 500 mM NaCl conditions. The activity of hIYD ($0.08 \mu\text{M}$) with DIT was determined using the standard discontinuous D^{125}IT iodide release assay.

Concerns over irreversible denaturation of hIYD led to a literature search for flavoenzyme reconstitution methods. One article⁷⁰ highlighted the effects of buffer conditions on generation and reconstitution of apoflavoprotein. High salt concentrations, while generally useful for apoenzyme stability, can create an environment that inhibits the uptake of flavin due to electrostatic repulsion⁷⁰. The dialysis buffer initially used for reconstitution contained the standard 500 mM NaCl used for preparation of hIYD. During the preparation of hIYD for protein crystallography studies⁶⁴, purified hIYD was found to be stable in buffer containing 100 mM NaCl. Consequently, solutions of apoenzyme and FMN were dialyzed

against buffer containing 100 mM NaCl after incubation. Lowering of the salt concentration resulted in uptake of FMN and return of deiodinase activity. While these results were promising, active site occupancy was observed at only 80% for the reconstituted enzyme. For the native enzyme, flavin occupancy of 90% or greater is often observed. Attempts were then made to increase active site occupancy to using 40 equivalents of FMN. This also resulted in the expected return of activity, however a 1:1 FMN:active site ratio was never obtained. Instead occupancy was seen to be over 100%, indicating the presence of unbound FMN in the enzyme solution. Difficulty in removing of all the excess unbound FMN from solution, made it hard to assess how much FMN was bound to hIYD. Attempts to remove unbound FMN, whether by multiple buffer dialysis or spin column extractions proved to be ineffective. An intermediate of 5 equivalents of FMN was then settled on, as this amount was high enough to provide full flavin occupation, while being low enough that any unbound flavin could be removed from solution via overnight dialysis. Under these conditions, FMN was removed and replaced in hIYD resulting in the loss and recovery of deiodinase activity as expected (**Figure 3.2**). Michaelis-Menten kinetic constants obtained for the reconstituted holoenzyme were within an order of magnitude of native hIYD (**Table 3.1**).

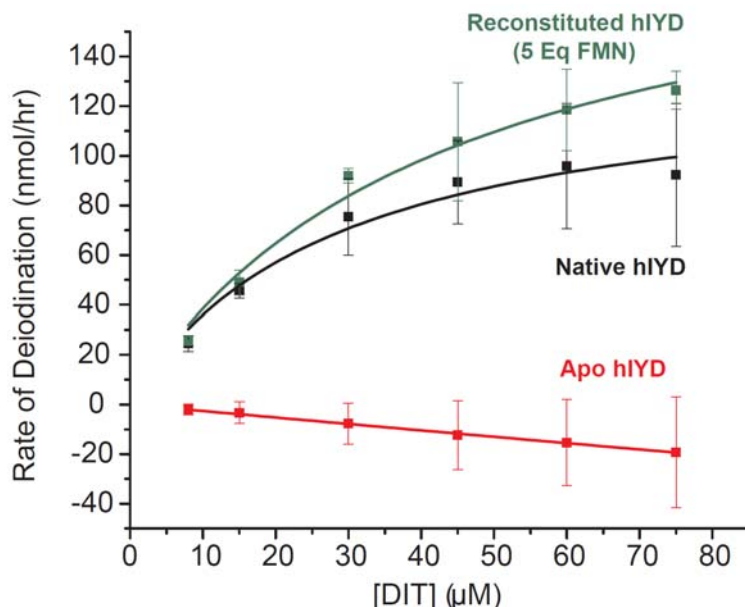


Figure 3.2 DIT deiodinase activity of native, apo and holo-hIYD reconstituted with 5 eq of FMN. The activity of hIYD (0.08 μM) was determined using the standard ¹²⁵I iodide release assay. Assays were performed in triplicate and the average data sets were fit to Michaelis-Menten kinetics using Origin 7.0. Error bars represent standard deviation at each concentration.

Table 3.1 Kinetic parameters of hIYD.

hIYD	K_M (μM)	V_{max} (μM/hr)	k_{cat} (1/s)
Native	28 ± 7.5	137 ± 14	0.48 ± 0.06
Apo	<0.02	<0.30	<0.002
Reconstituted (5 Eq FMN)	43 ± 10	204 ± 22	0.71 ± 0.08

Kinetic constants were obtained by fitting to Michaelis-Menten kinetics using Origin 7.0.

These results, while encouraging, ultimately proved to be irreproducible, as successive preparation of FMN reconstituted hIYD yielded large variability in observable deiodinase activity (30 to 100% recovery) due to active site occupancy (60 - 100%). Attempts to increase active site flavin occupancy drove the decision to double the quantity of FMN used during the apoenzyme incubation step from 5 to 10 equivalents of FMN. However the increased cofactor concentration had no effect on

the recovery of deiodinase activity (**Figure 3.3**). Problems seen in reproducibly of active site occupancy indicated decrease flavin uptake may be due to the decreased stability of the generated apoenzyme caused by irreversible damage during denaturing. Therefore, a means of stabilizing the apoprotein long enough to reincorporate flavin was sought.

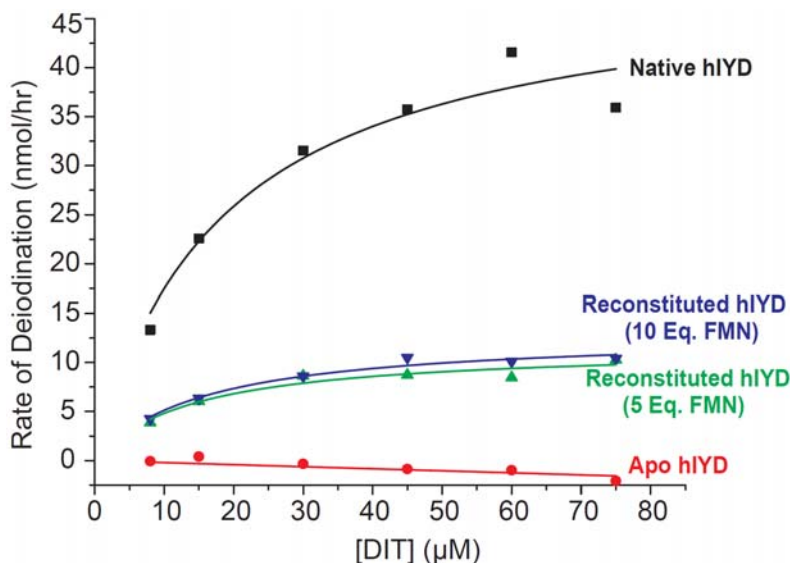


Figure 3.3 D¹²⁵I deiodinase activity of native, apo and holo-hIYD reconstituted with 5 and 10 equivalents of FMN. Activity was determined using the standard D¹²⁵I iodide release assay.

Efforts made to find a method that would effectively generate and stabilize the apoenzyme without inhibiting flavin uptake lead to a second review of the literature. A number of methods discussing the use of affinity chromatography to aid in apoenzyme stabilization were consulted^{82, 83} as affinity chromatography was used for generation of apo-hIYD. One affinity column protocol utilized immobilized metal affinity chromatography (IMAC) for both apoenzyme generation and reconstitution of the FAD-containing PAS domain of NifL⁸³. The main difference between this method and that used for hIYD was that the formed apoenzyme was not eluted off the

affinity column but instead reconstituted on-column by washing with a 10 mM flavin solution using a cyclic loop. The potential benefits of this method include: 1) increased apoenzyme stabilization during flavin uptake as the His tag helps the enzyme to correctly refold, 2) the ability to visualize flavin uptake before elution due to the large extinction coefficient of flavin and 3) recycling of the flavin containing solution. Recycling of the flavin solution made this method particularly attractive as limited supplies of 2-deoxyFMN were available for reconstitution.

To test the effectiveness of this new protocol⁸³ for hIYD, apo-hIYD was generated on an affinity column by stepwise washes with GdnHCl (0-1.5 M). The bound apo-hIYD was then washed with buffer containing 1 mM FMN and 100 mM NaCl. After 2 hours of recycling the FMN solution over the column bound enzyme, the column was washed with a flavin free buffer to remove any excess flavin that had not bound to the protein. At the end of that time a well-defined yellow band could be seen on the column, indicating flavin uptake and the generation of the reconstituted hIYD. Deiodinase activity of the initial on-column reconstituted hIYD was less than 20 % of native hIYD. While these results showed hIYD could be reconstituted using the on-column method, optimization was needed to improve the recovery of enzymatic activity. Furthermore, since synthesis of the 2-deoxyFMN analog provided milligram amounts of the desired product, millimolar flavin concentrations would not be ideal for its incorporation into hIYD. A modified on-column procedure using buffer containing 10 fold less FMN was then attempted to see how enzyme activity would compare. To compensate for the decrease in flavin concentration the FMN containing buffer was recycled over the column for 4 hours to increase flavin

uptake. This resulted in an improved recovery of enzymatic activity compared to the initial 1 mM FMN reconstitution. The 100 μ M FMN reconstituted enzyme had regained approximately 70% of the native deiodinase activity (**Figure 3.4**).

Encouraged by this data, reconstitution trials with 2-deoxyFMN were carried out.

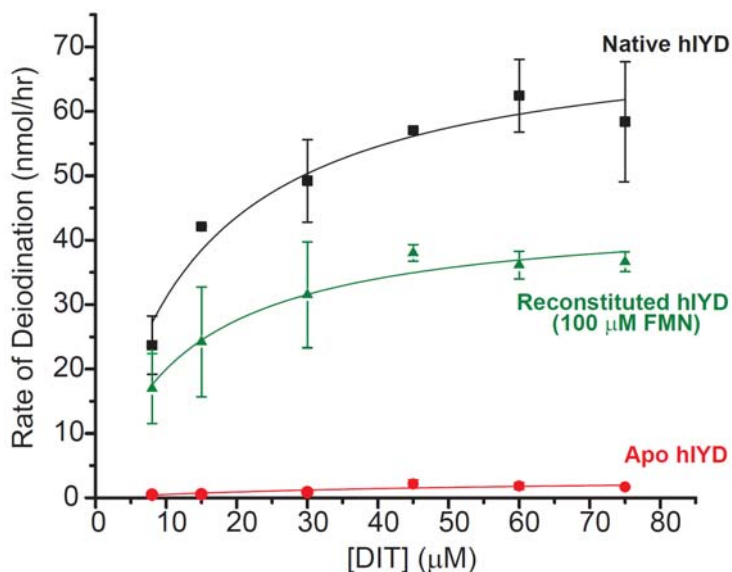


Figure 3.4 $D^{125}I$ deiodinase activity of native, apo and holo-hIYD reconstituted on Ni^{2+} affinity column using 100 μ M FMN. Activity of hIYD (0.08 μ M) was determined using the standard $D^{125}I$ iodide release assay. Assays were performed at least twice. Error bars represent standard deviation at each concentration.

Initial attempts at the formation of 2-deoxyFMN reconstituted hIYD with the newly modified on-column method produced a reconstituted enzyme that was stable for several hours, but began to precipitate after 24 hours. Short lived stability of 2-deoxyhIYD suggested that while hIYD was indeed able to recombine with 2deoxyFMN, enzyme aggregation, possible due to the presence of irreversible damage enzyme, was causing precipitation. To remedy this problem on-column reconstitution of the membrane truncated hIYD fusion protein (SUMO-hIYD(Δ tm)) was performed in hopes that the SUMO fusion protein would provide added stability

in the refolding process of the apoenzyme. Also, the use of gel filtration chromatography to purify the reconstituted hIYD would remove excess FMN as well as any remnants of damaged apoenzyme from the denaturation step. To date this method has produced the best result, as FMN reconstitution enzyme with 95-100% flavin occupancy and the return of native level deiodinase activity (**Figure 3.5**). In addition, the stability of reconstitution hIYD was comparable to that of purified native hIYD. 2-DeoxyhIYD generated following the same method was now stable enough for characterization.

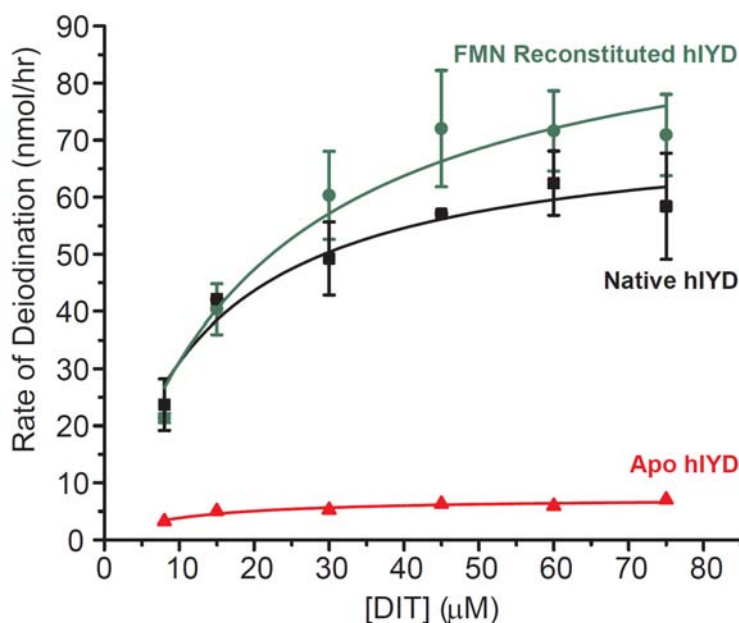


Figure 3.5 DIT deiodinase activity of native, apo and holo-hIYD reconstituted on Ni^{2+} affinity column using 100 μM FMN. The activity of hIYD (0.08 μM) was determined using the standard ^{125}I iodide release assay. Assays were performed in triplicate. The averaged data was fit to Michaelis-Menten kinetics using Origin 7.0. Error bars represent standard deviation at each concentration.

3.2.2 Equilibrium binding of MIT and DIT to 2-deoxyhIYD

Characterization of 2-deoxyhIYD began with measurement of substrate affinity. Binding of MIT to 2-deoxyhIYD was monitored by the decrease of the active

site flavin fluorescence upon ligand association. This data was compared to similar affinity measurements of MIT to FMN reconstituted hIYD (**Figure 3. 6**). Removal of the 2'OH significantly decreased affinity of the enzyme for substrate >4,000 fold compared to both wildtype and FMN reconstituted hIYD (**Table 3.2**). Measurements of DIT binding to 2-deoxyhIYD (**Appendix B.1**) also showed a drastic >3,000 fold decrease in substrate affinity (**Table 3.2**). This suggests the hydrogen bond between substrate and the ribtyl 2'OH is necessary for efficient substrate binding. Decreased affinity for DIT when compared to MIT was expected for 2-deoxyhIYD due to the steric bulk of DIT. 2-deoxyhIYD was observed to bind DIT 5 fold less tightly than MIT. This difference is doubled for native hIYD which binds DIT 10 fold less tightly than MIT. A possible reason for this observation is that removal of the 2'OH allows for better active site accommodation of bulkier DIT.

Table 3.2 Equilibrium binding constants of native, FMN reconstituted and 2-deoxyhIYD.

hIYD	K_D (μM)	
	MIT	DIT
Native*	0.15 ± 0.04	1.5 ± 0.15
FMN Reconstituted	0.42 ± 0.13	-
2-DeoxyFMN	996 ± 58.7	5029 ± 155.0

Dissociation constants were calculated by nonlinear fit of data to Equation 3.1 (See Figure 3.6 and Appendix B).

*Values for native hIYD were obtained from ⁸⁴.

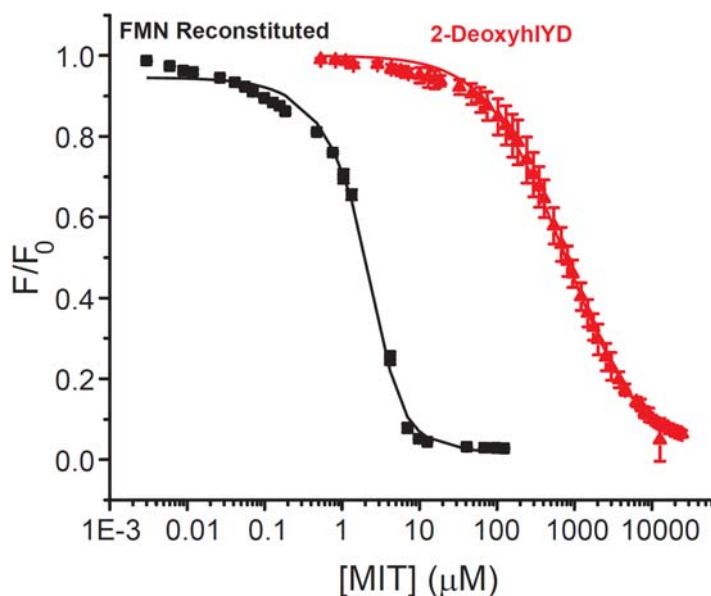


Figure 3.6 Equilibrium binding of MIT to FMN reconstituted hIYD and 2-deoxyhIYD. Binding was monitored by the change in fluorescence of flavin bound to enzyme (4.5 μM) in solution of 100 mM potassium phosphate and 200 mM potassium chloride (pH 7.4) at 25°C using λ_{ex} of 450 nm and λ_{em} of 527 nm. The average of three independent measurements were normalized and plotted against MIT concentrations. Error bars represent the standard deviation of three measurements.

3.2.2 Deiodinase Activity of FMN and 2-DeoxyFMN Reconstituted hIYD

Michaelis-Menten kinetic constants for the FMN reconstituted hIYD were determined by the previously mentioned discontinuous D^{125}IT assay (**Figure 3.5**). It was found that removal and replacement of the native FMN cofactor had no significant effects on the catalytic ability of hIYD towards native substrate (**Table 3.3**). The calculated $k_{\text{cat}}/K_{\text{m}}$ of $0.74 \pm 0.08 \text{ min}^{-1} \mu\text{M}^{-1}$ was close to that of native hIYD ($0.54 \pm 0.01 \text{ min}^{-1} \mu\text{M}^{-1}$) and falls within the range of $0.28 \text{ min}^{-1} \mu\text{M}^{-1}$ to $3.5 \text{ min}^{-1} \mu\text{M}^{-1}$ detected for a series of IYD obtained from highly diverse organisms⁸⁰. This indicates that the process of reconstitution itself is not detrimental to the deiodinase.

Table 3.3 Kinetic parameters of native, FMN reconstituted and 2-deoxyhIYD with DIT.

	MIT			DIT		
	K_M (μM)	k_{cat} (min^{-1})	k_{cat}/K_m ($\text{min}^{-1} \mu\text{M}^{-1}$)	K_M (μM)	k_{cat} (min^{-1})	k_{cat}/K_m ($\text{min}^{-1} \mu\text{M}^{-1}$)
Native*	12 ± 2.5	7.3 ± 1.0	0.60 ± 0.02	73 ± 3.7	15.2 ± 0.7	0.54 ± 0.01
FMN Reconstituted	—	—	—	22.5 ± 3.3	16.7 ± 1.0	0.74 ± 0.08
2-DeoxyFMN	327 ± 94.7	19.0 ± 3.50	0.06 ± 0.04	1820 ± 703.0	74.5 ± 11.7	0.04 ± 0.01

Kinetics constants were calculated by fit to Michaelis-Menten kinetics.

*Values for native hIYD were obtained from ⁸⁴.

To determine the effects of 2-deoxyFMN on the catalytic activity of IYD, protein dependence of MIT turnover was monitored by HPLC (**Figure 3.6**). Varying concentration of 2-deoxyhIYD (0.4, 2.5 and 4.5 μM) were reduced by sodium dithionite in the presence of 1 mM MIT. HPLC analysis of each reaction revealed the formation of tyrosine at each enzyme concentration. A reaction time course was obtained for MIT deiodination by 0.4 μM 2-deoxyhIYD (**Appendix B.2**). Michaelis-Menten kinetic constants obtained for 2-deoxyhIYD (k_{cat}/K_m of $0.06 \pm 0.04 \text{ min}^{-1} \mu\text{M}^{-1}$) showed an approximately 10 fold decrease in catalytic efficiency when compared to native hIYD (k_{cat}/K_m of $0.60 \pm 0.02 \text{ min}^{-1} \mu\text{M}^{-1}$) (**Figure 3.7**). Similarly, numbers were obtained using the standard D¹²⁵IT assay (**Table 3.3, Appendix B.3**). These results were surprising. Considering the large decrease in substrate binding affinity, 2-deoxyhIYD was expected to be unable to support catalysis. The hydrogen bond between FMN and substrate was thought to be necessary for substrate orientation, possibly acting as an anchor to help position substrate over the isoxallozine ring ⁶⁴. Moreover, the ribityl 2'OH had been hypothesized to be important for substrate

activation, through stabilization of a substrate intermediate during turnover, as will be discussed further in Chapter 4.

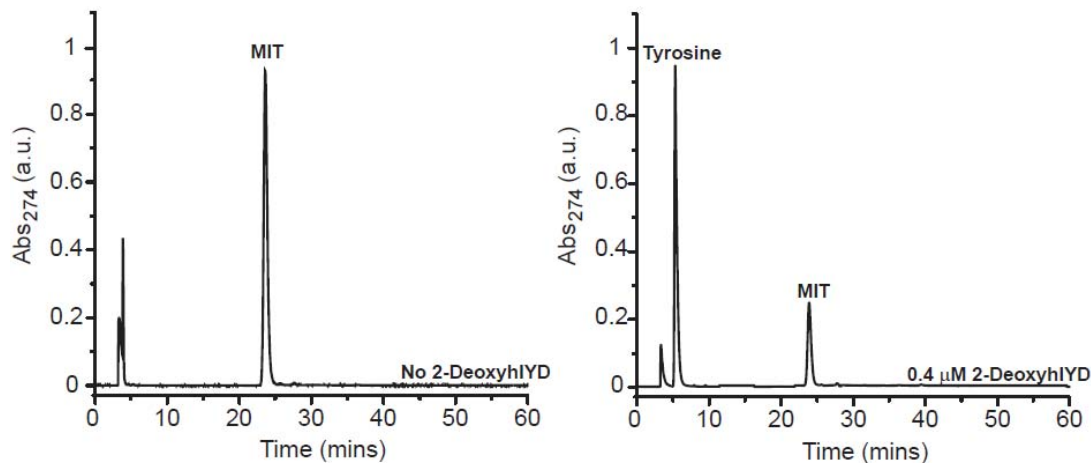


Figure 3.6 Representative HPLC chromatographs of the deiodination of MIT by 2-deoxyhIYD. Deiodination was monitored in the absence (A) and presence (B) of 0.4 μM 2-deoxyhIYD. Product purification using a 45 min linear gradient from 100% TEAA pH 5.5 to 45% acetonitrile. Product formation was monitored at 274.

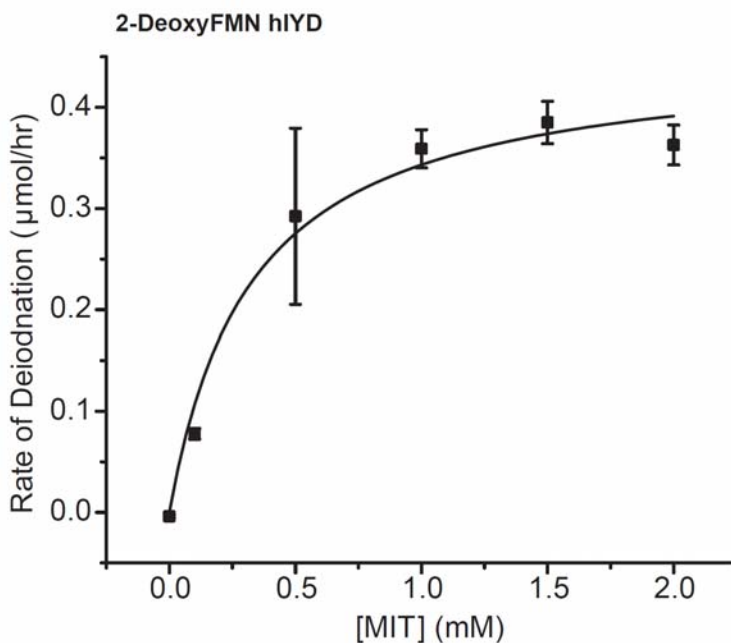


Figure 3.7 MIT deiodinase activity of 2-deoxyhIYD. The activity of 2-deoxyhIYD (0.4 μM) was determined using a HPLC assay. Assays were performed in triplicate. The averaged data was fit to Michaelis-Menten kinetics using Origin 7.0. Error bars represent standard deviation at each concentration.

3.3 Summary

Reliable reconstitution of hIYD requires removal of the native FMN in a manner that denatures the native protein without causing irreversible damage. Immobilized metal affinity chromatography (IMAC) provides added stabilization to apoIYD during enzyme refolding and flavin replacement. Low salt concentrations of 100 mM are crucial during hIYD reconstitution, as increased ionic strength inhibits flavin uptake by apo-hIYD. Gel filtration chromatography provides efficient purification of reconstituted hIYD from irreversibly denatured enzyme, generating a stable FMN haloenzyme with deiodinase activity comparable to native IYD. Removal of the FMN ribityl 2'OH in hIYD decreases substrate affinity greater than >3,000 fold, however does not significantly alter catalytic activity. This data suggest that the hydrogen between the FMN 2'OH and MIT is important for substrate binding but not turnover.

3.4 Experiments

Materials

Na¹²⁵I used for radiolabeling of DIT was obtained from Perkin Elmer (Waltham, MA). All other reagents were obtained at the highest grade available and used without further purification. Amicon Ultra-15 centrifugal filters were purchased from Millipore (Billerica, MA). HisTrap HP column (1 mL and 5 mL) and SephacrylTM S-200 resin were purchased from GE Healthcare Life Sciences. The pET28-SUMO-JH1 plasmid was prepared by Dr. Jimin Hu⁶⁴. Plasmids containing pET-SUMO-hIYD(Δ tm)His₆ were transformed into Escherichia coli Rosetta2 (DE3). All protein purifications were carried on an AKTA Prime FPLC (GE Healthcare Bio-sciences

Corp.) unless otherwise stated. UV-Vis measurements were made using a Hewlett-Packard 8453 spectrophotometer. Fluorescence intensities were measured with a HORIBA Scientific FluoroMax fluorescence spectrophotometer. High performance liquid chromatography (HPLC) was performed on a Varian Microsorb-MV 300 (250 x 4.6 mm) C₁₈ reverse-phase column using 10 mM TEAA buffer pH 5.5 (A) and acetonitrile (B) as the elution solvent. Compound elution was detected by UV at 274 nm and 280 nm.

3.4.1 Protein Expression and Purification of hIYD

E. coli transformed with pET-SUMO-hIYD(Δ tm)His₆ was grown in LB media with chloramphenicol (34 μ g/mL) and kanamycin (50 μ g/mL) at 37°C to an OD₆₀₀ between 0.6 and 0.8. The medium was then cooled to 16°C and induced via shaking incubation with 20 μ M isopropyl- β -D-thiogalactopyranoside (IPTG) for 18 hours. Cells were then harvested by centrifugation (5,000 x g for 5 min (4°C)) and resuspended for affinity purification in buffer containing 500 mM sodium chloride, 50 mM sodium phosphate pH 8.0, 0.01 mM dithiothreitol, and 10% glycerol. Cells were then flash frozen and stored at -80 °C until use.

Cells were lysed via 4 passages through a EmulsiFlex C-3homogenizer (Avestin) at approximately 15000 psi in affinity purification buffer supplemented with 180 μ M FMN. Lysates were centrifuged at 40,000 x g for 3 hour at 4°C to remove cellular debris. Supernatants were then filtered (0.22 μ m PES) to remove additional particulate matter before affinity purification. Soluble lysates were loaded on a 1 mL HisTrapTM HP column chelated with Ni²⁺, washed with 6 column volumes of wash buffer (500 mM sodium chloride, 50 mM sodium phosphate pH 7.9, 0.01 mM

dithiothreitol, 10% glycerol, 20 mM imidazole) and eluted using stepwise increases in imidazole (6 column volumes of 20 mM, 6 column volumes of 70 mM, 2 column volumes of 100 mM, and finally 3 column volumes 250 mM imidazole). Fractions containing SUMO-hIYD(Δ tm)His₆ as identified by SDS-PAGE, were pooled and incubated with approximately 1:100 ratio of Ulp1 protease per mg of fusion protein for 12 h at 4°C. Digested SUMO-hIYD(Δ tm)His₆ was concentrated to 1 mL using an Amicon Ultra-15 centrifugal concentrator (MWCO = 10 KDa) before being loaded onto SephacrylTM S-200 resin for gel filtration purification using buffer containing 100 mM sodium chloride, 50 mM sodium phosphate pH 7.4, 1 mM dithiothreitol, and 10% glycerol. Concentrations of the final purified hIYD(Δ tm)His₆ was determined using an ϵ_{280} of 38,000 M⁻¹ cm⁻¹. The concentration of bound FMN cofactor was determined using an ϵ_{450} 12,500 M⁻¹ cm⁻¹.

3.4.2 Generation of apo-hIYD

Purified hIYD(Δ tm)His₆ was loaded on a 1 mL HisTrapTM HP column chelated with Ni²⁺. Using an AKTA Prime FPLC, the protein was washed with 10 column volumes of native wash buffer (50 mM sodium phosphate pH 7.4, 500 mM sodium chloride, 0.1 mM dithiothreitol, 10% glycerol and 20 mM imidazole) before being washed by a stepwise gradient of native wash buffer supplemented with 1.5 M guanidine hydrochloride (GdnHCl). The stepwise gradient consisted of sequential 10 columns volumes washes with 0.0 M, 0.6 M and 1.05 M GdnHCl respectively, followed by one 20 column volume wash with 1.5 M GdnHCl. The protein was then refolded on the column by sequential 10 columns volume washes with 1.05 M, 0.6 M and 0.0 M GdnHCl respectively, before being eluted with 250 mM imidazole.

3.4.3 Reconstitution of apo-hIYD

Using an AKTA Prime FPLC soluble lysates of SUMO-hIYD(Δ tm)His₆ were loaded onto a 5 mL HisTrapTM HP column chelated with Ni²⁺ and washed with 6 column volumes of native wash buffer (NWB) (500 mM sodium chloride, 50 mM sodium phosphate pH 7.9, 0.01 mM dithiothreitol, 10% glycerol, 20 mM imidazole) followed by stepwise increases in imidazole to remove extracellular debris (6 column volumes of 70 mM imidazole in NWB, 2 column volumes of 100 mM imidazole in NWB). Apo-SUMO-hIYD(Δ tm)His₆ was then generated using a stepwise gradient of native wash buffer containing 1.5 M GdnHCl as described above. Column bound apo-SUMO-hIYD(Δ tm)His₆ was then washed with reconstitution wash buffer (RWB) (50 mM sodium phosphate pH 7.4, 100 mM sodium chloride, 0.1 mM dithiothreitol, 10% glycerol and 20 mM imidazole) supplemented with 200 μ M of either FMN or 2-deoxyFMN for 4 hours at 4°C at a flow rate of 1 ml/min. Reconstituted SUMO-hIYD(Δ tm)His₆ was then washed with at least 20 column volumes of flavin free RWB before being eluted with 250 mM imidazole in RWB. Fractions containing reconstituted SUMO-hIYD(Δ tm)His₆ as identified by SDS-PAGE, were pooled and incubated with approximately 1:100 ratio of Ulp1 protease per mg of fusion protein for 12 h at 4°C. Digested reconstituted SUMO-hIYD(Δ tm)His₆ was concentrated to 1 mL using an Amicon Ultra-15 centrifugal concentrator (MWCO = 10 KDa) and purified on SephacrylTMS-200 resin as described above.

3.4.4 Fluorescence Binding

Substrate dissociation constants were calculated based on the change in fluorescence of enzyme bound flavin upon titration of substrate as previously described⁶⁸. FMN reconstituted hIYD and 2-deoxyhIYD were titrated with Tyr

derivatives over a range of concentrations centered at that necessary for a 50% quenching of the emission signal. Fluorescence intensities were normalized by dividing the initial fluorescence (F_0) and plotted against the ligand concentrations using Origin 7. Dissociation constants (K_D) were obtained from the nonlinear fitting to the Equation 3.1⁸⁵. Reported K_D values were derived from the average value of 3 independent determinations and their error was based on the results of least squares fitting.

Equation 3.1.

$$F = F_0 + \Delta F \times \left(\frac{(K_D + [E]_0 + [S]_0) - \sqrt{(K_D + [E]_0 + [S]_0)^2 - 4 [E]_0 [S]_0}}{2[E]_0} \right)$$

3.4.5 Deiodinase Activity

Discontinuous D¹²⁵IT Activity Assay

Deiodination of D¹²⁵IT by hIYD(Δ tm) were measured by a discontinuous assay as previously described⁸¹. Assay of hIYD(Δ tm) and FMN reconstituted hIYD were typically performed by addition of a final concentration of 0.4 μ M protein to 100 mM potassium phosphate pH 7.4, 200 mM KCl, 0.50 mM methimazole, 50 mM 2-mercaptoethanol, D¹²⁵IT (20,000 cpm) and unlabeled DIT (0-75 μ M). Reactions were initiated by addition of sodium dithionite in sodium bicarbonate. Samples were incubated under ambient temperature for 1 hour and quenched by addition of 100 μ L of 0.1% DIT (w/v) in 0.1 NaOH. A 250 μ L aliquot (S) of the 1.1 mL final assay volume was removed and transferred to a vial containing 10% acetic acid (4.75 mL) in order to determine the total radioactivity for each reaction sample. The remaining mixture (850 μ L) was then passed through a cation exchange column (3.5 mL, AG

50W-X8 resin), washed an initial time with 10% acetic acid (4.15 mL), and the eluent collected (A). The column was then washed a second time with 10% acetic acid (5.00 mL) and the eluent was again collected (B). Each sample (S, A, and B) was diluted with 15 mL of Fisher Scientific Scintisafe Plus 50% scintillation fluid and the amount of [¹²⁵I]-iodide present in each sample was quantified using a Packard 1600 TR liquid scintillation analyzer. Assays of 2-deoxyhiYD were performed in a similar manner using 0 -5 mM unlabeled DIT and quenched by addition of 100 μL of 1% DIT (w/v) in 0.1 NaOH. The rate of iodide release was calculated by subtracting the ratio of eluted ¹²⁵I (F) from the background radiation (F₀) as seen in **equations 3.2** and **3.3**, where t is the time (hours) after initiation and n is the moles of DIT (i.e. nmol). This value is multiplied by a factor of 2 because two deiodination sites exist on the DIT but statistically only one of the two is labeled with ¹²⁵I. Values were then normalized for the amount of IYD (μg) added to each reaction. Kinetic constants were calculated by fitting the data obtained from three independent assays trials to the Michaelis-Menten equation in Origin 7.0 k_{cat} values were obtained from the V_{max} and the respective molar concentration of the hiYD protein. Reported error is based on the results of least squares fitting.

Equation 3.2

$$\frac{\frac{\text{dpm A} + \text{dpm B}}{850}}{\frac{\text{dpm S}}{250}} = F$$

Equation 3.3

$$(F_1 - F_0) * \frac{60 \text{ min}}{30 \text{ min}} * [\text{DIT}] * 2 = \text{Rate of DIT deiodination (nmol/hr)}$$

Where: F₀ = Negative control, F₁ = hiYD sample

MIT HPLC Deiodinase Activity Assay

Catalytic deiodination of MIT was measured by formation of tyrosine as detected by HPLC. Reactions were performed in buffer containing 100 mM potassium phosphate pH 7.4 with 200 mM KCl (1 mL total volume). MIT concentrations were centered around the substrate K_D of 1 mM. 0.5% Sodium dithionite in sodium bicarbonate was used to initiate reactions. Samples were incubated under ambient temperature for 2 hrs and terminated via injection onto HPLC (100% →45% A:B; 10mM TEAA pH 5.5: Acetonitrile). Product formation was monitored at 274 nm. Phenol (50 μ M) was used as in internal standard. Reaction rates were calculated using a generated standard curve for phenol/tyrosine in order to convert product area to nmol. The calibration curve of products (**Appendix B.4**) was normalized by the concentration of the internal standard. The response factor (RF) of product with internal standard was used to calculate the product formation by using **Equation 3.4**⁸⁶ where C_x = concentration of analyte, C_{is} = concentration of internal standard, A_x = peak area of the analyte, A_{is} = peak area of the internal standard.

Equation 3.4

$$RF = (A_x * C_{is}) / (A_{is} * C_x)$$

Product formation was determined by the RF and the peak area of the tyrosine as described above. All reactions were repeated at least twice. The average of at least measurements was plotted as product formation vs time by Origin 7.0. The slope of the linear range of the progress curve represents the initial rate of hIYD.

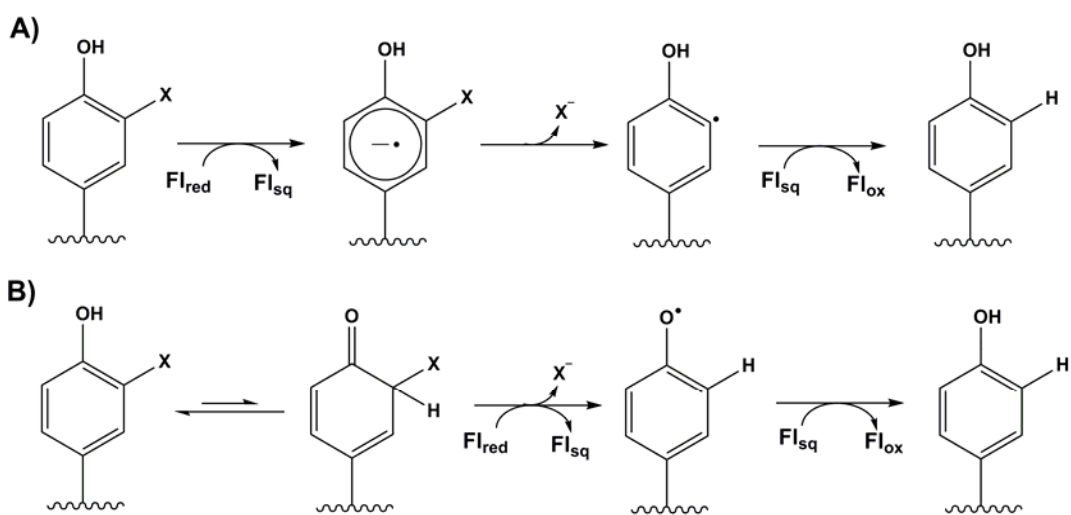
Chapter 4: 2-DeoxyhIYD Activity with Substrate Analogs

4.1 Introduction

The role of IYD in reductive dehalogenation is highly unusual for a flavoenzyme. Few literature examples present flavoenzyme as reductive dehalogenase. Many of these examples describe the necessity of flavin for enzymatic activity, but offer no mechanism for flavin involvement in dehalogenation^{36,87}. A broader search for examples of reductive dehalogenation in aerobic systems yielded two well characterized enzymes, the bacterial TCHQ and mammalian ID^{40,41,88}. Mechanisms for both TCHQ and ID rely on a nucleophilic active site cysteine or selenocysteine residue for dehalogenation. These mechanisms however, provide no insight for IYD, as mutagenesis studies in mIYD have shown the removal cysteine to have no effect on catalysis⁶⁷. Crystal structures of mIYD further confirmed this finding as the enzyme's active site was found to contain no cysteine residues⁶³.

Comparison of IYD's active site in the presence and absence of substrate has revealed an active site devoid of nucleophilic amino acids residues^{63,64}. The presence of substrate induces conformational changes in IYD. These changes include the formation of an active site lid that sequesters the active site from solvent as well as a 1.8 Å shift of the hydroxyl group of Thr239 (as observed in hIYD), placing this functionality within hydrogen bonding distance to the N5 of FMN⁶⁴. Additionally, MIT coordination to FMN in IYD mimics interaction typical seen between FMN and the protein in other flavoenzyme⁶³. Examples of this include but are not limited to hydrogen bonds formed between the zwitterion of MIT and the pyrimidine ring of FMN.

As a flavoenzyme, IYD is capable of catalyzing reductive dehalogenation via either a 1 or 2 electron transfer process. During sodium dithionite reduction of FMN bound to IYD in the presence of halotyrosine, the formation of a neutral Fl_{sq} was detected⁶⁸. Furthermore, anaerobic titrations of hIYD conducted with the inactive substrate analog mono-fluorotyrosine (MFT) have detected the formation of the distinct Fl_{sq} with a λ_{max} of 590 nm. Identical titrations in the absence of substrate only show disappearance of the characteristic FMN absorbance at λ_{max} of 446 nm⁶⁴. The previously mentioned detection of the Fl_{sq} suggests dehalogenation of MIT occurs via 2 sequential, 1 electron transfers.



Scheme 4.1 Proposed 1 e- mechanism for the reductive dehalogenation catalyzed by IYD.

The mechanism of IYD's reductive dehalogenation of MIT has been proposed to go through one of two 1 electron pathways (**Scheme 4.1**)⁴⁶. In the first pathway injection of a single electron from Fl_{red} directly into the phenyl ring of MIT is proposed to generate an aromatic anion radical intermediate. Collapse of this intermediate would result in formation of aryl radical and a free iodide. Transfer of a

second electron from Fl_{sq} and a proton would then yield tyrosine and Fl_{ox}. The second involves substrate tautomerization to a non-aromatic ketone. Injection of a single electron from Fl_{red} would result in release of iodide, forming a tyrosyl radical. The addition of a second electron followed by proton transfer would complete the catalytic cycle to give tyrosine and Fl_{ox}. To date, experimental data seems to support the second pathway. A non-aromatic pyridine analog, used to mimic of the propose substrate tautomer, was found to inhibit deiodinase activity in IYD purified from porcine thyroid, suggesting IYD may have an affinity for a substrate tautomer ⁸⁹.

More recently, pH dependence studies were conducted with hIYD in the presence of DIT to examine whether a preference for the phenol or phenolate form of substrate exist for hIYD binding ⁶⁴. The greatest affinity for substrate occurred at a neutral pH of 7.6 – 7.7⁶⁴. Any acidic or basic deviation from this pH resulted in decreased affinity for DIT. A plot of logK_D versus pH highlighted the significance of two ionizable groups with estimated pK_a values of ~6.6 and ~ 8.7, respectively for maximal binding ⁶⁴. Based on pK_a values, the phenol (pK_a = 6.4) and α-ammonium group (pK_a = 7.8) of DIT have been identified as the possible the ionizable groups. These results are consistent with preferential binding of the phenolate form of halotyrosines to hIYD.

Amongst the observed active site interaction, the phenolic group of MIT has been reported to share a possible a hydrogen bond with the 2'-OH of the FMN ribityl chain and the amide backbone of Ala126 in mIYD ⁶³. An analogous interaction between the 2'-OH of the FAD and the thioester carbonyl of acyl-CoA has been documented in MCAD. This polar contact has been proven to be critical for both orientation and

lower the pKa of acyl-CoA, activating the substrate for dehydrogenation by MCAD through reconstitution studies with 2-deoxyFAD²⁸. Likewise, another member of the nitro-reductase superfamily, BluB, forms a similar hydrogen bond between the 2'-OH of the FMN and its substrate molecular oxygen⁶⁵.

As described in Chapter 3, removal of the FMN ribityl chain 2'-OH decreased the binding affinity of hIYD for MIT and DIT greater than 3,000 fold. However, the loss of this hydrogen bond between substrate and FMN was not detrimental to catalytic activity. 2-DeoxyhIYD was still able to deiodinate both MIT and DIT, with only a 10 fold decreased in k_{cat}/K_m compared to wildtype hIYD. Questions about the chemical nature of these observations, such as effects on flavin chemistry and substrate activation, still remain. Discussed herein is the apparent function of the ribityl chain 2'-OH towards the reductive dehalogenation catalyzed by hIYD. 2-deoxyhIYD was used to probe the role of the 2'-OH of FMN for cofactor redox chemistry and pKa requirements for substrate activation. Binding and turnover studies were also carried out using an O-methyl-iodotyrosine (OMeMIT) substrate analog to block formation of the hypothesis of substrate tautomer.

4.2 Results and Discussion

4.2.1 The Effects of 2'OH on Flavin Reduction

Redox titrations of native hIYD revealed that the presence of bound substrate switches the redox chemistry of FMN from a 2 electron transfer process to a 1 electron transfer process, as observed by the accumulation of the neutral Fl_{sq} only in the presence of substrate⁶⁴. To verify that reinsertion of FMN had no effects on the redox chemistry of IYD, redox titrations were performed on the FMN reconstituted

hIYD as described⁶⁴. UV-Vis spectroscopy of the oxidized FMN reconstituted hIYD showed the characteristic absorbance max at 445 nm. Anaerobic reduction of FMN reconstituted hIYD using the xanthine /xanthine oxidase system rapidly decreased the absorbance at 445 nm, as expected (**Figure 4.1A**). For native hIYD, performance of this anaerobic reduction in the presence of excess 3-fluoro-L-tyrosine (MFT) was reported to yield accumulation of the neutral Fl_{sq}⁶⁴. MFT was selected for these experiments because it binds tightly to the hIYD ($K_D = 1.30 \pm 0.04 \mu\text{M}$)⁸⁴, but is not dehalogenated by the enzyme⁶⁸. Similarly, accumulation of the neutral Fl_{sq} was also observed during reduction of the FMN reconstituted enzyme with excess MFT (**Figure 4.1B**) These results again confirm that the process of reconstitution itself does not affect the enzymatic characteristics of hIYD.

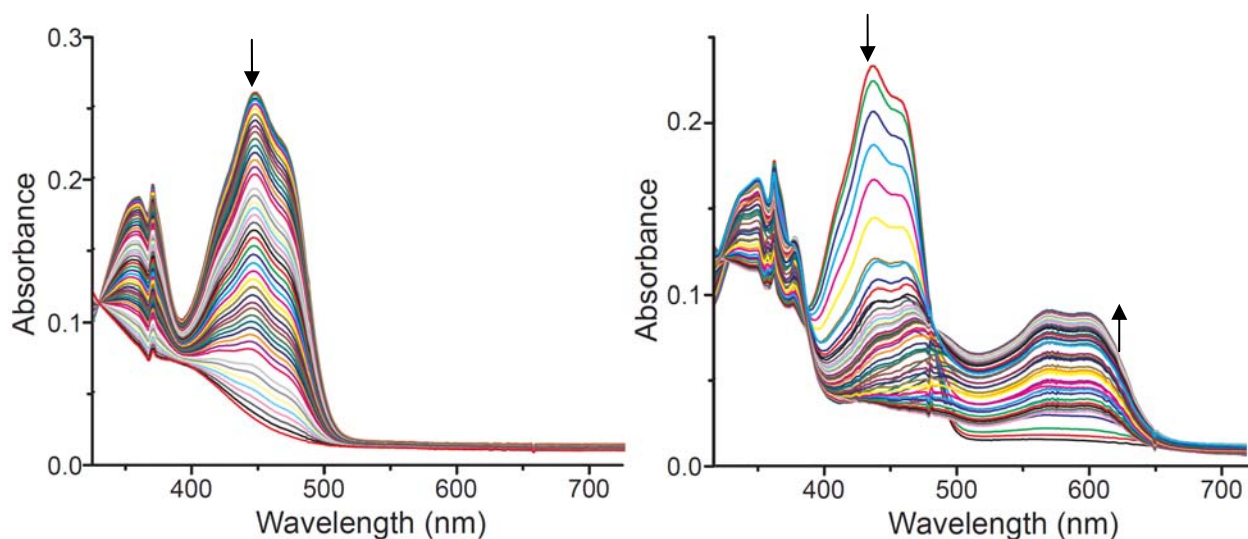


Figure 4.1 Selected spectra from the redox titration of 15 μM FMN reconstituted hIYD by xanthine/xanthine oxidase in the A) absence and B) presence of 0.6 mM MFT. Data was collected every 2 mins for over 120 mins.

To investigate the effects of the FMN ribityl chain 2'-OH on the redox chemistry of hIYD, redox titrations were then performed using 2-deoxyhIYD. Since

the isoalloxazine ring is responsible for controlling the redox chemistry of flavin, removal of the 2'-OH was not expected to have any effects on the reduction of FMN. Anaerobic reduction of oxidized 2-deoxyhIYD in the absence of substrate, resulted in the expected full reduction to the 2-deoxyFl_{hq}. Similar to MIT, 2-deoxyhIYD has an extreme decreased affinity for MFT ($K_D = 1.49 \pm 0.07$ mM, **Appendix C**). As a result an excess of 5 mM MFT was used for redox titrations of 2-deoxyhIYD. In the presence of MFT, however, the 2-deoxyFl_{sq} was never detected (**Figure 4.2**). This result was surprising was not insular. The Fl_{sq} also went undetected during previous redox titrations of native hIYD with two substrate analogs, 3-iodotyramine and 4-hydroxy-3-iodophenyl propionic acid⁸⁴. Similar to 2-deoxyhIYD's decreased affinity for MIT, native hIYD shown a significant decrease in affinity for these analogs ($K_D = 400 \pm 45$ μ M for 3-iodotyramine and $K_D = 1000 \pm 120$ μ M for and 4-hydroxy-3-iodophenyl propionic acid), but was still able to support the turnover of both compounds⁸⁴. For these analogs it was suggested that the removal of their hydrogen bonds with the N3-O4 edge of FMN may prevent stabilization of the Fl_{sq}⁸⁴. This interaction remains intact in 2-deoxyhIYD. However, the lack of Fl_{sq} detection for 2-deoxyhIYD could possibly be explained by the crystal structure of IYD which show the 2'-OH to be within 3.3Å of the N1 position, suggesting a possible hydrogen bond between these two groups (**Figure 4.3**). While is unclear how this interaction would affect stabilization of the neutral Fl_{sq}, hydrogen bonds between ribityl chain hydroxyl and the N1 position in FAD have been shown to stabilize the anionic Fl_{sq} in human electron transfer flavoprotein (ETF)¹³). Further investigations will be necessary to

understand if a similar relationship can be derived in hIYD, as the ionic states of the Fl_{sq} required for these two flavoproteins, hIYD and ETF, appear to differ.

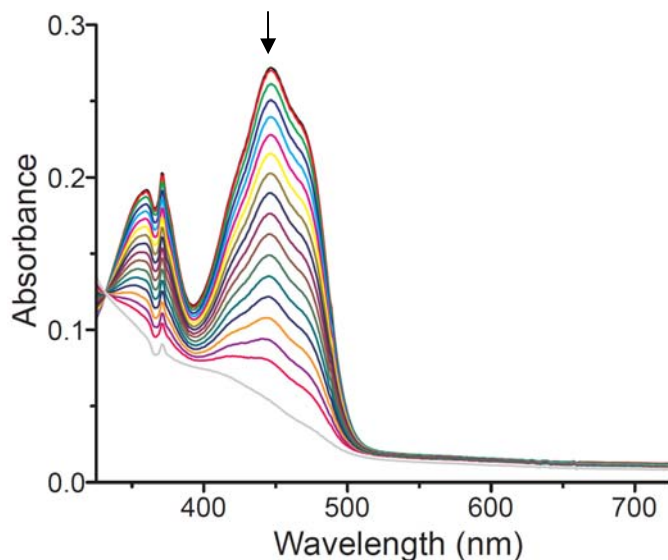


Figure 4.2 Selected spectra from the redox titration of 15 μ M 2-deoxyhIYD in the presence of 5 mM MFT by xanthine/xanthine oxidase. The data was recorded every 2 mins for over 120 mins.

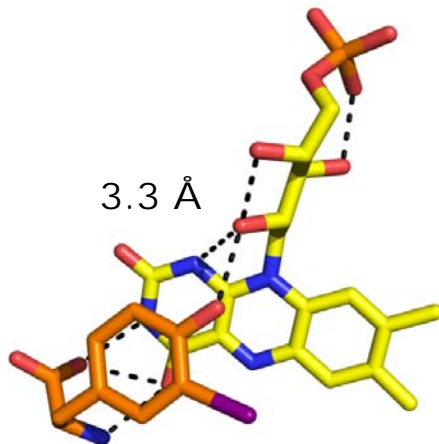


Figure 4.3 Polar contacts between the ribityl chain 2'-OH and N1 of FMN in IYD. PDB 4TTC.

4.2.2 Importance of 2'OH for Substrate Binding

As described in Chapter 3, removal of the 2'OH was found to significantly decrease the binding affinity of hIYD towards MIT and DIT. Based on findings from

a pH dependence of DIT binding⁶⁴, this decreased affinity may be attributed to destabilization the preferred phenolate form of the substrate from the loss of hydrogen bonding with the 2'OH. To test this hypothesis, two alternate methods were sought. The first involved repeating the report pH dependence of DIT binding using 2-deoxyhIYD. It was assumed that, if the phenolate form was indeed the preferred form for enzyme binding, removal of the 2'OH would result in no difference in DIT binding at a lower pH. Unfortunately, due to the already observed decreased affinity for DIT in 2-deoxyhIYD, solution of DIT at concentrations greater than 10 mM were necessary to quench 50% of flavin fluorescence. At these high millimolar concentrations, DIT is known to have low solubility in acidic media. Mock assays were conducted to test the solubility of DIT under these conditions for the planned pH dependence assays. A final concentration of 1 mM DIT was added to 3 mL of 100 mM potassium phosphate 200 mM potassium chloride buffer at pH 6 and stirred at 25°C for 2 -10 mins. While the initial addition of DIT to this solution appeared to dissolve, it was observed that after approximately 2 mins, DIT began to precipitate out of solution. This trial assay was repeated at pH 6.5 with a similar precipitation observed after approximately 5 mins. Therefore, we were unable to test the pH dependence of substrate binding on 2-deoxyhIYD.

The second method used to test the importance of the 2'OH hydrogen bond for substrate binding involved use of the substrate analog, OMeMIT. As an aromatic ether, OMeMIT is not capable of forming a phenolate via deprotonation. If the phenolate form is indeed necessary for substrate binding in hIYD, it was expected that OMeMIT would lose binding affinity to native hIYD. However, in 2-deoxyhIYD

no preference should exist, therefore OMeMIT was expected to retain some level of binding.

Equilibrium binding of OMeMIT was performed for both native hIYD and 2-deoxyhIYD. For native hIYD, a slight drop in fluorescence was observed but only at a final OMeMIT concentration greater than 5 mM (**Figure 4.4A**). This observation was right in line with the hypothesis that the inability of OMeMIT to form a phenolate would inhibit its binding to native hIYD. More interesting was the observation that OMeMIT did not decrease flavin fluorescence in 2-deoxyhIYD (**Figure 4.4B**). Removal of the ribityl 2'OH should have eliminated the preference for the phenolate form of the substrate. In addition, the slight increase of the active site binding pocket due to the absence of the 2'OH should allow for small variations in substrate. This result may indicate that there is another factor necessary for substrate binding. A suggested hydrogen bond between the MIT phenol group and the amide backbone of Ala126 in mIYD may also play a role in substrate binding⁶³. In MCAD, the thioester carbonyl oxygen of acyl-CoA is believed to share hydrogen bonds with both the 2'OH of FAD and a Glu376 residue²⁶. The cumulative effect of these interactions that have been assumed to be responsible for lower the α proton pKa in acyl-CoA²⁷. Similarly in IYD, hydrogen bonds between the phenol group of MIT to both the FMN 2'OH and Ala126 may be necessary for substrate binding and activation.

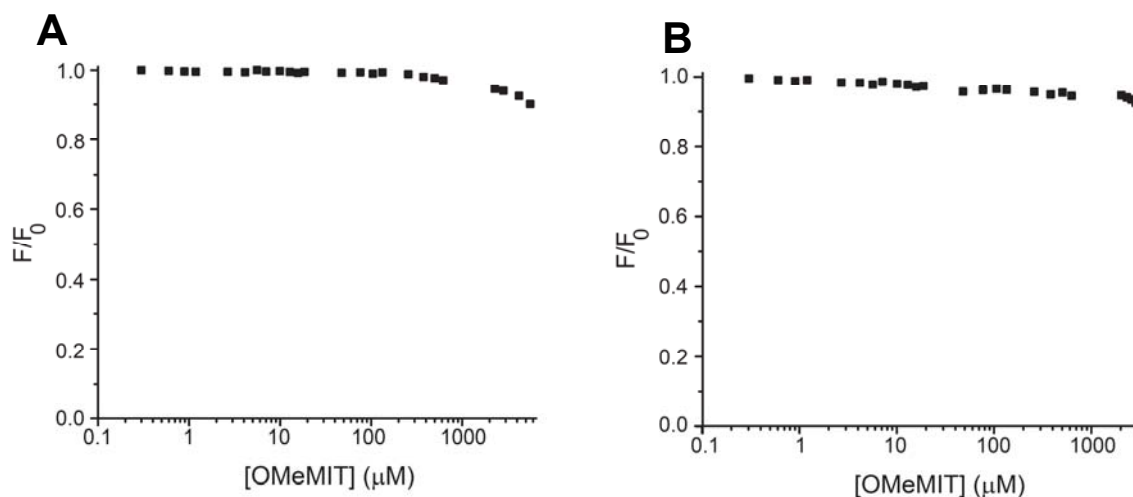


Figure 4.4 Equilibrium binding of OMeMIT to A) native hIYD and B) 2-deoxyhIYD. Binding was monitored by the change in fluorescence of flavin bound to enzyme (4.5 μM) in solution of 100 mM potassium phosphate and 200 mM potassium chloride (pH 7.4) at 25°C using λ_{ex} of 450 nm and λ_{em} of 527 nm

4.2.3 2-DeoxyhIYD does not Support Turnover of OMeMIT

The currently proposed mechanism for the reductive dehalogenation of MIT by hIYD involves substrate tautomerization to an electron deficient keto-intermediate⁴⁶. To investigate the formation of the proposed intermediate, OMeMIT was used. OMeMIT is unable to tautomerize to the non-aromatic ketone. Therefore turnover of this analog should not be observed. Although binding of this substrate was not observed for either hIYD or 2-deoxyhIYD, these studies were still attempted. For 2-deoxyhIYD a > 4,000 fold decrease in affinity for MIT did not hinder deiodinase activity in the enzyme. Additionally, deiodination in 2-deoxyhIYD may occur via a 2 electron process, as the 2-deoxyFl_{sq} was not detected during anaerobic reduction of the enzyme. These factors taken into consideration, we believed it could be possible for 2-deoxyhIYD to turnover OMeMIT, even though substrate binding was not observed.

Deiodination of OMeMIT as monitored by HPLC, showed no formation of the OMeTyr product after 4 hours with either native hIYD or 2-deoxyhIYD (**Figure 4.5**). These observations were confirmed by the addition of 10 μ M OMeTyr to the reaction mixture. The lack of turnover may be the result of hIYD and 2-deoxyhIYD's inability to efficiently bind substrate. Further studies, possibly with other substrate mimics, will need to be conducted to confirm this hypothesis.

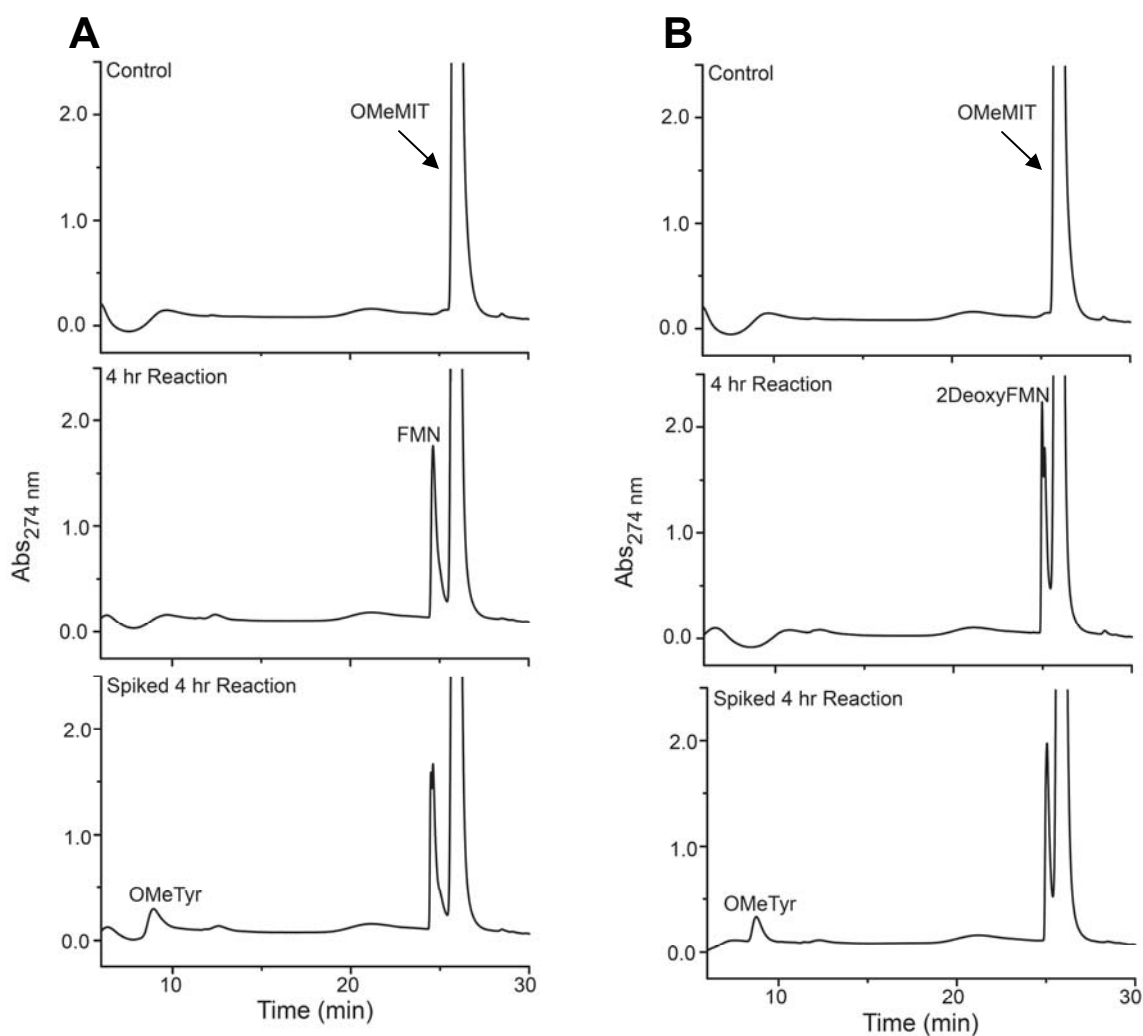


Figure 4.5 HPLC chromatograph of the deiodination of OMeMIT by A) 4.5 μ M hIYD and B) 4.5 μ M 2-deoxyhIYD using a 45 min linear gradient from 100% TEAA pH 5.5 to 45% acetonitrile. Production formation was monitored at 274 nm. Reaction were conducted for 4 hr and spiked with 10 μ M OMeTyr to confirm no turnover had occurred.

4.3 Summary

Anaerobic titrations of 2-deoxyhIYD carried out in the absence and presence of MFT resulted in the direct transformation of 2-deoxyFl_{ox} to the fully reduced 2-deoxyFl_{hq}. 2-deoxyFl_{sq} was not detected, suggesting that the 2'-OH may play a role in stabilizing the Fl_{sq} formed during catalysis in hIYD. Due to the insolubility of substrate at low pH, determination of the pH dependence on DIT binding in 2-deoxyhIYD could not be performed. Binding and turnover studies conducted with OMeMIT, showed that neither native hIYD nor 2-deoxyhIYD to have an affinity towards this substrate analog. Similarly, neither enzyme was able to support enzymatic turnover of the analog. These results, though they may indicate a requirement for substrate tautomerization and therefore phenolate formation, will need to be investigated further.

4.4 Experimental

Materials

Biochemical reagents including xanthine oxidase were purchased from Sigma Chemicals and used without purification unless specified. 3-Fluoro-L-tyrosine was purchased from Astatech, Inc. O-methyl-tyrosine was purchased from Bachem. O-methyl-3-iodo-L-tyrosine was synthesized by Qi Su.

4.4.1 Anaerobic Redox Titration

Redox titrations were performed at 25°C using xanthine/xanthine oxidase as the reducing system⁹⁰. Individual samples within sealable quartz cuvettes (1.2 mL total volume) contained 100 mM potassium phosphate pH 7.4, 200 mM KCl, 900 µM xanthine and 2 µM methyl viologen. Reaction solutions were purged by continuously

flushing with argon for at least 1 hour, prior to addition of 15 μ M hIYD. Reaction solutions were then purged for an additional 30 minutes, prior to initiation by addition of 40 μ g/mL xanthine oxidase. Argon flow was maintained over the head space for the duration of the reaction. Spectra changes were monitored every 2 minutes for over 2 hours. Titrations were repeated in the presence of MFT (0.6 mM for hIYD, 5 mM for 2-deoxyhIYD) to investigate the effects of ligand binding on the oxidation-reduction properties of the enzyme-bound FMN.

4.4.2 Fluorescence Binding

Substrate dissociation constants for OMeMIT were calculated based on the change in fluorescence of enzyme bound flavin upon titration of substrate as described in Chapter 3,

4.4.3 HPLC Deiodinase Activity Assay of OMeMIT

Catalytic deiodination of OMeMIT as measured by formation of OMeTyr as detection by HPLC was performed as described in Chapter 3.

Chapter 5: Conclusions

The chemical diversity of riboflavin has been extended through its derivatives FMN and FAD to a large number of biological processes via nature's use of flavoenzymes. This diversity includes the ability to catalyze both 1 and 2 electron redox processes as well as the activation of dioxygen. In flavoenzymes, the modulation of flavin chemistry can be attributed to protein-cofactor interactions such as hydrogen bonding and π -stacking^{8, 11}. In order to determine which interactions are most important for enzymatic activity, methods like site-directed mutagenesis and enzymatic reconstitution with modified flavin have been utilized.

IYD is critical for proper thyroid function through its salvage of iodide from MIT and DIT. As one of the few flavoenzymes capable of supporting reductive dehalogenation, no literature precedence for its mechanism has been reported. Advances in heterologous expression of IYD in *E. coli* have resulted in the large scale production of IYD for mechanistic studies⁶². Detection of the Fl_{sq} intermediate during anaerobic reduction of IYD in the presence of substrate suggests deiodination occurs via a two sequential single electron transfer processes^{64, 68}. Currently proposed 1 electron mechanisms for IYD involving formation of a substrate keto-tautomer⁴⁶ are supported by the enzyme's apparent preference for the phenolate form of substrate during binding⁶⁴. Analysis of a co-crystal of IYD and MIT show the involvement of substrate in extensive interactions with the FMN cofactor, including a hydrogen bond between the FMN ribityl 2'-OH and the phenolate of MIT⁶³. This hydrogen bond has been hypothesized to activate substrate for deiodination by facilitating formation of the propose substrate tautomerization. Additional, this bond may be necessary for

substrate recognition. The goal of this dissertation was to synthesize and enzymatically phosphorylate 2-deoxyriboflavin for reconstitution with hIYD to probe how disruption of this hydrogen bond affects enzyme behavior.

Removal of the FMN ribityl 2'-OH was observed to significantly decrease substrate binding affinity but did not inhibit deiodinase activity. The Fl_{sq} was not detected during anaerobic reduction of 2-deoxyhIYD in the presence of MFT. Crystal structures of IYD show the ribityl 2'-OH to be within 3.3 Å of N1⁶³. This distance suggests possible formation of a hydrogen bond that may be necessary to promote 1 electron redox chemistry. Further studies will need to be conducted to confirm whether deiodination proceeds via a 1 or 2 electron transfer process. Reconstitution of hIYD with the 1- and 5-deazaFMN analogs should be helpful in this regard. 1-deazaFMN, while still able to promote both 1 and 2 electron transfers disrupts the hydrogen bond to the ribityl 2'-OH, clarifying the significance of this possible interaction¹⁸. 5-deazaFMN can only support 2 electron transfers¹⁸. Therefore this analog would clearly distinguish between the proposed 1 electron deiodination mechanism and a 2 electron mechanism. The enzyme's preference for the phenol versus phenolate form of substrate could not be determined due to the low solubility of halotyrosines at concentrations necessary for fluorescence quenching. However, 2-deoxyhIYD was shown to not support turnover of OMeMIT, possibly suggesting a requirement for substrate tautomerization and therefore a preference for the phenolate form of MIT.

Investigations into the requirements for substrate recognition and activation for IYD using halogenated substrate analogs that mimic the proposed keto-tautomer

would be helpful in gaining more insights on the mechanism of deiodination. Additionally, IYD has been shown to have a propensity to dehalogenation of bromo- and chlorotyrosines, broadening the substrate specificity this enzyme ⁶⁸. If the substrate scope for IYD could be expanded to include haloaromatics the enzyme may have an application in the area of bioremediation ^{91,92}. In order to tap into this potential, better understanding of IYD and its mechanism of action are needed.

Appendices

Appendix A. Supporting Information for Chapter 2

Figure A.1 ^1H NMR of 2-Deoxyribitylated-3,4-dimethylaniline (**2.2**) taken in d_4 -MeOD.

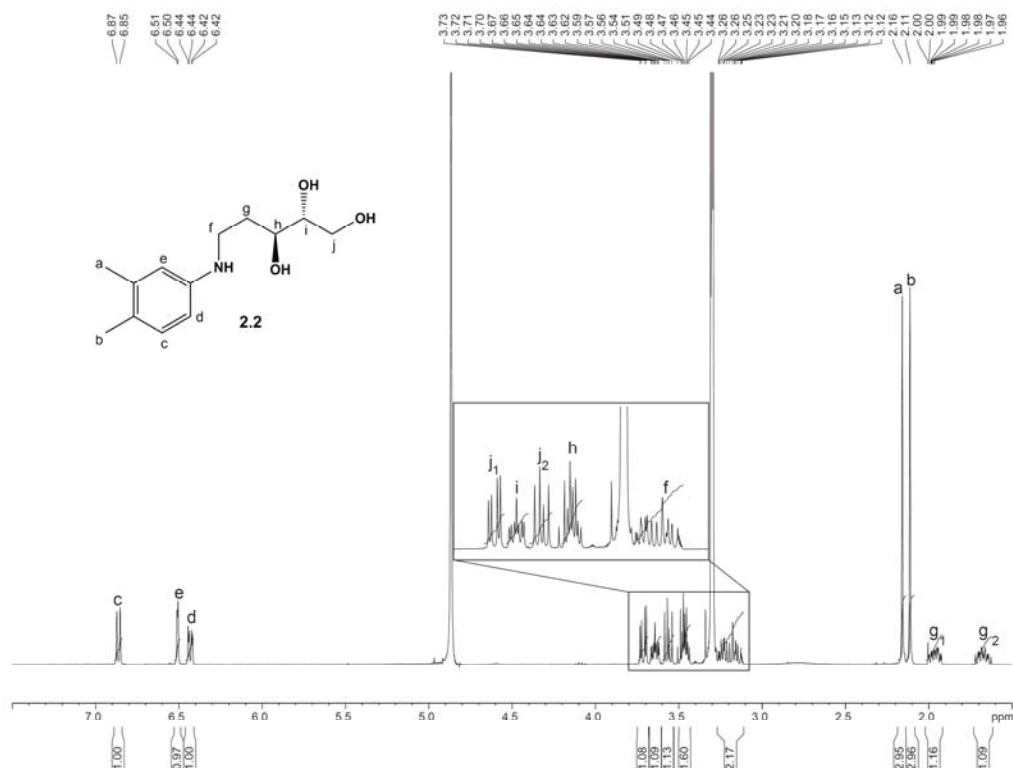


Figure A.2 ESI^+ -MS of 2-Deoxyribitylated-3,4-dimethylaniline (**2.2**) (m/z) $[\text{M}+\text{H}]^+$ for $\text{C}_{13}\text{H}_{21}\text{NO}_3$ calculated: 240.1555, found: 240.1464.

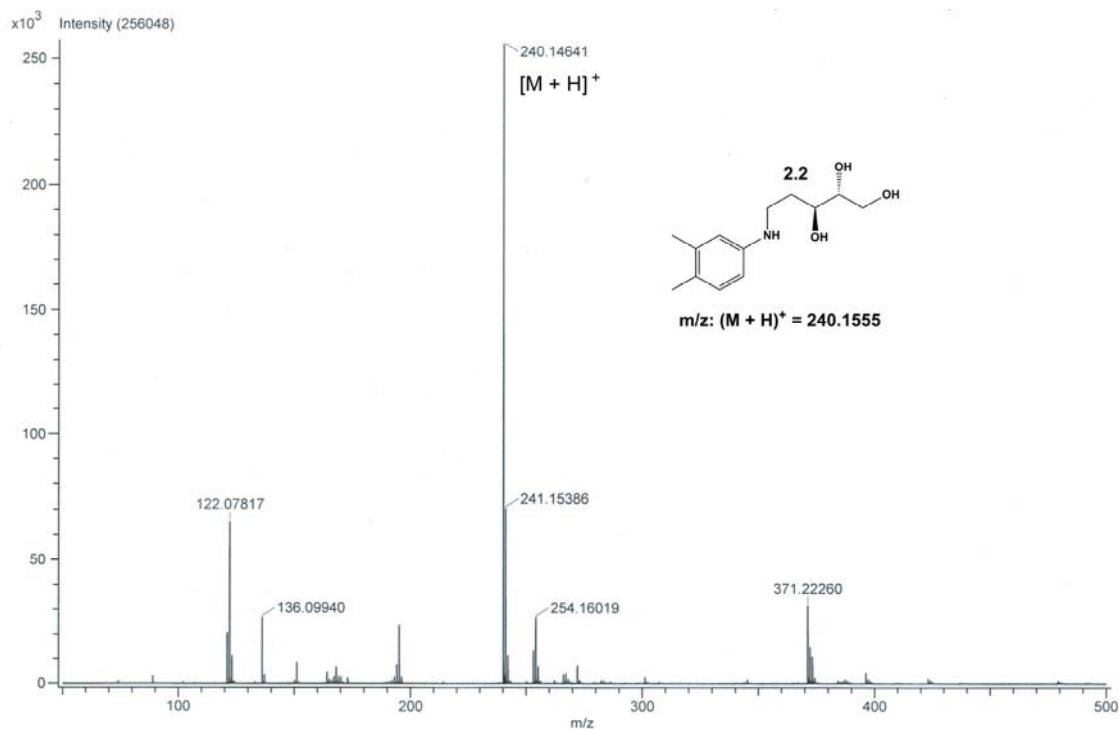


Figure A.3 ^1H NMR of crude Diazo-2-Deoxyribitylated-3,4-Dimethylaniline (**2.3**) taken in d_6 -Acetone.

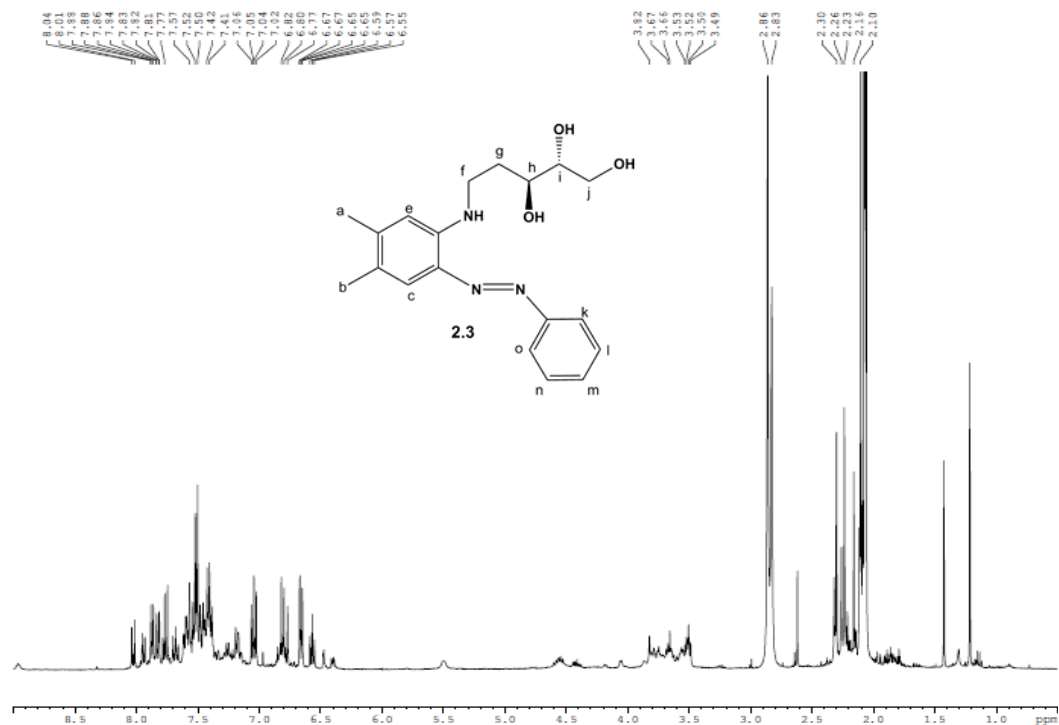


Figure A.4 ^1H NMR of Diazo-2-Deoxyribitylated-3,4-Dimethylaniline (**2.3**) taken in d_6 -Acetone.

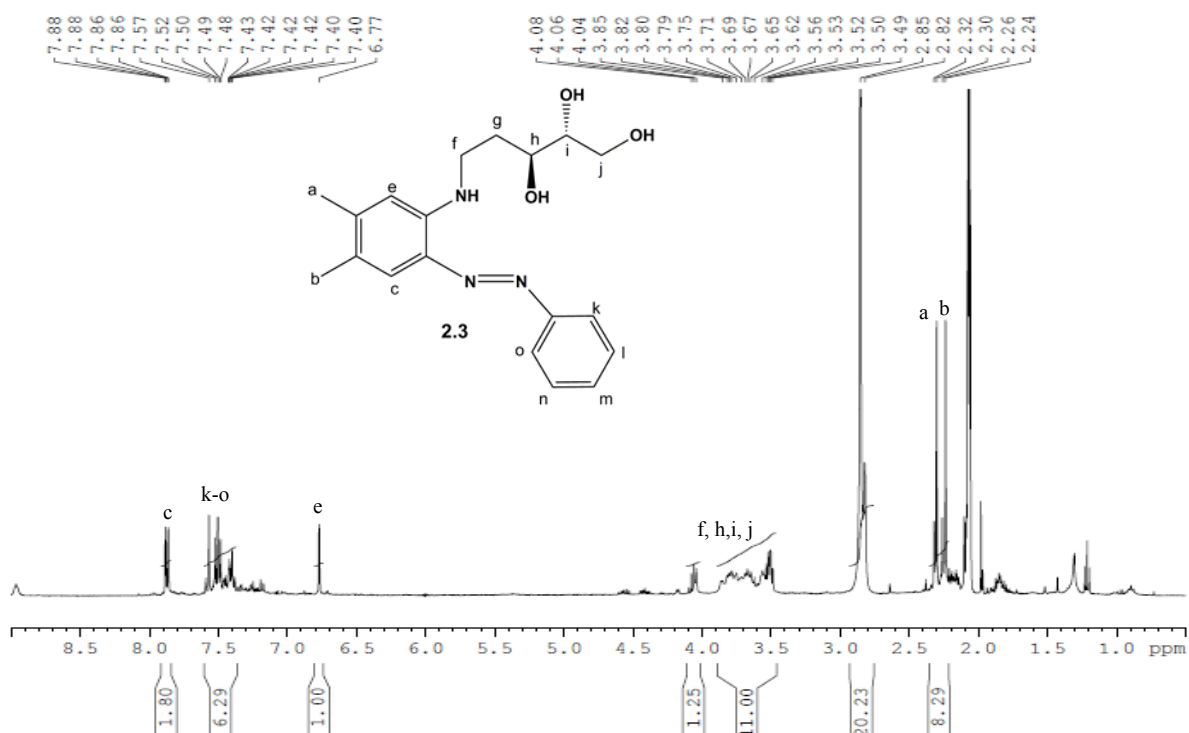


Figure A.5 ESI⁺- MS for Diazo-2-Deoxyribitylated-3,4-Dimethylaniline (**2.3**) (m/z) [M+H]⁺ for C₁₉H₂₅N₃O₃ calculated: 344.1929, found: 344.2645.

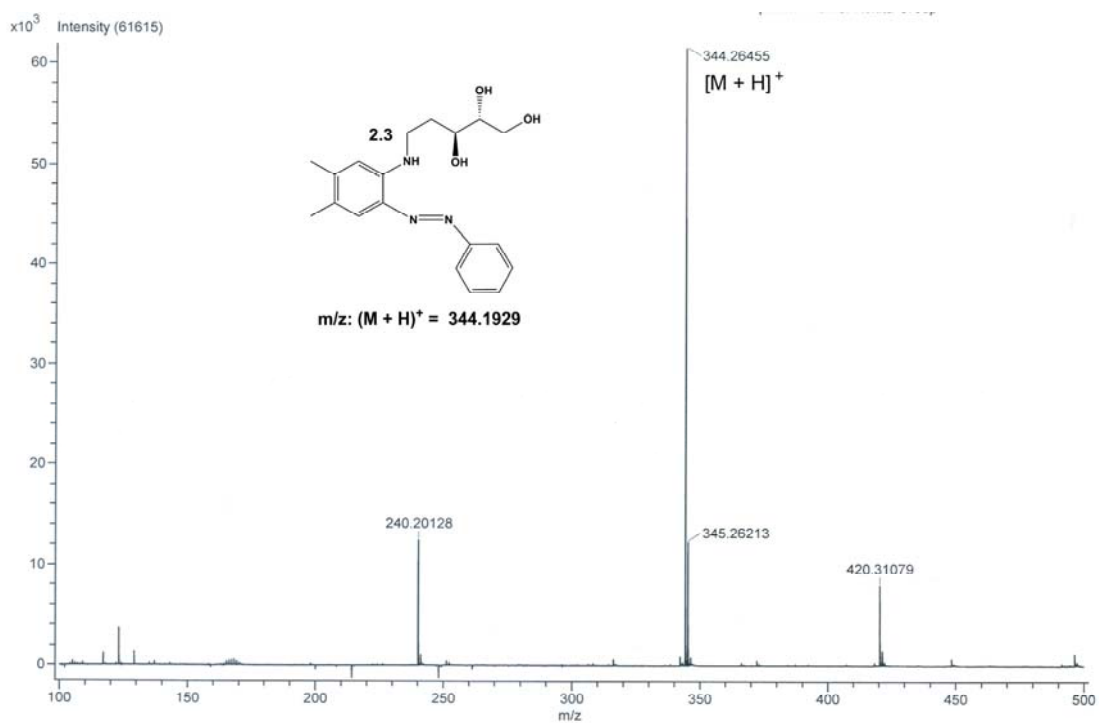


Figure A.6 ^1H NMR of 2-Deoxyriboflavin taken in d_4 -MeOD.

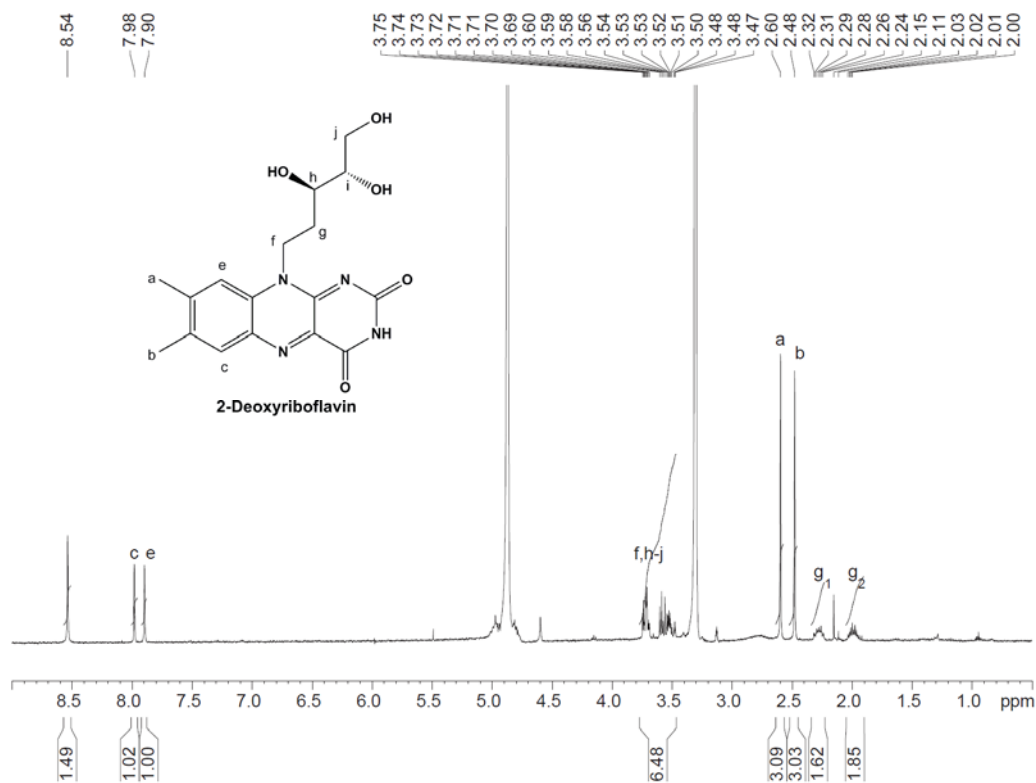


Figure A.7 UPLC- MS for 2-Deoxyriboflavin (m/z) $[\text{M}+\text{H}]^+$ for $\text{C}_{17}\text{H}_{20}\text{N}_4\text{O}_5$ calculated: 361.1467, found: 361.1508.

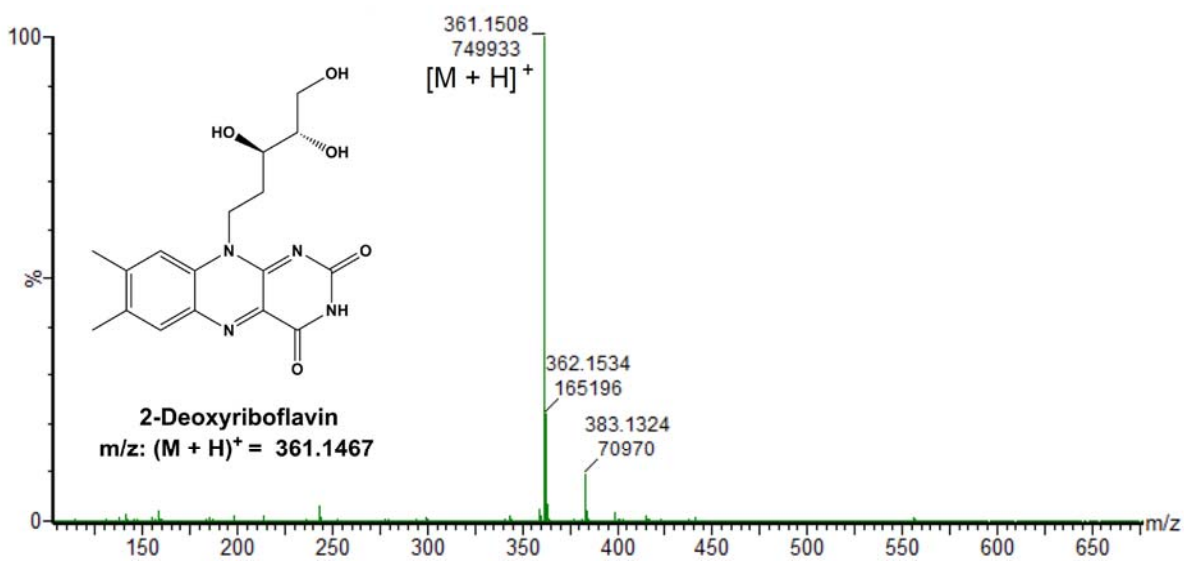


Figure A.8 ^1H NMR of 2-DeoxyFMN taken in D_2O .

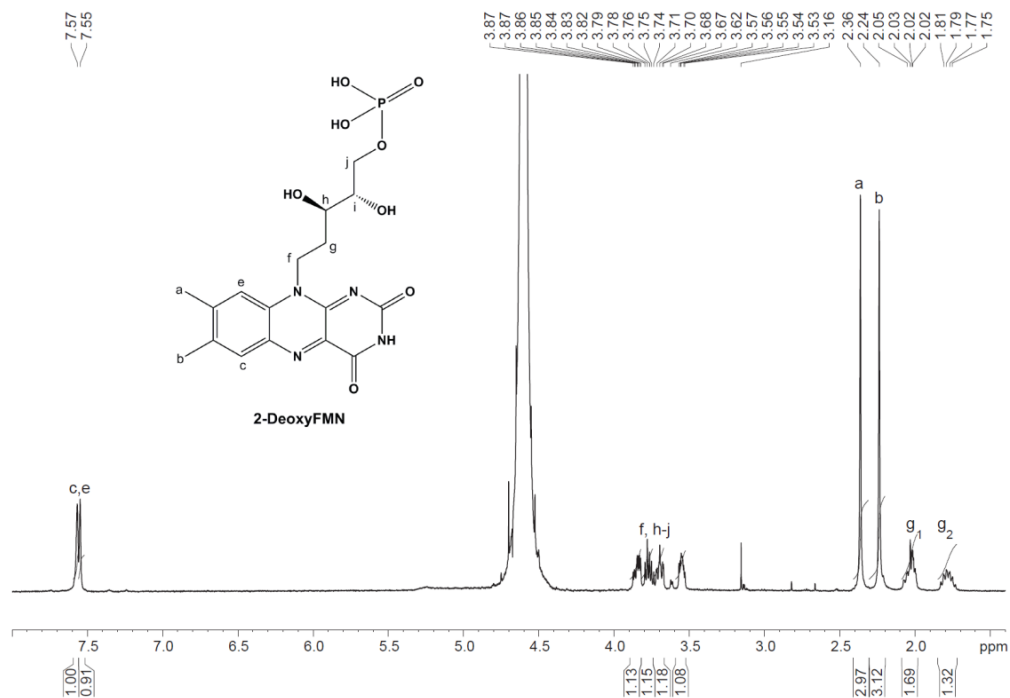
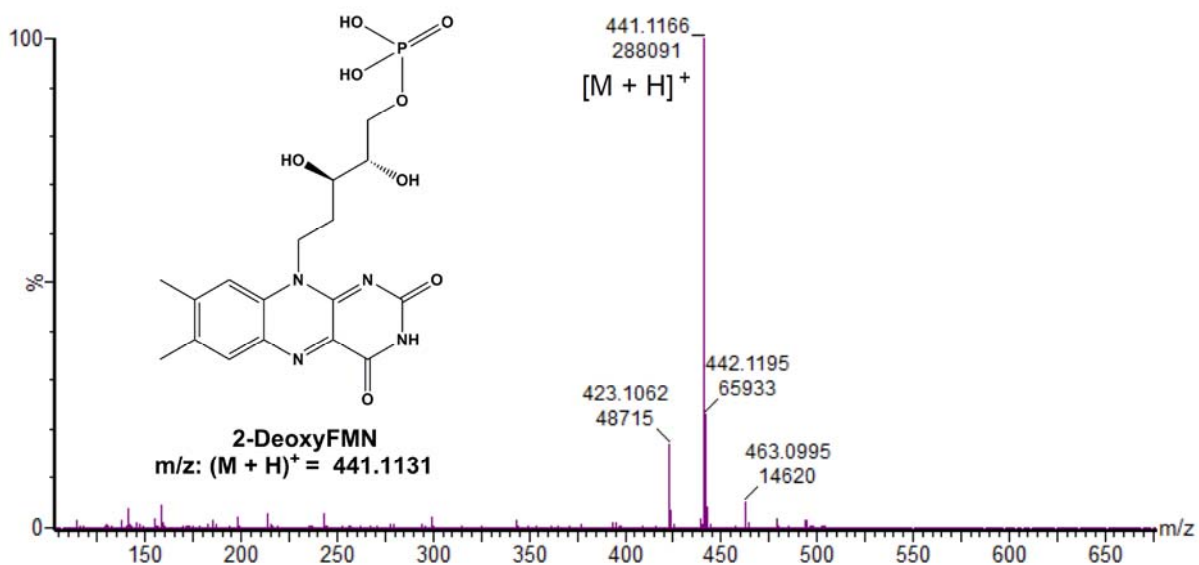


Figure A.9 UPLC- MS for 2-DeoxyFMN (m/z) $[\text{M}+\text{H}]^+$ for $\text{C}_{17}\text{H}_{20}\text{N}_4\text{O}_5$ calculated: 441.1131, found: 441.1166.



Appendix B. Supporting Information for Chapter 3

Figure B.1 Equilibrium binding of DIT to 2-deoxyhIYD.

DIT binding was monitored by the change in fluorescence of flavin bound to hIYD (4.5 μM) in solution of 100 mM potassium phosphate and 200 mM potassium chloride (pH 7.4) at 25°C using λ_{ex} of 450 nm and λ_{em} of 527 nm. The average of three independent measurements were normalized and plotted against DIT concentrations. Error represents the standard deviation of three measurements. A dissociation constant of 5.03 ± 0.16 mM was obtained by nonlinear fitting of the data to Eq. 3.1 by Origin 7.0 as described in Chapter 3.

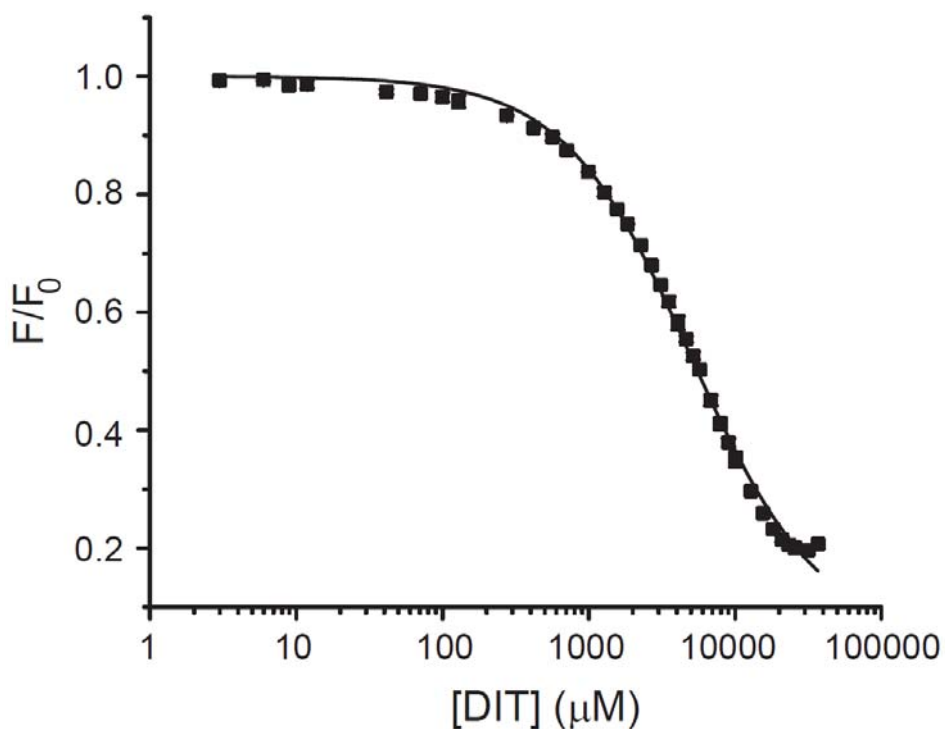


Figure B.2. Time Course MIT deiodinase activity of 2-deoxyhIYD.

The deiodination of MIT by 2-deoxyhIYD (0.4 μ M) was monitored by HPLC as described in Chapter 3 from 0 – 4 hours. The increase of tyrosine formation, as determined by the increase area of the tyrosine signal, was plotted against time and fit to a linear regression.

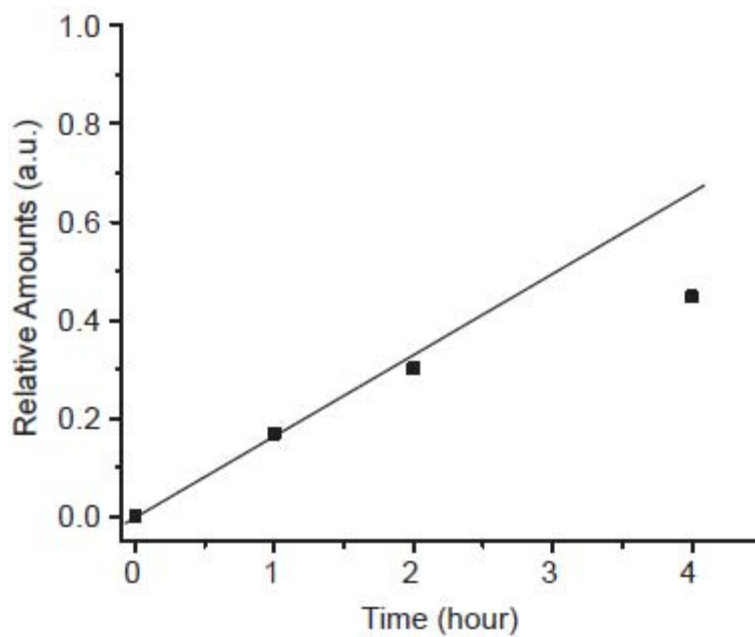


Figure B.3. $D^{125}IT$ deiodinase activity of 2-deoxyhIYD.

The activity of 2-deoxyhIYD ($0.4 \mu M$) with DIT was determined using the standard $D^{125}IT$ iodide release assay. Assays were performed in triplicate. Kinetic constants were obtained by fitting the average of the three independent measurements to Michaelis-Menten kinetics using Origin 7.0. Error bars represent standard deviation at each concentration. The kinetic parameter obtained from the fitting was a K_M of $1820 \pm 703.0 \mu M$ and a k_{cat} of $74.5 \pm 11.7 \text{ min}^{-1}$.

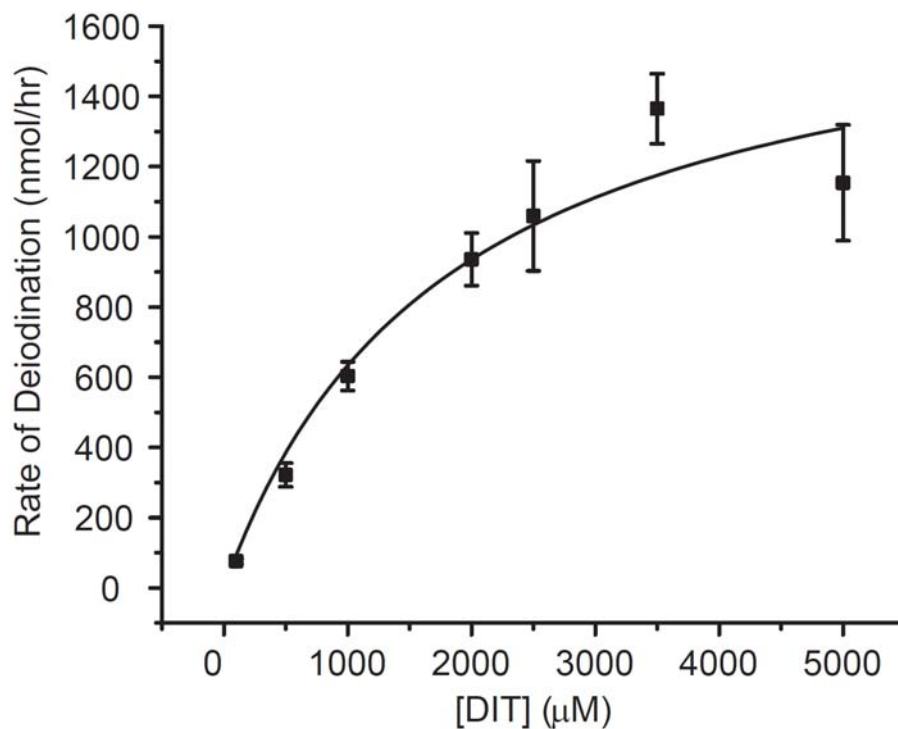
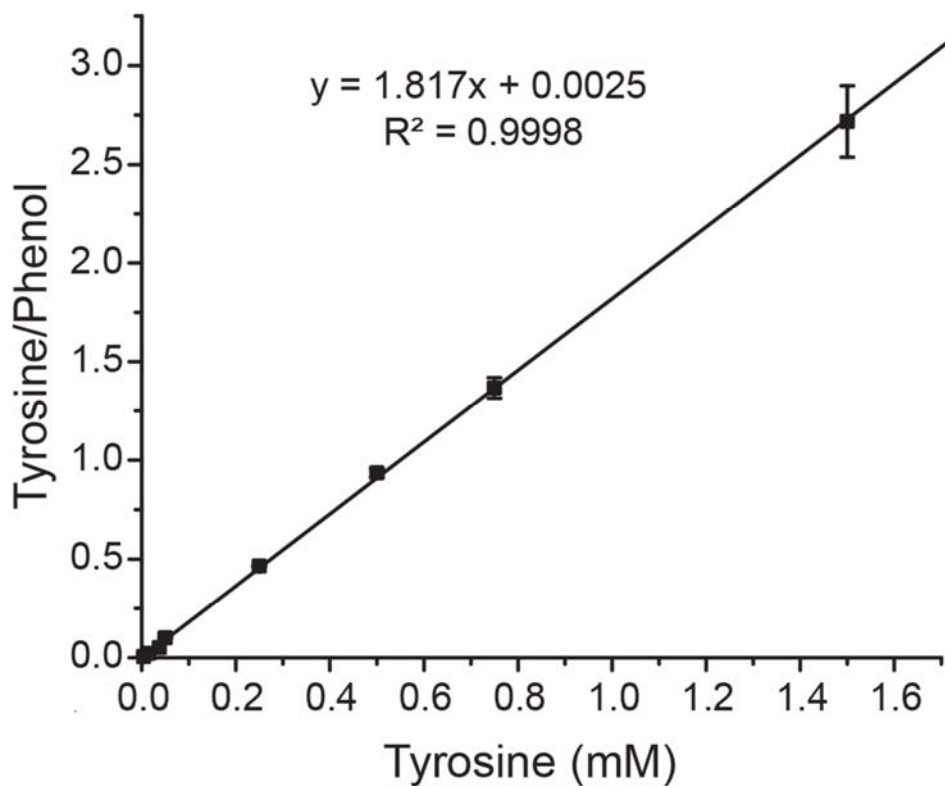


Figure B.4. Standard Curve of Tyrosine.

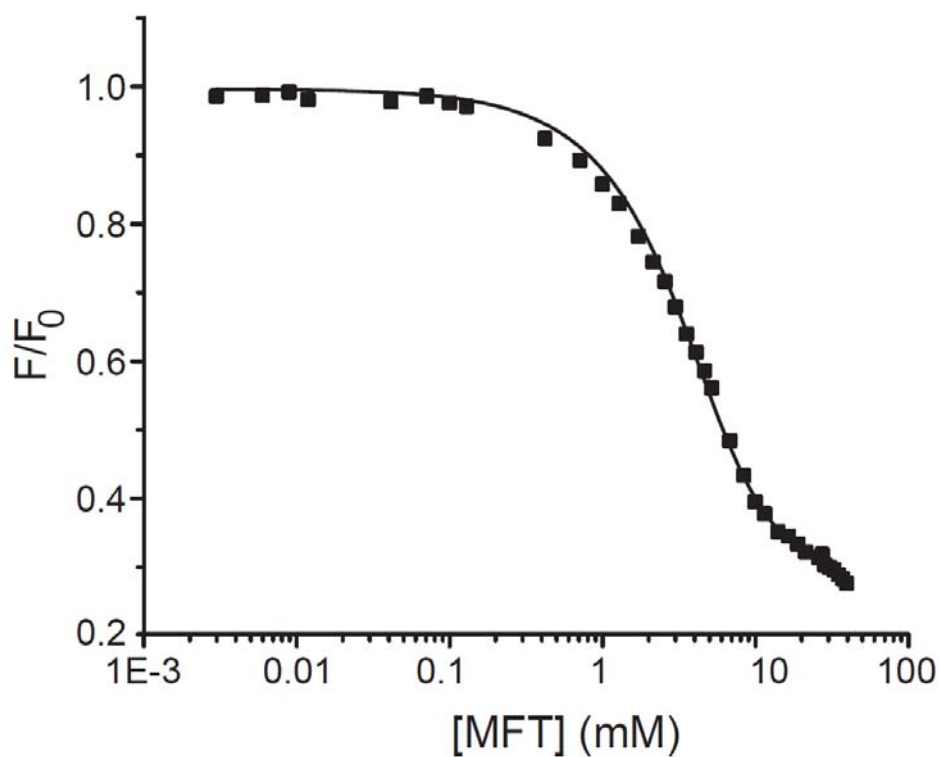
The standard curve of tyrosine was used to calculate reaction rates for the MIT deiodination assay monitored by HPLC as described in Chapter 3. The calibration curve was generated by injection of known amount of tyrosine and phenol onto the HPLC ⁸⁶. Measurements were performed in duplicate and the average of the two trials were normalized and plotted against tyrosine concentrations. Error represents the standard deviation of two measurements. RF was calculated using **Equation 3.4** by Microsoft Excel 2010.



Appendix C. Supporting Information for Chapter 4

Figure C.1. Equilibrium binding of MFT to 2-deoxyhIYD.

MFT binding was monitored by the change in fluorescence of flavin bound to hIYD (4.5 μM) in solution of 100 mM potassium phosphate and 200 mM potassium chloride (pH 7.4) at 25°C using λ_{ex} of 450 nm and λ_{em} of 527 nm. A dissociation constant of 1.49 ± 0.07 mM obtained by nonlinear fitting of the data to Eq. 3.1 by Origin 7.0 as described in Chapter 3.



Reference

1. Massey, V., The Chemical and Biological Versatility of Riboflavin. *Biochem. Soc. Trans.* **2000**, 28, 283-296.
2. Massey, V.; Hemmerich, P., Active-site probes of flavoproteins. *Biochemical Society Transactions* **1980**, 8, 246-257.
3. Chaiyen, P.; Fraaije, M. W.; Mattevi, A., The enigmatic reaction of flavins with oxygen. *Trends in Biochemical Sciences* **2012**, 37, (9), 373-380.
4. Müller, F., Flavin Radicals - Chemistry and Biochemistry *Free Radical Biol. Med.* **1987**, 3, (3), 215-230.
5. Kao, Y.-T.; Saxena, C.; He, T.-F.; Guo, L.; Wang, L.; Sancar, A.; Zhong, D., Ultrafast Dynamics of Flavins in Five Redox States. *J. Am. Chem. Soc.* **2008**, 130, (39), 13132-13139.
6. Hemmerich, P.; Nagelschneider, G.; Veeger, C., Chemistry and Molecular Biology of Flavins and Flavoproteins. *FEBS Lett.* **1970**, 8, (2), 69-83.
7. Ghisla, S.; Massey, V., New Flavin for Old -Artificial Flavins as Active-Site Probes of Flavoproteins *Biochem. J.* **1986**, 239, (1), 1-12.
8. Ghisla, S.; Massey, V., MECHANISMS OF FLAVOPROTEIN-CATALYZED REACTIONS. *European Journal of Biochemistry* **1989**, 181, (1), 1-17.
9. Rotello, V., *Models systems for flavoenzyme activity. Redox-induced modulation of flavin-receptor hydrogen bonding.* 1998; p 479-482.
10. Breinlinger, E. C.; Keenan, C. J.; Rotello, V. M., Modulation of flavin recognition and redox properties through donor atom-pi interactions. *Journal of the American Chemical Society* **1998**, 120, (34), 8606-8609.
11. Fraaije, M. W.; Mattevi, A., Flavoenzymes: Diverse Catalysts with Recurrent Features. *Trends Biochem. Sci.* **2000**, 25, (3), 126-132.
12. Walsh, C., Flavin Coenzymes: At the Crossroads of Biological Redox Chemistry. *Acc. Chem. Res.* **1980**, 13, (5), 148-155.
13. Dwyer, T. M.; Mortl, S.; Kemter, K.; Bacher, A.; Fauq, A.; Frerman, F. E., The Intraflavin Hydrogen Bond in Human Electron Transfer Flavoprotein Modulates Redox Potentials and May Participate in Electron Transfer. *Biochemistry* **1999**, 38, (30), 9735-9745.

14. Hemmerich, P.; Massey, V.; Fenner, H., Flavin and 5-Deazaflavin: A Chemical Evaluation of 'Modified' Flavoproteins with Respect to the Mechanisms of Redox Biocatalysis. *FEBS Lett.* **1977**, 84, (1), 5-21.
15. Xu, D.; Kohli, R. M.; Massey, V., The role of threonine 37 in flavin reactivity of the old yellow enzyme. *Proceedings of the National Academy of Sciences of the United States of America* **1999**, 96, (7), 3556-3561.
16. Pitsawong, W.; Sucharitakul, J.; Prongjit, M.; Tan, T. C.; Spadiut, O.; Haltrich, D.; Divne, C.; Chaiyen, P., A Conserved Active-site Threonine Is Important for Both Sugar and Flavin Oxidations of Pyranose 2-Oxidase. *Journal of Biological Chemistry* **2010**, 285, (13), 9697-9705.
17. Thibodeaux, C. J.; Mansoorabadi, S. O.; Kittleman, W.; Chang, W. C.; Liu, H. W., Evidence for the Involvement of Acid/Base Chemistry in the Reaction Catalyzed by the Type II Isopentenyl Diphosphate/Dimethylallyl Diphosphate Isomerase from *Staphylococcus aureus*. *Biochemistry* **2008**, 47, (8), 2547-2558.
18. Hersh, L. B.; Walsh, C., Preparation, Characterization, and Coenzymic Properties of 5-Carba-5-Deaza and 1-Carba-1-Deaza Analogs of Riboflavin, FMN, and FAD. *Methods Enzymol.* **1980**, 66, 277-287.
19. Fox, K. M.; Karplus, P. A., Old Yellow Enzyme at 2 Å Resolution: Overall Structure, Ligand Binding, and Comparison with Related Flavoproteins. *Structure* **1994**, 2, (11), 1089-105.
20. Karplus, P. A.; Schulz, G. E., Substrate Binding and Catalysis by Glutathione Reductase as Derived from Refined Enzyme: Substrate Crystal Structures at 2 Å Resolution. *J. Mol. Biol.* **1989**, 210, (1), 163-180.
21. Mattevi, A.; Schierbeek, A. J.; Hol, W. G., Refined Crystal Structure of Lipoamide Dehydrogenase from *Azotobacter vinelandii* at 2.2 Å Resolution. A Comparison with the Structure of Glutathione Reductase. *J. Mol. Biol.* **1991**, 220, (4), 975-994.
22. Zhou, B. P.; Wu, B.; Kwan, S. W.; Abell, C. W., Characterization of a Highly Conserved FAD-Binding Site in Human Monoamine Oxidase B. *J. Biol. Chem.* **1998**, 273, (24), 14862-14868.
23. Murthy, Y.; Massey, V., Chemical Modification of the N-10 Ribityl Side-Chain of Flavins - Effects on Properties of Flavoprotein Disulfide Oxidoreductases. *J. Biol. Chem.* **1995**, 270, (48), 28586-28594.
24. Murthy, Y.; Massey, V., Syntheses and Applications of Flavin Analogs as Active Site Probes for Flavoproteins. In *Methods Enzymol.*, 1997; Vol. 280, pp 436-460.

25. Palfey, B. A.; Murthy, Y.; Massey, V., Altered Balance of Half-Reactions in p-Hydroxybenzoate Hydroxylase Caused by Substituting the 2'-Carbon of FAD with Fluorine. *J. Biol. Chem.* **2003**, 278, (25), 22210-22216.
26. Kim, J. J. P.; Wang, M.; Paschke, R., Crystal Structures of Medium-Chain Acyl-CoA Dehydrogenase from Pig-Liver Mitochondria with and without Substrate *Proc. Natl. Acad. Sci. U.S.A.* **1993**, 90, (16), 7523-7527.
27. Ghisla, S.; Thorpe, C., Acyl-CoA Dehydrogenases - A Mechanistic Overview. *Eur. J. Biochem.* **2004**, 271, (3), 494-508.
28. Engst, S.; Vock, P.; Wang, M.; Kim, J. J. P.; Ghisla, S., Mechanism of Activation of Acyl-CoA Substrates by Medium Chain Acyl-CoA Dehydrogenase: Interaction of the Thioester Carbonyl with the Flavin Adenine Dinucleotide Ribityl Side Chain. *Biochemistry* **1999**, 38, (1), 257-267.
29. Macheroux, P.; Kappes, B.; Ealick, S. E., Flavogenomics - a genomic and structural view of flavin-dependent proteins. *Febs Journal* **2011**, 278, (15), 2625-2634.
30. Tu, S.-C.; Mager, H. I. X., Biochemistry of Bacterial Bioluminescence. *Photochem. Photobiol.* **1995**, 62, (4), 615-624.
31. Tomiki, T.; Saitou, N., Phylogenetic Analysis of Proteins Associated in the Four Major Energy Metabolism Systems: Photosynthesis, Aerobic Respiration, Denitrification, and Sulfur Respiration. *J. Mol. Evol.* **2004**, 59, (2), 158-176.
32. Dagley, S., Lesson from Biodegradation. *Annual Review of Microbiology* **1987**, 41, 1-23.
33. van Pee, K. H.; Unversucht, S., Biological Dehalogenation and Halogenation Reactions. *Chemosphere* **2003**, 52, 299-312.
34. van Pee, K. H.; Patallo, E. P., Flavin-dependent halogenases involved in secondary metabolism in bacteria. *Applied Microbiology and Biotechnology* **2006**, 70, (6), 631-641.
35. Blasiak, L. C.; Drennan, C. L., Structural Perspective on Enzymatic Halogenation. *Acc. Chem. Res.* **2009**, 42, (1), 147-155.
36. Rokita, S. E., Flavoprotein dehalogenases. *Handbook of Flavoproteins, Vol 1: Oxidases, Dehydrogenases and Related Systems* **2013**, 337-350.
37. Orser, C. S.; Dutton, J.; Lange, C.; Jablonski, P.; Xun, L. Y.; Hargis, M., Characterization of a Flavobacterium Glutathione-S-Transferase Gene Involved in Reductive Dechlorination. *J. Bacteriol.* **1993**, 175, (9), 2640-2644.

38. Kiefer, P. M.; Copley, S. D., Characterization of the Initial Steps in the Reductive Dehalogenation Catalyzed by Tetrachlorohydroquinone Dehalogenase. *Biochemistry* **2002**, 41, (4), 1315-1322.
39. McCarthy, D. L.; Navarrete, S.; Willett, W. S.; Babbitt, P. C.; Copley, S. D., Exploration of the Relationship between Tetrachlorohydroquinone Dehalogenase and the Glutathione S-Transferase Superfamily. *Biochemistry* **1996**, 35, (46), 14634-14642.
40. Visser, T. J., Mechanism of Action of Iodothyronine-5'-Deiodinase. *Biochim. Biophys. Acta* **1979**, 569, (2), 302-308.
41. Bianco, A. C.; Salvatore, D.; Gereben, B.; Berry, M. J.; Larsen, P. R., Biochemistry, cellular and molecular biology, and physiological roles of the iodothyronine selenodeiodinases. *Endocr. Rev.* **2002**, 23, (1), 38-89.
42. Tortora, G. J.; Anagnostakos, N. P., *Principles of anatomy and physiology*. 6th ed.; Harper & Row: New York, 1990; p xxv, 956, 102 p.
43. Johnson, K. S.; Coale, K. H.; Jannasch, H. W., ANALYTICAL-CHEMISTRY IN OCEANOGRAPHY. *Analytical Chemistry* **1992**, 64, (22), A1065-A1075.
44. De La Vieja, A.; Dohan, O.; Levy, O.; Carrasco, N., Molecular analysis of the sodium/iodide symporter: impact on thyroid and extrathyroid pathophysiology. *Physiol. Rev.* **2000**, 80, (3), 1083-105.
45. Medeiros Neto, G. A. d.; Stanbury, J. B., *Inherited Disorders of the Thyroid System*. CRC Press: Boca Raton, FL, 1994; p 221 p.
46. Rokita, S. E.; Adler, J. M.; McTamney, P. M.; Watson, J. A., Efficient Use and Recycling of the Micronutrient Iodide in Mammals. *Biochimie* **2010**, 92, (9), 1227-1235.
47. DeGroot, L. J.; Stanbury, J. B.; Means, J. H., *The Thyroid and Its Diseases*. 4th ed.; Wiley Biomedical Division, Wiley: New York, 1975; p xiv, 823 p.
48. Zimmermann, M. B.; Jooste, P. L.; Pandav, C. S., Iodine-Deficiency Disorders. *Lancet* **2008**, 372, (9645), 1251-62.
49. World Health Organization, U., *ICCIDD Assessment of Iodine Deficiency Disorders and Monitoring Their Elimination. A Guide for Programme Managers*; 978 92 4 159582 7; 2008; p 98.
50. Roche, J.; Michel, R.; Michel, O.; Lissitzky, S., Sur la Deshalogénéation Enzymatique des Iodotyrosine par le Corps Thyroïde et sur son Rôle Physiologique. *Biochim. Biophys. Acta* **1952**, 9, 161-169.

51. Roche, J.; Michel, O.; Michel, R.; Gorbman, A.; Lissitzky, S., Sur la Deshalogénéation Enzymatique des Iodotyrosine par le Corps Thyroïde et sur son Rôle Physiologique. II. *Biochim. Biophys. Acta* **1953**, 12, (1), 570-576.
52. Stanbury, J. B., Deiodination of the Iodinated Amino Acids *Ann. N.Y. Acad. Sci.* **1960**, 86, (2), 417-439.
53. Rosenberg, I. N.; Goswami, A., Purification and Characterization of a Flavoprotein from Bovine Thyroid with Iodotyrosine Deiodinase Activity *J. Biol. Chem.* **1979**, 254, (24), 12318-12325.
54. Goswami, A.; Rosenberg, I. N., Characterization of a Flavoprotein Iodotyrosine Deiodinase from Bovine Thyroid - Flavin Nucleotide Binding and Oxidation-Reduction Properties. *J. Biol. Chem.* **1979**, 254, (24), 12326-12330.
55. Moreno, J. C.; Pauws, E.; van Kampen, A. H.; Jedlicková, M.; de Vijlder, J. J.; Ris-Stalpers, C., Cloning of Tissue-Specific Genes Using Serial Analysis of Gene Expression and A Novel Computational Substraction Approach. *Genomics* **2001**, 75, (1-3), 70-6.
56. Moreno, J. C., Identification of Novel Genes Involved in Congenital Hypothyroidism Using Serial Analysis of Gene Expression. *Horm. Res.* **2003**, 3, 96-102.
57. Gnidehou, S.; Caillou, B.; Talbot, M.; Ohayon, R.; Kaniewski, J.; Noel-Hudson, M. S.; Morand, S.; Agnangji, D.; Sezan, A.; Courtin, F.; Virion, A.; Dupuy, C., Iodotyrosine Dehalogenase 1 (DEHAL1) is a Transmembrane Protein Involved in the Recycling of Iodide Close to the Thyroglobulin Iodination Site. *FASEB J.* **2004**, 18, (11), 1574-1576.
58. Moreno, J. C.; Klootwijk, W.; van Toor, H.; Pinto, G.; D'Alessandro, M.; Leger, A.; Goudie, D.; Polak, M.; Gruters, A.; Visser, T. J., Mutations in the Iodotyrosine Deiodinase Gene and Hypothyroidism. *N. Engl. J. Med.* **2008**, 358, (17), 1811-1818.
59. Afink, G.; Kulik, W.; Overmars, H.; de Randamie, J.; Veenboer, T.; van Cruchten, A.; Craen, M.; Ris-Stalpers, C., Molecular Characterization of Iodotyrosine Dehalogenase Deficiency in Patients with Hypothyroidism. *J. Clin. Endocrinol. Metab.* **2008**, 93, (12), 4894-4901.
60. Burniat, A.; Pirson, I.; Vilain, C.; Kulik, W.; Afink, G.; Moreno-Reyes, R.; Corvilain, B.; Abramowicz, M., Iodotyrosine Deiodinase Defect Identified via Genome-Wide Approach. *Journal of Clinical Endocrinology & Metabolism* **2012**, 97, (7), E1276-E1283.
61. Friedman, J. E.; Watson, J. A.; Lam, D. W. H.; Rokita, S. E., Iodotyrosine Deiodinase is the First Mammalian Member of the NADH Oxidase/Flavin Reductase Superfamily. *J. Biol. Chem.* **2006**, 281, (5), 2812-2819.

62. Buss, J. M.; McTamney, P. M.; Rokita, S. E., Expression of a Soluble Form of Iodotyrosine Deiodinase for Active Site Characterization by Engineering the Native Membrane Protein from *Mus musculus*. *Protein Sci.* **2012**, 21, (3), 351-361.
63. Thomas, S. R.; McTamney, P. M.; Adler, J. M.; LaRonde-LeBlanc, N.; Rokita, S. E., Crystal Structure of Iodotyrosine Deiodinase, a Novel Flavoprotein Responsible for Iodide Salvage in Thyroid Glands. *J. Biol. Chem.* **2009**, 284, (29), 19659-19667.
64. Hu, J. M.; Chuenchor, W.; Rokita, S. E., A Switch between One- and Two-electron Chemistry of the Human Flavoprotein Iodotyrosine Deiodinase Is Controlled by Substrate. *Journal of Biological Chemistry* **2015**, 290, (1), 590-600.
65. Taga, M. E.; Larsen, N. A.; Howard-Jones, A. R.; Walsh, C. T.; Walker, G. C., BluB Cannibalizes Flavin to Form the Lower Ligand of Vitamin B-12. *Nature* **2007**, 446, (7134), 449-453.
66. Rosenberg, I. N., Purification of Iodotyrosine Deiodinase from Bovine Thyroid *Metabolism* **1970**, 19, (10), 785-798.
67. Watson, J. A.; McTamney, P. M.; Adler, J. M.; Rokita, S. E., Flavoprotein Iodotyrosine Deiodinase Functions without Cysteine Residues. *ChemBioChem* **2008**, 9, (4), 504-506.
68. McTamney, P. M.; Rokita, S. E., A Mammalian Reductive Deiodinase has Broad Power to Dehalogenate Chlorinated and Brominated Substrates. *J. Am. Chem. Soc.* **2009**, 131, (40), 14212-14213.
69. Müller, F., *Chemistry and Biochemistry of Flavoenzymes*. CRC Press: Boca Raton, 1991; p v. <1-3 >.
70. Hefti, M. H.; Vervoort, J.; van Berkel, W. J. H., Deflavination and Reconstitution of Flavoproteins - Tackling Fold and Function. *Eur. J. Biochem.* **2003**, 270, (21), 4227-4242.
71. Kittleman, W.; Thibodeaux, C. J.; Liu, Y. N.; Zhang, H.; Liu, H. W., Characterization and Mechanistic Studies of Type II Isopentenyl Diphosphate:Dimethylallyl Diphosphate Isomerase from *Staphylococcus aureus*. *Biochemistry* **2007**, 46, (28), 8401-8413.
72. Miller, J. R.; Guan, N. N.; Hubalek, F.; Edmondson, D. E., The FAD Binding Sites of Human Liver Monoamine Oxidases A and B: Investigation of the Role of Flavin Ribityl Side Chain Hydroxyl Groups in the Covalent Flavinylation Reaction and Catalytic Activities. *Biochim. Biophys. Acta* **2000**, 1476, (1), 27-32.
73. Tishler, M.; Wellman, J. W.; Ladenburg, K., The Preparation of Riboflavin. 3. The Synthesis of Alloxazines and Isoalloxazines. *J. Am. Chem. Soc.* **1945**, 67, (12), 2165-2168.

74. Carlson, E. E.; Kiessling, L. L., Improved Chemical Syntheses of 1-and 5-Deazariboflavin. *J. Org. Chem.* **2004**, 69, (7), 2614-2617.
75. Kasai, S.; Nakano, H.; Kinoshita, T.; Miyake, Y.; Maeda, K.; Matsui, K., Intestinal - Absorption of Riboflavin, Studied by an in situ Circulation System using Radioactive Analogs. *J. Nutr. Sci. Vitaminol.* **1988**, 34, (3), 265-280.
76. Karthikeyan, S.; Zhou, Q.; Mseeh, F.; Grishin, N. V.; Osterman, A. L.; Zhang, H., Crystal Structure of Human Riboflavin Kinase Reveals a beta Barrel Fold and a Novel Active Site Arch. *Structure* **2003**, 11, (3), 265-273.
77. Karthikeyan, S.; Zhou, Q.; Osterman, A. L.; Zhang, H., Ligand Binding-Induced Conformational Changes in Riboflavin Kinase: Structural Basis for the Ordered Mechanism. *Biochemistry* **2003**, 42, (43), 12532-12538.
78. Mack, M.; van Loon, A.; Hohmann, H. P., Regulation of Riboflavin Biosynthesis in *Bacillus subtilis* is Affected by the Activity of the Flavokinase/Flavin Adenine Dinucleotide Synthetase Encoded by ribC. *J. Bacteriol.* **1998**, 180, (4), 950-955.
79. McTamney, P. M., Catalytic Features of the Iodine Salvaging Enzyme Iodotyrosine Deiodinase. Ph.D. Dissertation. *Department of Chemistry and Biochemistry, University of Maryland, College Park.* **2009**.
80. Phatarphekar, A.; Buss, J. M.; Rokita, S. E., Iodotyrosine deiodinase: a unique flavoprotein present in organisms of diverse phyla. *Molecular Biosystems* **2014**, 10, (1), 86-92.
81. Rosenberg, I. N.; Goswami, A.; Finn, W.; Kivie, M., Iodotyrosine Deiodinase from Bovine Thyroid. *Methods Enzymol.* **1984**, Volume 107, 488-500.
82. van Berkel, W. J. H.; van den Berg, W. A. M.; Müller, F., Large-Scale Preparation and Reconstitution of Apo-Flavoproteins with Special Reference to Butyryl-CoA Dehydrogenase from *Megasphaera elsdenii*. *Eur. J. Biochem.* **1988**, 178, (1), 197-207.
83. Hefti, M. H.; Milder, F. J.; Boeren, S.; Vervoort, J.; van Berkel, W. J. H., A His-tag Based Immobilization Method for the Preparation and Reconstitution of Apoflavoproteins. *Biochim. Biophys. Acta* **2003**, 1619, (2), 139-143.
84. Hu, J. M., The Interplay of Substrate, Protein and Its Cofactor in Controlling the Catalytic Properties of Human Iodotyrosine Deiodinase. Ph.D. Dissertation *Department of Chemistry and Biochemistry, University of Maryland, College Park.* **2014**.
85. Warner, J. R.; Copley, S. D., Pre-steady-State Kinetic Studies of the Reductive Dehalogenation Catalyzed by Tetrachlorohydroquinone Dehalogenase. *Biochemistry* **2007**, 46, 13211-13222.

86. Moldoveanu, S. e.; David, V., *Sample preparation in chromatography*. Elsevier: Amsterdam ; Boston, 2002; p xi, 930 p.
87. Kitamura, S.; Kuwasako, M.; Ohta, S.; Tatsumi, K., Reductive debromination of (alpha-bromoiso-valeryl)urea by intestinal bacteria. *Journal of Pharmacy and Pharmacology* **1999**, 51, (1), 79-84.
88. Kiefer, P. M.; McCarthy, D. L.; Copley, S. D., The Reaction Catalyzed by Tetrachlorohydroquinone Dehalogenase does not Involve Nucleophilic Aromatic Substitution. *Biochemistry* **2002**, 41, (4), 1308-1314.
89. Kunishima, M.; Friedman, J. E.; Rokita, S. E., Transition-State Stabilization by a Mammalian Reductive Dehalogenase. *J. Am. Chem. Soc.* **1999**, 121, (19), 4722-4723.
90. van den Heuvel, R. H. H.; Fraaije, M. W.; van Berkel, W. J. H., Redox properties of vanillyl-alcohol oxidase. *Redox Cell Biology and Genetics, Pt B* **2002**, 353, 177-186.
91. Fetzner, S.; Lingens, F., Bacterial Dehalogenases - Biochemistry, Genetics, and Biotechnological Applications *Microbiol. Rev.* **1994**, 58, (4), 641-685.
92. Fetzner, S., Bacterial Dehalogenation. *Appl. Microbiol. Biot.* **1998**, 50, (6), 633-657.